E-ISSN: 2655-8777

3Bio

JOURNAL OF BIOLOGICAL SCIENCE, TECHNOLOGY AND MANAGEMENT

Volume 3, No 1, 2021

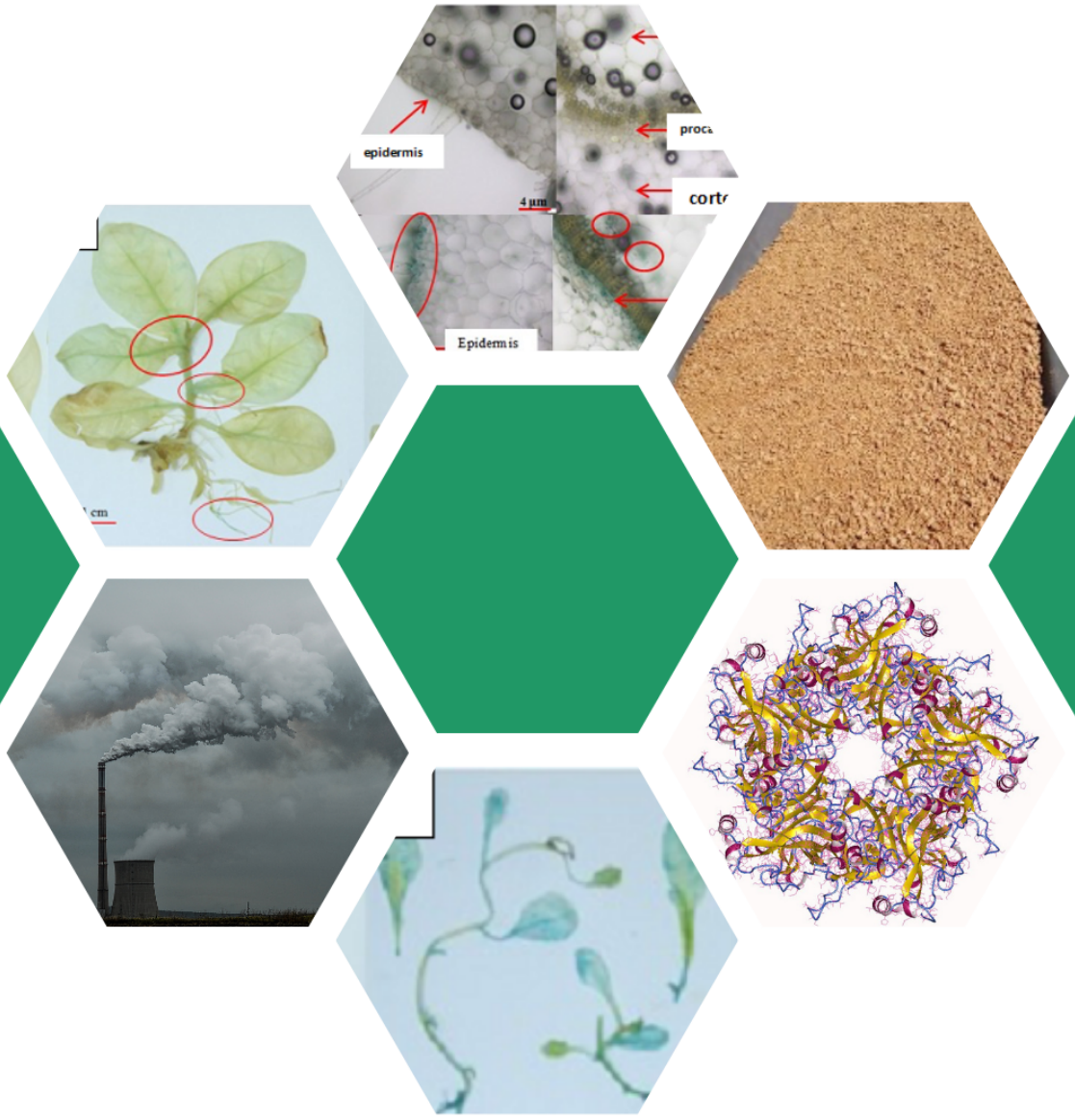

School of Life Sciences and Technology
Institut Teknologi Bandung - Indonesia

3BIO: Journal of Biological Science, Technology and Management

Volume 3 • No 1 • 2021

This journal and individual articles are published at http://journals.itb.ac.id/index.php/3bio
a series imprint of the ITB Journal – an open access publisher.

ISSN 2655-8777 (Online)

3Bio: Journal of Biological Science, Technology and Management is a peer-refereed journal which is published twice a year. It is an interdisciplinary journal with its core in basic and applied life sciences and aims to address sustainability issues.

AIMS AND SCOPE

Journal of Biological Science, Technology and Management (3BIO) is the official journal of the School of Life Sciences and Technology, Institut Teknologi Bandung, Indonesia. 3BIO is an open access journal and published by ITB Journal. It is an interdisciplinary peer-reviewed journal in a wide aspect related to the field of life sciences and other related fields of study. The journal aims to promote scientific discourse and disseminate research on various branches and applications of bio-science, biotechnology and bio-based management.

This journal invites original empirical research, literature reviews, theoretical or methodological contributions, or short communications on, but not limited to, the following topics:

- Ecology and Biosystematics
- Microbiology
- Genetics and Molecular Biology
- Animal Development and Physiology
- Plant Development and Physiology
- Entomology
- Biomedical science
- Biochemistry
- Agronomy
- Forestry
- Bioengineering
- Bioethics
- Management of Biological Resources.

The journal also invites contributions from other associated disciplines.

ITB Journal (formerly Proceedings ITB), the official ITB scientific journal, has been published since 1961. It serves a vehicle for ITB's Faculty members and contributors from outside of ITB to publish research findings in science, technology and fine arts.

For more information about how to submit an article, please refer to our website: http://journals.itb.ac.id/index.php/3bio

COPYRIGHT

TABLE OF CONTENTS

3BIO: Journal of Biological Science, Technology and Management 3(1):1-8
e-ISSN: 2655-8777 http://journals.itb.ac.id/index.php/3bio

Analysis of MeEf1A6 Gene Promoter Activity with In-vitro and In-vivo using Transient and Stable Expression Techniques in Tobacco Plant (*Nicotiana tabacum*)

Galih Gibral Andalusia, Sony Suhandono*, Ima Mulyama Zainuddin

School of Life Sciences and Technology, Bandung Institute of Technology, Indonesia.

Corresponding author; e-mail: sony@sith.itb.ac.id
Received 7 August, 2020
Accepted for publication 6 April, 2021

Abstract

The promoter is a part of the gene that functions in carrying out the gene expression, and its work activity becomes a matter of concern to ensure that expression works effectively. MeEF1A6 (*Manihot esculenta* Elongation Factor 1 Alfa - 6) is a promoter derived from cassava plants (*Manihot esculenta*). In previous studies, the MeEF1A6 promoter was successfully isolated, introduced, and characterized into the pBI121 plasmid, replacing the CaMV35S promoter. This study aims to analyze the activity of MeEF1A6 promoters in-vivo and in-vitro by using transient and transgenic techniques in tobacco plants. The pBI121 plasmid containing the MeEF1A6 promoter was introduced into *Agrobacterium tumefaciens* strain AGL1 and LBA4404. The promoter's work was then analyzed by the result of introducing it into the tobacco plant using the transient and stable transformation. The whole part of explants was used for transient study and tested in a minimum of two biological replicates. Sixty sheets of explant leaves that have been cut were used for stable transformation. The promoter work analysis was carried out with the GUS gene expression that integrated with the promoter with histochemical GUS assay. The transient produced a blue color in the roots, stems, and leaves on the whole repetition. The transverse incision in the stem shows the blue color on the epidermis and procambium tissue. Stable transformation using AGL1 as vector produced 43 shoots from 40 calli. A total of 43 shoots were selected with antibiotics and produced 27 plantlets that were successfully grown. Some plantlets are then reacted with x-gluc as histochemical GUS assay substrat and produced a blue color in the explants, indicating that the MeEF1A6 promoter has been successfully introduced. The results indicate that the MeEF1A6 promoter could work on plant tissue in roots, stems, leaves, and tissues that connect meristems such as procambium in tobacco plants. This reinforces the suspicion that the MeEF1A6 promoter performs work constitutionally as a constitutive promoter.

Keywords: Promoter, Transformation, MeEF1A6*, N. tabacum*

1. Introduction

Genetic engineering has made substantial progress in recent years. One of these advances was the discovery of several components that could support the introduction of genetic engineering, for instance, promoters. In genetic engineering, especially in gene introduction, the role of the promoter is very important for the success of protein expression. In process of protein expression, the transcription initiation is a very important initial step, since this process is the starting point for attaching RNA polymerase to the DNA sequence before the transcription process begins [1]. The DNA sequences where the initiation of transcription (attachment of RNA polymerase and transcription factors) begin are called promoter sequences. Without the promoter sequence, the transcription process will not be induced [2]. The promoter sequence consists of a specific base sequence and serves to support the initiation of transcription [3]. Studies of promoters have been carried out to see the expression patterns of a gene. The control of the promoter can be an important factor that can explain how a gene can be expressed or inhibited.

Studies on promoter have been widely carried out, for instance, on the EF1A gene (Elongation factor 1 alpha).

DOI: https://doi.org/10.5614/3bio.2021.3.1.1

EF1A presents as abundant proteins in cells, which fills up to 3 - 10% of the total soluble protein in cells [4]. EF1A protein is included in the Moonlight protein group, a protein that has more than one function [5]. This protein can interact with several types of proteins including actin protein [6], microtubules [7], and calmodulin [8]. This protein is also known to play a role in the process of apoptosis [9], regulation of viral infections [10], and DNA replication [11]. Variation in function and high amount of protein makes the EF1A gene family promoter expected to be one source of promoters that can be actively varied and have a high level of expression [12].

Several promoters of the EF1A gene family derived from cassava (*Manihot esculenta*) have been successfully isolated in previous research [13]. This study isolated promoter of MeEF1A3, MeEF1A5, and MeEF1A6 genes. MeEF1A promoters have different levels of expression in the studied plant model. MeEF1A3 can be expressed in cotyledons but cannot be expressed at the root of tobacco. MeEF1A5 can be expressed in bananas and tomatoes, but cannot be expressed in tobacco shoots. MeEF1A6 can be active in all parts of tobacco shoots, bananas, and tomatoes and has a high level of expression [13]. This makes the MeEF1A6 promoter a constitutive promoter candidate because it could be active continuously and had a very high level of activation. To find out the exact work of the MeEF1A6 promoter, further research is needed on the analysis of this promoter. This study focused on promoter transformation, which was carried out using *Agrobacterium tumefaciens* strain AGL1 and LBA4404. The results of the promoter expression were carried out by an integrated histochemical GUS assay on the pBI121 plasmid.

2. Material and Methods

2.1. Material

Agrobacterium tumefaciens (AGL1 and LBA4404 Strains) were used as a vector. AGL1 was used from the genetic lab of Bandung Institut of Technology (ITB) and LBA4404 was used from Biorin lab Bogor Agricultural University (IPB). Tobacco plant CV SR1 (*Nicotiana tabacum*) 3-4 week age was used as a plant model for expression analysis. pBi121 plasmid was used as a plasmid vector. Kanamycin antibiotic was used for plasmid selection, Ampicillin and streptomycin antibiotic was used for selection *A tumefaciens* strain AGL1 and LBA4404.

2.2. Introduction of MeEF1A6 Promoter to Agrobacterium tumefaciens

Gene introduction was carried out using the electroporation method using electrocompetent cells. Electrocompetent cells were made by following the method described by Debler [14]. Electrocompeten cells were made by incubating *Agrobacterium tumefaciens* until it reached exponential phase (2-3 days) and centrifuge gradually until the volume reaches a quarter of the previous volume (every step must conducted in ice-cold temperature). The final pellet was resuspended with 10% glycerol and stored at -80ºC. Introduction plasmid to *Agrobacterium tumefaciens* begins by mixing 1 µL of the promoted plasmid (plasmid concentration of not more than 20 µg/mL) with 40 µL of electrocompetent cells in the electroporation cuvette. Electroporation conditions were regulated on the Xcell Electroporation System Gene pulser with the choice of *Agrobacterium tumefaciens* electroporation method. The electroporation cuvette was placed on the Xcell Shock Pod and the electroporation process begins by pressing the pulse button. After the graph appears on the electroporator screen, the culture is quickly transferred to the refresher media (LB medium for LBA4404 and YEP medium for AGL1). The culture was then incubated on the incubator Shaker at 250 rpm at 30ºC for 3 hours. After that, the culture is spread on solid media that have been mixed with antibiotic selection (ampicillin 100 ppm for AGL1 and Streptomycin 50ppm for LBA4404).

2.3. Confirmation of Plasmids Carrying MeEF1A6 and CaMV35S Promoter in Agrobacterium tumefaciens Cultures

Plasmid confirmation was performed using the Polymerase Chain Reaction (PCR) method using specific primers to confirm that plasmid carrying MeF1A6 and CaMV35S promoter. The primers used are specific primers between the promoter base (forward) and the uidA gene coding base (GUS) (reverse). Specific primers were obtained from Apriyanto research [15]. The PCR condition follows used anealing temperature for MeEF1A6 promoters, which is 55 ºC and CaMV35S 60 ºC. MeEF1A6 bp fragment is 1311 bp, while CaMV35S is 675 bp. PCR results were obtained by running the electrophoresis method in agarose gel 1%. The DNA sequence tape was confirmed by visualization in UV light.

2.4. Introduction of MeEF1A6 promoter linked to the GUS gene into the tabacco plant

Introduction promoter was used by two methods, i.e., transient transformation and stable transformation. The introduction was carried out to investigate the work of the MeEF1A6 promoter in tobacco plants (*N. tabaccum*). *A. Tumefaciens* cultures that had been confirmed for the presence of pBI-MeEF1A6 and pBI-CaMV35S plasmids were sampled and transferred into liquid media containing the antibiotic selection. The culture was incubated at room temperature for 2-3 days. After incubation,

DOI: https://doi.org/10.5614/3bio.2021.3.1.1

20 µL of liquid culture was transferred back to the liquid medium with a volume of 20 mL that had been added to selected antibiotics. The liquid culture is re-incubated for 12-15 hours. After that, the culture was then confirmed OD600 until it reached 0.3-0.5. The culture was then centrifuged at 5000 rpm at 4ºC for 15 minutes. The supernatant was removed and the pellet was transferred to the infiltration media (MS0 with acetosyringone) which has been added with 20 ppm acetosyringone and 0.005% silwet.

The transient transformation plants prepared were separated per individual consisting of roots, stems, and leaves. The plants were then soaked in a co-cultivation solution with 20 ppm acetosiringone and siltettt 0.005% added. Then the infiltration stage was carried out using a vacuum and desiccator. The vacuum was done for 30 minutes. The infiltration process was carried out aseptically in the Laminar airflow cabinet (LAFC). Vacuumed plants in an infiltration medium then tightly closed in a container and incubated at 26ºC for 2-3 days. After 2-3 days, the plants are ready for further testing.

The stable transformation was carried out by following the method from Fajri (2015) [16]. The stable transformation begins with cutting 1x1 cm plant leaves. A total of 60 leaves that have been cut were immersed in the co-cultivation solutions containing *A. tumefaciens* and 20 ppm acetosyringone. The culture was then shaken with a 100 rpm speed shaker for 10 minutes. The culture was dried with sterile tissues for 10 minutes. After incubation, culture was then planted on solid infiltration media (Appendix A2). The abaxial position of the leaves is in the down position and submerged in solid co-cultivation media. The culture was then incubated in a dark room for 2-3 days. After incubation, the culture was washed with sterile deionized water 3 times and cefotaxime 200 ppm antibiotics 1 time. The culture was dried with sterile tissue and re-planted into callus growth media (Appendix A3). After two weeks, the culture was transferred to callus growth media that had been given antibiotic selection. Every 2 weeks the culture was transferred to a new callus growth media. The shoots that have emerged from the callus are transferred to the root induction medium (Appendix A4) containing selection antibiotics and left until the roots appear and become a new plantlet.

2.5. Analysis of uidA gene expression by Histochemical GUS Assay

Explants that had been incubated for 2 days and explants that had been successfully transformed were immersed in X-Gluc solution (1 mM 5-bromo-4-choloro-3-indolyl-β-D-glucuronide; Sigma), 100 mM sodium phosphate buffer pH 7 , 0.5 mM K3 [Fe(CN)6], 0.5 mM K4 [Fe(CN)6], 10 mM Na2EDTA, 0.1% (v / v), Triton X-100, then incubated at 37ºC for 18 hours in dark conditions. Then the explants were rinsed with 70% alcohol until the green color in the explants disappeared. Blue appearance was analyzed on the roots, stems, and leaves. The blue color indicated the promoter had been actived and stimulated expression of *GUS* gene that reacted with the substrate (X-Gluc) from colorless to blue. Samples that have been analyzed were then photographed using SLR (Canon EOS 1100 DC).

3. Results and discussion

3.1. Introduction and promoter sequence analysis

Introduction of promoters into *A. tumefaciens* was carried out by electroporation methods and selected by selection of antibiotics. The results of electroporation were performed by PCR test and obtained a band according to positive control. According to Apriyanto [15]. the CaMV35S :: uidA promoter PCR resulted in a base length of 675 bp fragment, while the MeEF1A6 :: uidA promoter produced a base length of 1311 bp fragment. The electrophoresis of AGL1 and LBA4404 PCR resulted containing CaMV35S promoters was showed band of about 675 bp fragment. These results are consistent with the positive control of the pBI121-CaMV35S plasmid. The electrophoresis of AGL1 and LBA4404 PCR resulted containing MeEF1A6 promoter was showed band about 1311 bp fragment. These results were also consistent with the positive control of the pBI121-MeEF1A6 plasmid (Figure 1). Therefore, it can be concluded that the plasmids pBI121-CaMV35S and pBI121-MeEF1A6 have been successfully introduced into *A. tumefaciens* strains AGL1 and LBA4404.

3.2. Qualitative Analysis of GUS activity with transien and stable transformation

The results of the introduction promoter with *A. tumefaciens* to tobacco plant (*N. tabacum*) was analyzed with histochemical GUS assay. The result from the histochemical GUS assay was showed a blue spot in the root, stems, and leaves in plants. The blue spot on the root was found in the transient transformation results using *A. tumefaciens* LBA4404 strain. The blue spot on leaves and stems was seen in the results of the transformation of the transient with both strains of *A. tumefaciens* (LBA4404 and AGL1) (Figure 2). Positive results were indicated by the blue spot in the explants. This was due to the association between MeEF1A6 and CaMV35S promoters with the *uidA* gene that expresses the β-glucuronidase enzyme. The *uidA* gene is located under the control of the MeEF1A6 promoter on the pBi121-MeEF1A6 plasmid and the CaMV35S promoter on the pBi121-CaMV35S plasmid. The expression of the *uidA* gene as a marker gene was controlled by the active promoters of MeEF1A6 and CaMV35S. The β-glucuronidase enzyme can hydrolyze the X-Gluc substrate which was

DOI: https://doi.org/10.5614/3bio.2021.3.1.1

previously a colorless compound to color (5.5'-dibromo-4,4'-dichloro-indigo) blue with the help of K3Fe (CN)6 and K4Fe (CN)6 [17].

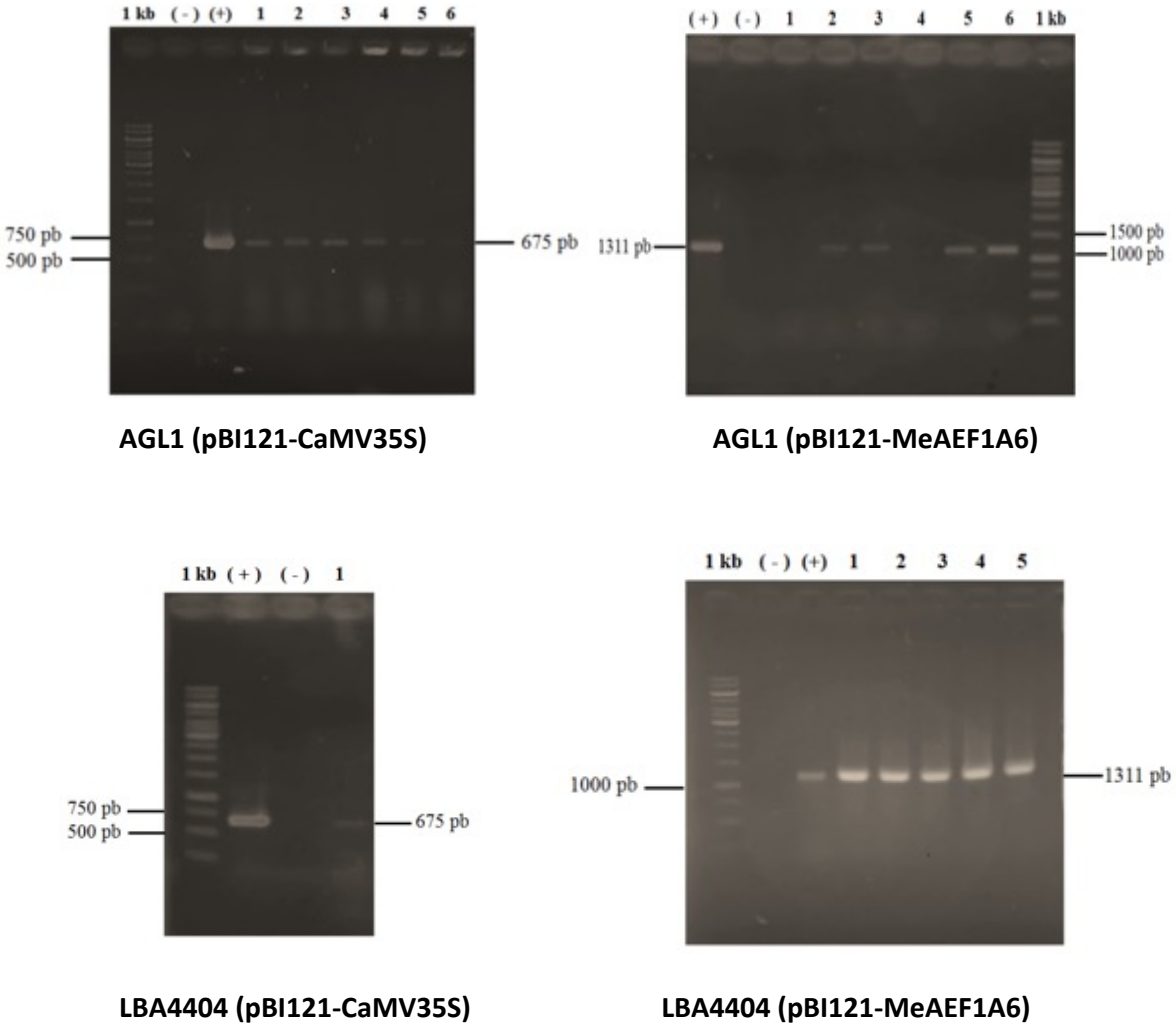

Figure 1. Confirmation PCR results of MeEF1A6 and CaMV35S promoter electroporation into *Agrobacterium tumefaciens* strain AGL1 and LBA4404. (+) shows positive control (plasmid containing promoter), (-) indicates negative control and number (1,2,3 etc) shows the number of samples tested

The transformation results using *A. tumefaciens* strain LBA4404 showed blue color on the roots, stems, and tobacco leaves. This is consistent with Apriyanto research [15] which shows that the MeEF1A6 promoter can work in all parts of tobacco sprouts. This proves that the MeEF1A6 promoter can activate the expression in roots, stems, and leaves. To see in more detail the specific work of the MeEF1A6 promoter, a cut on the trunk of the transient transformation results was made with LBA4404. Specimens of transient tobacco incision with MeEF1A6 promoter were compared with transient tobacco incision with CaMV35S promoter as positive control and wild-type tobacco incision as negative control (Figure 3).

The red circle shows a blue spot on the picture. The incision results show that the MeEF1A6 promoter can be expressed in the procambium tissue that lies between the xylem and phloem. This is different from the results of previous studies [18] which states that the color blue was found in the cortex, pith (not comprehensive), and xylem (a small part). In this study, blue also appeared in a small portion of the heartwood near procambium. The blue color in some of these tissues can prove that the MeEF1A6 promoter can work in tobacco plant tissue, although it is not comprehensive. The promoter MeEF1A6 and CaMV35S showed the same blue spot. This reinforces the notion that the MeEF1A6 promoter has the same constitutive nature as the CaMV35S promoter, which is a universal promoter in genetic engineering.

DOI: https://doi.org/10.5614/3bio.2021.3.1.1

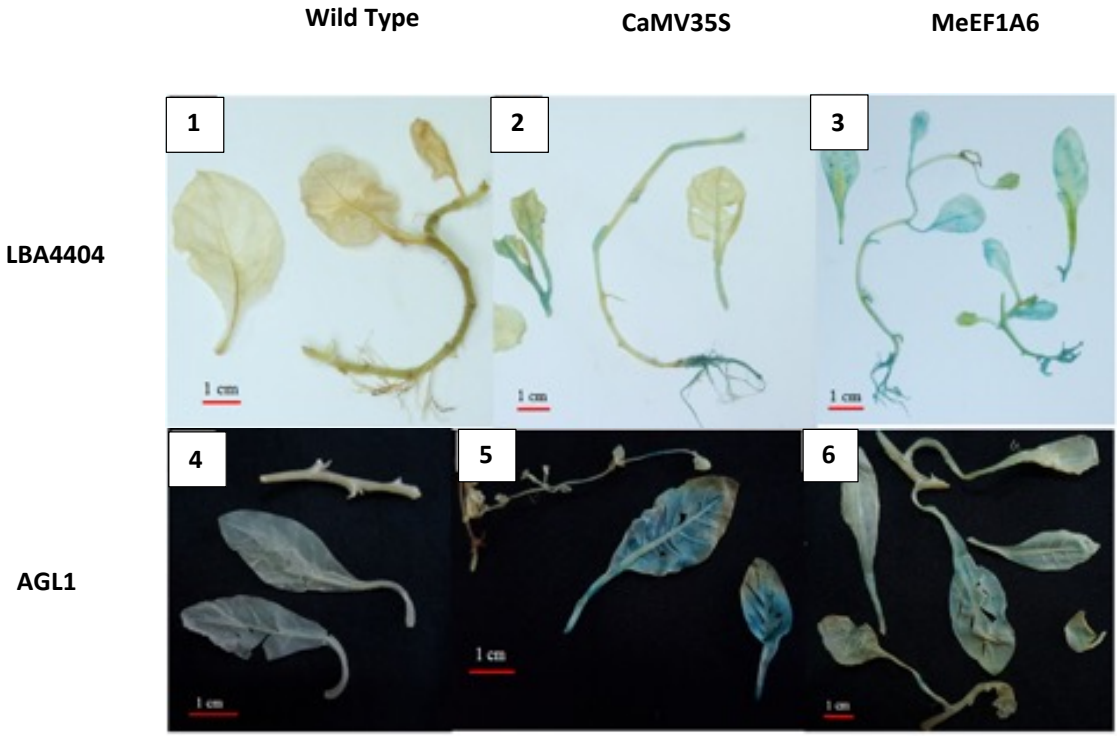

Figure 2. Transient transformation of tobacco plants (N.tabaccum) with A.tumefaciens strains AGL1 and LBA4404 which carry promoters MeEF1A6 and CaMV35S. (1-3) Showed transien transformation for LBA4404, (4-6) Showed transien transformation for AGL1.

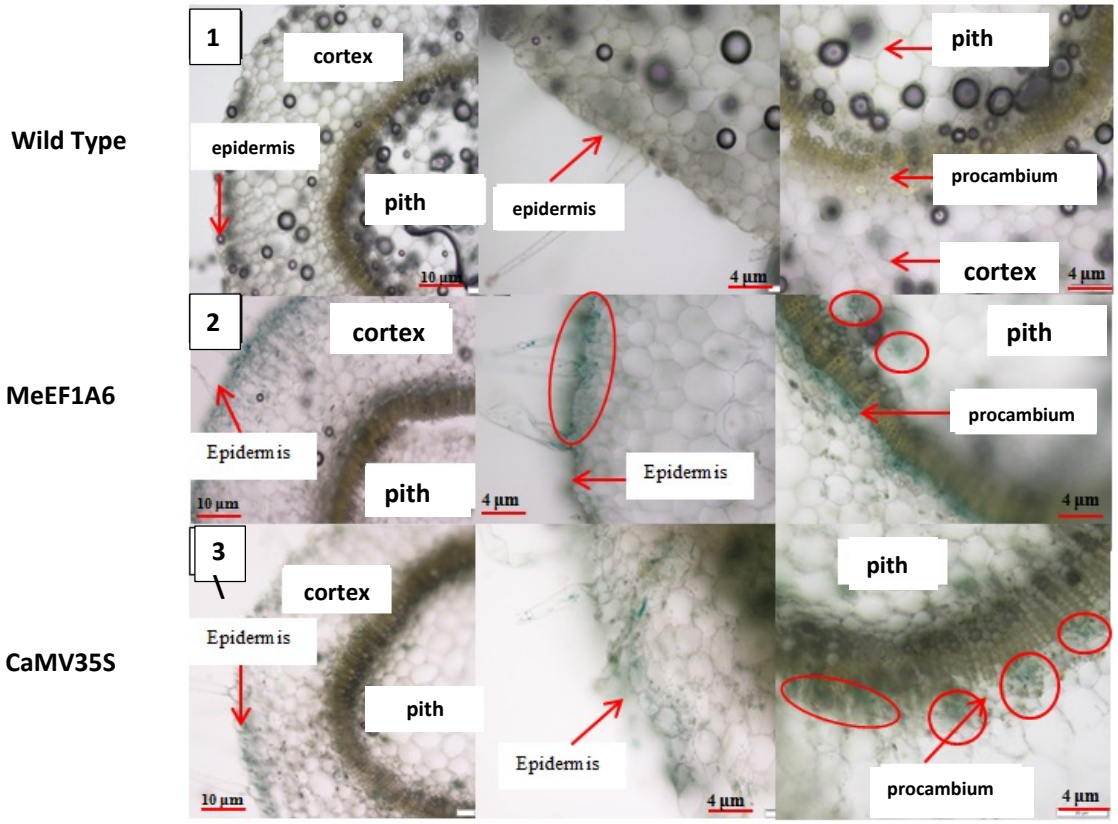

Figure 3. Cross-cutting incision of tobacco stem. (1) Wildtype tobacco, (2) LBA4404 transient transformation with pBI121-MeEF1A6,(3). LBA4404 transient transformation with pBI121-CaMV35S

DOI: https://doi.org/10.5614/3bio.2021.3.1.1

Stable transformation using Agrobacterium strain AGL1 was obtained in the shoots, which then a GUS histochemical test was performed. In the stable transformation process, cefotaxime antibiotics are used to kill *A. tumefaciens* and kanamycin antibiotics to select explants. Cefotaxime 100 ppm antibiotics have been known to kill *A. tumefaciens* [16] and 50 ppm kanamycin antibiotics have been known to reduce plant growth [18]-[20]. The results of stable transformation with *A. tumefaciens* strain AGL1 can be seen in Table 1.

The stable transformation results with Agrobacterium strain AGL1 (Table 1) resulted in 12 living explants for pBI121-CaMV35S and 27 living explants pBI121-MeEF1A6. Live expansions have been inserted into the target promoter but it was uncertain whether they have been integrated into plant DNA or not. Explants that had died were confirmed by looking at the yellowing of the explants that had not grown. The explants then performed a GUS histochemical test to see whether the promoters of MeEF1A6 and CaMV35S could work on stable transformation plants (Figure 4).

The blue color that appears indicates that the promoters CaMV35S and MeEF1A6 have successfully worked on tobacco plants that have been transformed. A study of Octacviana [18] showed that the blue color was very bright in almost all parts of the plant while in this study the blue color was only found in a few parts of the plant even though it included roots, stems, and leaves. To see more clearly whether the promoter is expressed in all types of plant tissue, a transverse incision is performed on the stem. The incision results can be seen in Figure 5.

Table 1. The result of stable transformation of Agrobacterium strain AGL1

Plants	Σ Leafs	Σ Leafs that had been grown by callus	Σ Shoots	Σ Explants	
				Dead	Live
pBI121-CaMV35S	60	45	20	8	12
pBI121-MeEF1A6	70	40	43	16	27

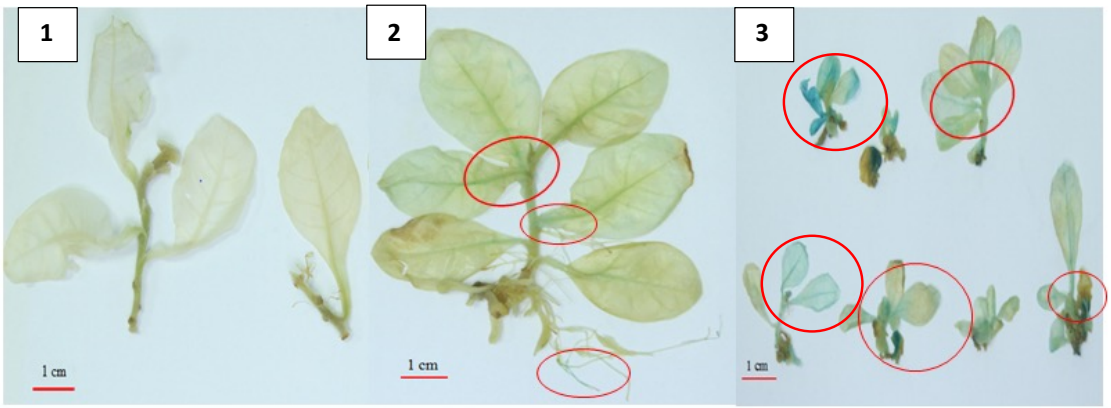

Figure 4. The result of stable transformation of Agrobacterium strain AGL1. (1) Tobacco wildtype, (2) pBI121-CaMV35S,(3) pBI121-MeEF1A6

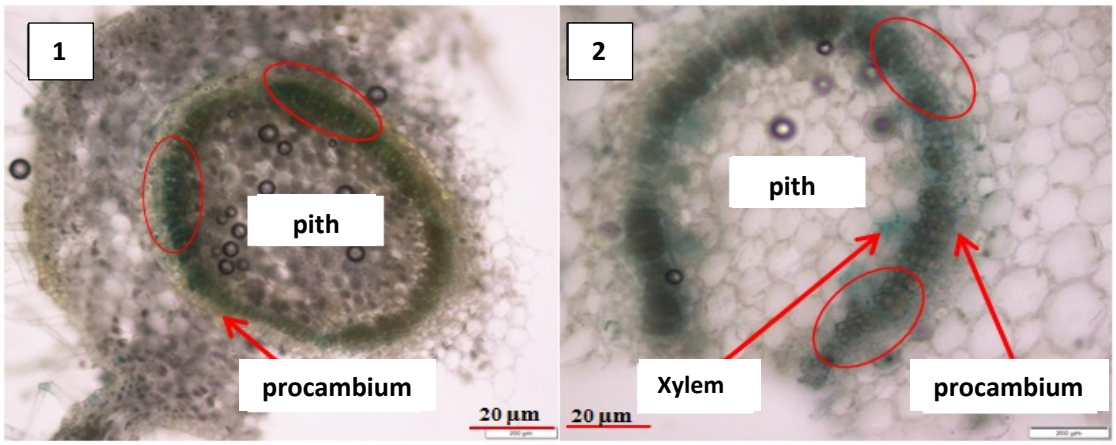

Figure 5. Transverse incision resulting from stable transformation with Agrobacterium strain AGL1; a. pBI121-CaMV35S; b. pBI121-MeEF1A6

DOI: https://doi.org/10.5614/3bio.2021.3.1.1

Figure 5 showing that the MeEF1A6 promoter can work in the procambium, xylem, and some pith tissue. This is consistent with the results of research before [18] who also stated that the MeEF1A6 promoter can work in the cortex, xylem, and pith network. In this study, the blue color did not spread evenly to the cortex. This also happened to the positive control (CaMV35S). This is possible because the results of the stable transformation are still not evenly distributed in all host cells or chimeras / chimeric. Chimera is a condition where individuals have different genomes in several cells, resulting in variations in expression/phenotypes in one individual [21]. So the MeEF1A6 promoter is only expressed in a few cells/tissues and cannot be maximally expressed in GMO tobacco plants.

4. Conclusion

Promoter MeEF1A6 can actively work on tobacco plants (*N. tabacum*), though not showing high activity. This study proved that the promoter MeEF1A6 could work in several tobacco plant tissues; procambium, epidermis, cortex, and pith. This adds to the suspicion that the MeEF1A6 promoter can work constitutively on tobacco plants of SR1 variety (*Nicotiana tabacum* cv SR1).

Acknowledgements

The authors thanked the Genetic research group of SITH ITB and PPSHB IPB for all supports and facilities that support this research. The authors also thanked Ian for helping during the research in the laboratory.

References

[1] Maston, G.A., Evans, S.K., dan Green, M. R: Transcriptional Regulatory Elements in the Human Genome. Genet [Internet]. 2006 Sep [cited 2020 Mar 18]:7:29-59. DOI: https://doi.org/10.1146/annurev.genom.7.080505.115623

[2] Peramuna A, Bae H, Rasmussen E.K, Dueholm B, Waibel T, Critchley J.H, Berzezek K, Roberts M, Simonsen H.T: Evaluation of synthetic promoters in Phycomitrella patens. Biochemical and Biophysical Reserch Communications [Internet]. 2018 Jun [cited 2020 Mar 17] :500: 418-422. DOI: https://doi.org/10.1016/j.bbrc.2018.04.092

[3] Alberts, B., Johnson, A., Lewis, J., Raff, M., Roberts, K., dan Walter, P.: Molecular Biology of The Cell. 5th edition. Garland science [Internet]. 2008 Jul [cited 2020 Mar 18]. DOI: https://doi.org/10.1002/bmb.20192

[4] Merrick, W. C. dan Nyborg, J: The Protein Biosynthesis Elongation Cycle, Translational control of gene expression, edited Nahum Sonenberg, Jhon W. B. Hersey. Michael B. Mathews, Cold Spring Harbor Laboratory Press [Internet]. 2000 [cited 2020 Mar 17] : 39: 89-125. Available from : https://www.forskningsdatabasen.dk/en/catalog/2440359660

[5] Ejiri S : Moonlighting functions of polypeptide elongation factor 1: from action bundling to zine finger protein R1-associated nuclear localization. Biosci. Biotechnol. Biochem [Internet]. 2014 May [cited 2020 Mar 17]: 66: 1-21. DOI: https://doi.org/10.1271/bbb.66.1

[6] Yang F, Demma M, Warren V, Dharmawardhane S, Condeelis J : Identification of an actin-binding protein from Dictyostelium as elongation factor 1a. Nature [Internet]. 1990 Oct [cited 2020 Mar 17]:347: 494–496. DOI: https://doi.org/10.1038/347494a0

[7] Sasikumar, A. N., Perez, W. B., dan Kinzy, T. G: The many roles of the eukaryotic elongation factor 1 complex, WIREs RNA [Internet]. 2012 May [cited 2020 Mar 17]:3:543-55. DOI: https://doi.org/10.1002/wrna.1118

[8] Kaur KJ, Ruben L: Protein translation elongation factor-1 alphafrom Trypanosoma brucei binds calmodulin. J Biol Chem [Internet]. 1994 Sept [cited 2020 Mar 17]:269: 23045–23050. Available from : https://www.jbc.org/content/269/37/23045.full.pdf

[9] Duttaroy, A., Bourbeau, D., Wang, X. L.,dan Wang, E : Apoptosis rate can be accelerated or decelerated by overexpression or reduction of the level of elongation factor-1 alpha, Exp. Cell Res [Internet]. 1998 Jan [cited 2020 Mar 17] :238:168–176. DOI: https://doi.org/10.1006/excr.1997.3819

[10] Yamaji Y, Sakurai K, Hamada K, Komatsu K, Ozeki J, et al : Significance of eukaryotic translation elongation factor 1A in tobacco mosaic virus infection. Archives of Virology [Internet]. 2009 Des [cited 2020 Mar 18]:155: 263–268. DOI: https://doi.org/10.1007/s00705-009-0571-x

[11] Toueille M, Saint-Jean B, Castroviejo M, Benedetto JP : The elongation factor 1a: a novel regulator in the DNA replication/repair protein network in wheat cells?. Plant Physiol Biochem [Internet]. 2007 Feb [cited 2020 Mar 17]: 45: 113–118. DOI: https://doi.org/10.1016/j.plaphy.2007.01.006

[12] Suhandono S, Hughes J, Brown K, Hughes M.A : Expression and structure of an elongation factor-1α gene (MeEF1) from cassava (Manihot esculenta Crants). Euphytica [Internet]. 2001 Jun [cited Mar 2020 17]:120: 49-58. DOI: https://doi.org/10.1023/a:1017543318423

[13] Suhandono S, Apriyanto A, Ihsani N : Isolation and Characterization of Three Cassava Elongation Factor 1 Alpha (MeEF1A) Promoters. PloS ONE [Internet].

DOI: https://doi.org/10.5614/3bio.2021.3.1.1

2014 Jan [cited 2020 Mar 17] :9(1), e84692. DOI: https://doi.org/10.1371/journal.pone.0084692.

[14] Debler J W. : Making electrocompeten agrobacterium tumefaciens [Internet]. 2019 Available from https://dx.doi.org/10.17504/protocols.io.xyqfpvw. [Accessed: 2019-12-01]

[15] Apriyanto, A. Isolation and Characterization of Eukaryotic Elongation Factor 1 Alpha (EF1a) Gene Promoters from Cassava (Manihot esculenta Crantz.) [thesis]. Bandung: Bandung Insititute of technology. 2012.

[16] Fajri Hayatul. Genetic engineering of Nicotiana tabacum cv. SR1 with the Gα gene cDNA [thesis]. Bogor: Bogor Agricultural University. 2015.

[17] Jefferson, R. A., Kavanagh, T.A., dan Bevan, M.W.: GUS fusions: ,B-glucuronidase as a sensitive and versatile gene fusion marker in higher plants, The EMBO journal [Internet].1987 Dec [cited 2020 Mar 17]: 6: 3901-3907. PMCID: PMC553867. PMID: 3327686

[18] Oktaviani Indah. MeEF1A6 promoter activity in Nicotiana tabacum L. Putative transgenic [thesis]. Bandung: Bandung Insititute of technology. 2016

[19] Verdaguer, B., Kochko, A., Beachy, R. N., dan Fauquet, C. : Isolation and expression in transgenic tobacco and rice plants, of the cassava vein mosaic virus (CVMV) promoter, Plant Molecular Biology [Internet]. 1996 Sept [cited 2020 Mar 17]:31: 1129-1139. DOI: https://doi.org/10.1007/BF00040830

[20] Delporte, A., Holle, S. V, dan Van Damme, E. J. M. : Qualitative and quantitative analysis of the Nictaba promoter activity during development in Nicotiana tabacum, Plant Physiology and Biochemistry [Internet]. 2013 Jun [cited 2020 Mar 18]: 67: 162-168. DOI: https://doi.org/10.1016/j.plaphy.2013.03.005

[21] Prina A.R, Landau A.M, Pacheco M.G. Chimeras and mutant gene transmission. In book Plant Mutation Breeding and Biotechnology, Edition: 2012, Chapter: Chapter 15. FAO/IAEA, Editors: Shu Q.Y., pp.179-187. 2012. Available from : https://www.researchgate.net/publication/262068626_Chimeras_and_Mutant_Gene_Transmission

DOI: https://doi.org/10.5614/3bio.2021.3.1.1

e-ISSN: 2655-8777 http://journals.itb.ac.id/index.php/3bio

Selection of Indonesian Medicinal Plant Active Compounds as Inhibitor Candidates of Oncoproteins E6 and E7 Human Papillomavirus Type 16 by Molecular Docking

Riyanti Weni Syavitri*, Azzania Fibriani, Reza Aditama

School of Life Sciences and Technology, Bandung Institute of Technology, Indonesia.

Corresponding author; e-mail: riyanti106@students.itb.ac.id
Received 7 March, 2021
Accepted for publication 22 April, 2021

Abstract

Cervical cancer cases caused by infection with Human Papillomavirus (HPV), especially HPV 16 (60.5% of cases) continue to increase every year with a high mortality rate. The current anti-cancer drugs were not only specifically targeting cancer cells, but healthy cells and can cause serious side effects. Therefore, it is necessary to find safer alternative therapies, e.g., using active compounds from natural products. The purpose of this study was to find the active compounds of Indonesian medicinal plants potentially as an inhibitor of oncoprotein E6 and E7 HPV 16, the main protein causing cervical cancer by in silico method. In this study, 711 active compounds from 187 medicinal plant species were selected based on molecular weight, solubility, gastrointestinal absorption index, and drug-likeness. Compounds that meet the criteria were tested for their affinity and interaction profile with E6 and E7 proteins through the molecular docking method. The results of this study showed 164 compounds that met the criteria. The molecular docking analysis showed nine of the most potent compounds as E6 inhibitors on the E6AP binding site and six compounds on the p53 binding site. Besides that, there were eleven most potent compounds as E7 inhibitors. The results of this study indicate that there are natural compounds that can inhibit E6 and E7 proteins and have further potential to be used as anti-HPV drugs. However, further research is needed to test these compounds in vitro and in vivo.

Keywords: cervical cancer, E6 HPV16, E7 HPV16, inhibitor, molecular docking

1. Introduction

Cervical cancer is the second most common type of cancer in Indonesia. Based on data from WHO, there were 36,633 new cases in 2020, while the death rate from cervical cancer in the same year reached 21,003 deaths [1]. The main cause of cervical cancer is the High-Risk Human Papillomavirus (HPV) infection, identified in over 99,7% of cervical cancers [2]. HPV 16 is the most prevalent type which is detected in 60.5% of cases [3]. Although effective prophylactic HPV vaccines are readily available commercially such as Merck's Gardasil (quadrivalent vaccine) and GlaxoSmithKline's Cervarix (bivalent vaccine), the high cost of vaccination is a major barrier. Besides, this vaccine is only effective if it is given to uninfected individuals [4]. Therefore, an effective and affordable therapeutic approach is urgently needed.

The ideal anticancer drugs are those that are specific and cytotoxic only in cancer cells [5]. In cervical cancer, there are two main oncoproteins in HPV (i.e., E6 and E7), which are only expressed in infected cells that could be potential therapeutic targets. Both proteins cause cell immortalization and are continuously expressed during cancer development [6].

E6 is an 18 kD protein consist of approximately 150 amino acids [7]. The main target of E6 is tumor suppressor protein p53. E6 HPV 16 causes ubiquitination and degradation of p53 in two ways. First by binding directly to p53 (E6AP independent) or second by forming the E6 / E6AP / p53 complex (E6AP dependent). The degradation of p53 causes the uncontrolled proliferation of cells that are resistant to apoptosis [8]

E7 is the first oncoprotein discovered. This protein is relatively small, about 100 amino acids, divided into three conserved regions: CR1, CR2, and CR3 [8]. Half of the

DOI: https://doi.org/10.5614/3bio.2021.3.1.2

N-terminal E7 terminals (amino acids 1-40) constituting the CR1 and CR2 regions are naturally unfolded (distinctly disordered) and are flexible with few conformational transitions [9]. Meanwhile, CR3 E7 HPV plays a role in the dimerization of E7 and becomes a medium for direct interaction with several proteins. In particular, CR3 interacts with the C-terminal portion of pRb. E7 full-length protein is 100 times more potential to bind pRb than E7 which only contains CR1 / CR2, this indicates an important role for CR3 in interactions with pRb [10]. E7 binds to pRb then causes ubiquitination of pRb so that E2F is released from pRb and becomes active. E2F is a transcription factor of genes that cells need to enter the synthesis phase in the cell cycle. The synthesis phase prompts the cell to activate DNA replication and initiates the process of self-division [8]. The combination action of E6 and E7 in cervical cells leads to cell transformation and cancer development. Hijacking E6 and E7 binding to cellular protein targets by an inhibitor could have an impact on their oncogenic activity [11].

Various types of therapies that target these two proteins have been developed, e.g., therapeutic vaccines targeting HPV 16/18 E6 / E7 for the treatment of advanced cervical cancer, genome editing using antisense oligonucleotides, ribozymes, DNAzymes, siRNA (small interfering RNA), shRNA (short-hairpin RNA), immunotherapy with synthetic E6 / E7 HPV16 / 18 DNA sequences, and tumor-infiltrating T cells (reviewed by Pal and Kundu [8]). Therapy with the E6 / E7 target gives promising results, but the high cost will be an obstacle to its application. Hence, discovering effective and more affordable alternatives becomes crucial.

The use of natural products promises a comparatively safer alternative therapeutic approach to cervical cancer. This therapy also offers less complicated treatments using abundantly available and inexpensive medicine compared to genome editing technologies or immunotherapeutic methods [8]. Natural compounds, such as plant extracts in either pure form or standardized extracts, provide unlimited opportunities for new drug discovery due to the unrivaled availability of chemical diversity [12]. The chemical diversity of natural compounds can be an excellent source of novel scaffolds. These chemical scaffolds are optimized further to get the new drug candidates.

Indonesia is a country with extraordinary high biodiversity. Indonesia's tropical rainforests, covering an area of approximately 143 million hectares, are home to about 80% of the world's medicinal plants [13]. Active compounds from Indonesian medicinal plants could be potential E6 and E7 inhibitors. A computational experiment or *in silico* method is conducted as a shortcut to seeking this great potential by creating computational models or simulations that can be used to make predictions, suggest hypotheses [14]. This method is more effective and efficient for screening new drugs for pre-eliminary research, the range of compounds being tested can be wider with a shorter time and lower cost. In this study, we explored Indonesian medicinal plants active compounds potency an oncoprotein E6 and E7 HPV 16 inhibitors by molecular docking.

2. Material and Methods

2.1. Hardware

DELL laptop with a specification of processor processor Intel® Core™ i5-7200U CPU @ 2,5 GHz RAM 8GB and 64-bit *Windows* 10 *operating system* was used in this research.

2.2. Software

Bioinformatics programs used included Marvin Sketch (ChemAxon, Budapest, Hungary), Modeller 9.16 (University of California San Francisco, USA), BIOVIA Discovery Studio Visualizer 2020 (Dassault Systèmes, San Diego), Autodock Tools1.5.6 (The Scripps Research Institute, USA), Autodock Vina (TheScripps Research Institute USA) [15], LigPlot+ 2.2 (EMBL-EBI, UK) [16], and Chimera 1.14 to visualize the ligand position on the protein [17].

2.3. Protein preparation

E6 HPV 16 3D structure (chain F) was separated from E6/E6AP/p53 complex crystal structure retrieved from Protein Data Bank (PDB), ID 4XR8, and a resolution of 2,25 Å. Visualization and separation were processed by BIOVIA Discovery Studio Visualizer 2020. Polar hydrogen atoms were added to the structure and convert to *.pdbqt format by Autodock Tools 1.5.6.

E7 protein used in this research was only the CR3 domain. E7 HPV 16 sequence was harvested from the Uniprot server. The template used for modeling the 3D structure was ID2B9D (PDB id), a crystal structure of E7-CR3 domain of HPV 1A dimer with 37% identity to E7-CR3 domain of HPV 16. E7-CR3 domain of HPV 16 3D dimer structure was built by MODELLER 9.25. YASARA Energy Minimization server was used for protein model structural refinement and energy minimization [18]. The refined structure then confirmed for reliability by ProSA-Web [19] and plot to The Ramachandran plot (Zhiping weng's laboratory, USA) [20].

2.4. Ligand preparation

There were 711 active compounds of 187 Indonesian medicinal plant species that were collected and filtered by molecular weight, solubility, GI absorption, and drug-likeness by Lipinski's Rules of Five. The selection was carried out by submitting the 2D structure of the active compound to SwissADME webserver [21]. Compounds that have MW of more than 200 g/mol, moderate to high

DOI: https://doi.org/10.5614/3bio.2021.3.1.2

solubility, high GI absorption, and fulfill drug-likeness criteria were selected and prepared for docking. The 3D conformations were drawn on Marvin Sketch by employing the dreiding force field as minimization energy.

2.5. Binding Site Identification

Identification of residues involved in E6-E6AP and E6-p53 interaction was based on E6/E6AP/p53 crystal structure complex resolved by Martinez-Zapien et al. [22] which also determined hot spot residues by mutational study and binding assay. CR3 E7 HPV 1A interaction with pRb was identified by Liu et al. [10]. Residues involved in CR3 E7 HPV 16-pRb interaction determined by amino acid sequence alignment between CR3 E7 HPV 16 and CR3 E7 HPV 1A. Pocket searching in the binding site areas of E6-E6AP, E6-p53, and CR3 E7 HPV 16-pRb were performed by fpocket webserver [23]. Those pockets were then used for the docking study.

2.6. Molecular Docking Simulation

Molecular docking was executed by Autodock Vina, a fast and accurate docking tool [15]. Grid box parameters were set in specific searching area to encompass binding site for effective docking simulation (Table 1). The docking results were visualized by LigPlot+ 2.2 in 2D and Chimera 1.14 in 3D molecular structures.

Table 1. Grid Box Parameters

No	Receptor	Protein Binding Patner (Binding Site)	Grid Center Coordinate			Grid Box Size (Å)		
			x	y	z	x	y	z
1.	E6	E6AP	-52,065	-7,059	-12,871	20	20	20
2.	E6	p53	-61,861	1,947	-17,234	20	20	20
3.	CR3 E7	pRb	22,31	24,86	50,682	20	20	20

3. Results and discussion

The major roles of E6 and E7 oncoprotein in cervical carcinogenesis make these proteins a potential target for cervical cancer therapy [24]. Blocking both protein interactions with its cellular protein targets will be expected to have a significant impact to suppress cancer development and lead to senescence. This research aims to find Indonesian medicinal plants' active compounds that have good potency to inhibit the interaction of oncoprotein E6 to E6AP, E6 to p53, and oncoprotein E7 to pRb. In this research, the inhibition potency of the active compounds was evaluated by molecular docking to E6 and E7.

3.1. Active compounds selection

Active compounds were filtered by molecular weight, solubility, GI absorption, and drug-likeness (Lipinski's rules of five). Low molecular weight compounds bound weakly to protein [25], so only compounds that have a molecular weight above 200 g/mol used in this study. Compound solubility in water is important for drug formulation to achieve the desired concentration of drug in systemic circulation for desired pharmacological response [26]. The GI absorption parameter was observed in this study because this parameter is related to the absorption rate of the compound in the intestine and its bioavailability. High GI absorption is very important for oral drug candidates. The oral route is the most common and preferred way of administration over other routes because of its many advantages. These advantages include safety, ease of administration, high patient compliance, painlessness, cost-effectiveness, and flexibility in dosage form design [27]. The Lipinski's rule of five helps to distinguish a drug-like compound from a non-drug based on five rules: molecular mass < 500 Da, lipophilicity (LogP < 5), hydrogen bond donors < 5, hydrogen bond acceptors < 10, molar refractivity should be within 40 to 130.28 [28]. Active compounds selection results in 164 compounds that meet the criteria.

3.2. Binding Affinity and Molecular Interaction Profile

E6 oncoprotein was docked in two binding sites: E6-E6AP interface and E6-p53 interface. Residues involved in E6-E6AP interaction are R10, K11, V31, Y32, L50, C51, V53, R55, V62, L67, Y70, S74, R77, H78, L100, R102, Q107, R129, and R131. L50, R102, and R131 are considered hot spot residues because of their high contribution for E6AP binding, mutation of these residues leads to binding perturbation, prevents p53 degradation, and disrupts the oncogenic activity of E6 [29].

Docking results of active compounds to E6 in E6AP interface are shown in Table 2. Table 2 shows active compounds with the best docking score to E6 at E6AP binding site and a standard anticancer drug (i.e., jaceosidin) as a positive control. Jaceosidin is a flavonoid from

DOI: https://doi.org/10.5614/3bio.2021.3.1.2

Artemisia princeps which experimentally through the ELISA method has the potential as an inhibitor of oncoproteins E6 and E7. In vitro testing on SiHa and CaSki cell lines containing the HPV 16 genome shows jaceosidin inhibits cancer formation [30]. Nine compounds, i.e., elephantin, roemerine, ginkgolide A, phaseollin, anonaine, chitranone, elephantopin, tetrahydroalstonine and vindolinine have significantly lower docking score (-8,3 to -8,7 kcal/mol) than positive control (-7,2 kcal/mol). The lower docking score or binding affinity indicate the more stable and favorable the interaction. The nine compounds have better affinity to E6 than jaceosidin because they have more hydrophobic interactions. Figure 2.a shows that the elephantin interact with nine hydrophobic residues of E6 (Y32, L50, V53, V62, L67, Y70, S71, S74, R102) or 47,37% compared to total 19 residues involved in E6-E6AP protein-protein interaction. While jaceosidin has only three hydrophobic interactions (L50, Q107, R131) or 31,58% (Figure 1.a). Elephantin atomic groups are mostly in the hydrophobic E6 protein residue (dark orange color), shown in Figure 2.b. Hydrophobic interaction can increase the affinity in the protein-ligand complex. The addition of the number of hydrophobic atoms at the active site of the target and drug interface affects the biological activity of the drug candidate. The increase in binding affinity to the target complex and the drug that results from the optimization of hydrophobic interactions shows better drug efficacy [31]

Table 2. Docking Results of Indonesian Medicinal Plant Active Compounds against Oncoprotein E6 on the Binding Site of E6AP

Active Compound	Plant Spesies	Docking Score/Binding Affinity (kcal/mol)	Hydrogen Bonds	Hydrophobic Interaction	Total Interaction
Jaceosidin (positive control)	*Artemisia princeps* (Mugwort Korea)	-7.2	L100, W132, **R102**, C51	**L50**, Q107, R131	31.58%
Elephantin	*Elephantopus scaber* (tapak liman)	-8,7	C51, Q107, **R131**	Y32, **L50**, V53, V62, L67, Y70, S71, S74, **R102**	47.37%
Roemerine	*Nelumbo nucifera* (teratai)	-8,7	-	V31, Y32, F45, **L50**, C51, V53, V62, Y70, S71, Q107, **R102**	47.37%
Ginkgolide A	*Ginkgo biloba* (ginkgo biloba)	-8,6	-	Y32, **L50**, C51, L67, Y70, S71, S74, Q107, **R131**	42.10%
Phaseollin	*Erythrina fusca* (cangkring)	-8,6	-	V31, Y32, F45, **L50**, C51, V53, A61, V62, L67, Q107, **R102, R131**	52.63%
Anonaine	*Annona squamosa* (srikaya)	-8,5	-	V31, Y32, **L50**, C51, V53, V62, L67, S71, **R102**, Q107	47.37%
Chitranone	*Plumbago zeylanica* (daun encok)	-8,4	C51, **R102**	**L50**, V62, L67, L100, Q107, **R 131**	42.10%
Elephantopin	*Elephantopus scaber* (tapak liman)	-8,4	C51, **R131**	Y32, **L50**, V53, V62, L67, Y70, S71, S74, Q107	52.63%
Tetrahydroalstonine	*Catharanthus roseus* (tapak dara)	-8,3	**R102**	V31, Y32, F45, **L50**, C51, V53, A61, V62, L67, S71, S74, Q107, **R131**	57.89%
Vindolinine	*Catharanthus roseus* (tapak dara)	-8,3	Q107	Y32, F45, **L50**, C51, V62, L67, Y70, S71	31.57%

DOI: https://doi.org/10.5614/3bio.2021.3.1.2

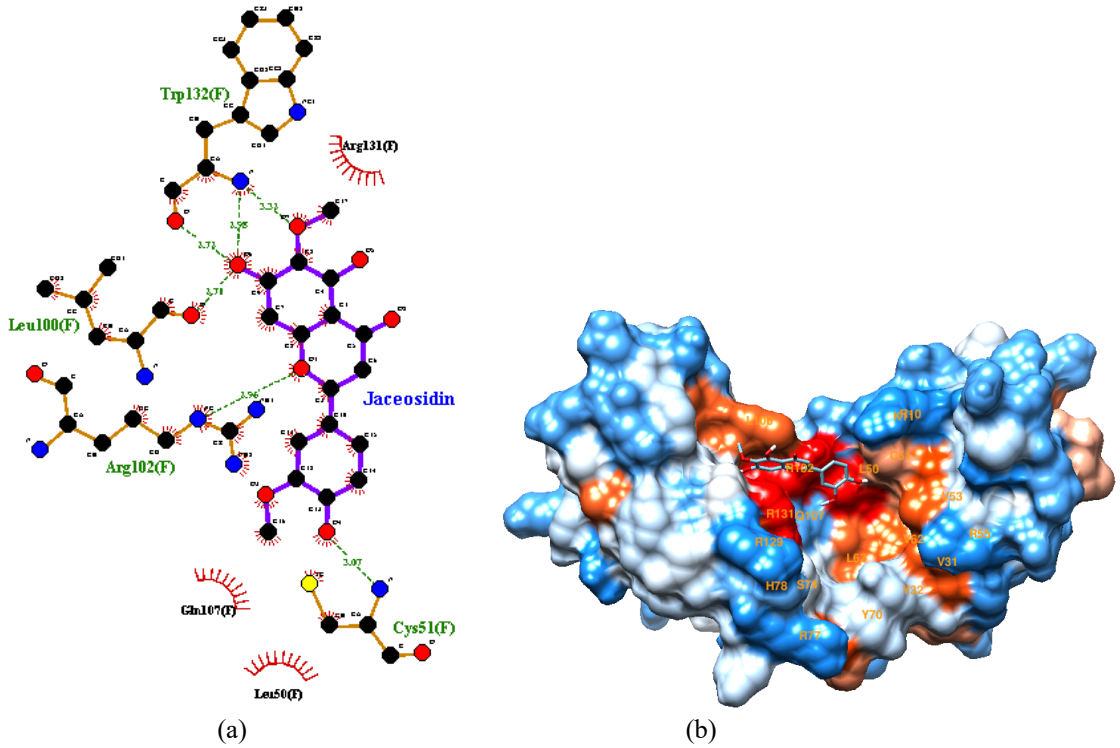

Figure 1. 2D visualization (a) and 3D visualization (b) of jaceosidin-E6 interaction on E6AP binding site.

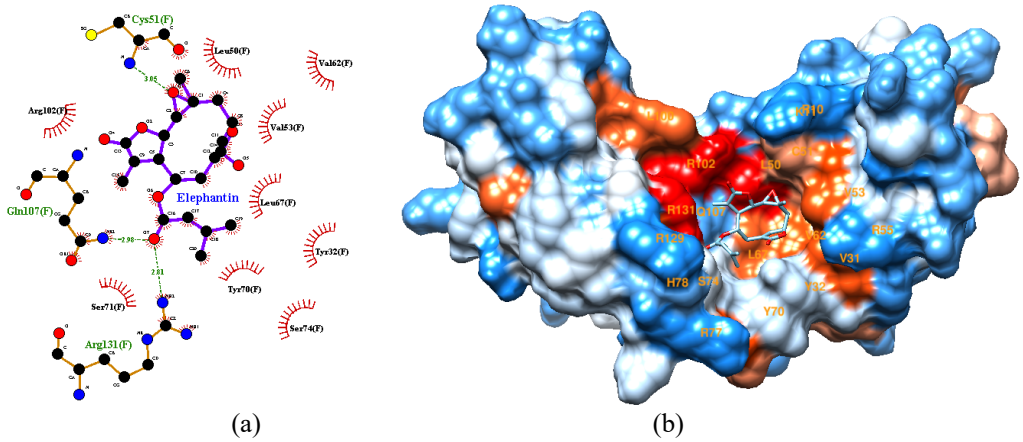

Figure 2. 2D visualization (a) and 3D visualization (b) of elephantin-E6 interaction on E6AP binding site.

Having three hydrogen bonds, elephantin has better specificity among the nine compounds. Hydrogen bonding is a fundamental interaction in protein-ligand complexes and is the main reason for the selectivity of ligand proteins, due to its specific nature, short spacing, and directionality [32-33]. Docking programs generally model hydrogen bond interactions better than hydrophobic interactions. This relates to the need for specificity in drug design [33].

The compound's interaction with hot spot protein residues also affects its potential as inhibitor. Hot spot residues are crucial residues for protein-protein interactions, so that intervention in these residues has an impact on their binding. L50, R102, and R131 are hot spot residues in E6-E6AP interaction. Elephantin, phaseolin, chitranone, and tetrahydroalstonine have interactions with all these residues via hydrogen bonding and/or hydrophobic interaction so that these compounds could have better potency as E6 inhibitors.

Molecular docking was also executed on p53 binding site, to simulate inhibition of E6-p53 direct interaction by active compounds. Molecular interaction profile of best docking

DOI: https://doi.org/10.5614/3bio.2021.3.1.2

score compounds shown in Table 3. D44, F47, and D49 were known to be E6 hot spot residues in E6-p53 interaction base on research conduct by Martinez-Zapien et al. [22]. E6 also interacts with p53 via I23, H24, and Y43. All these six residues lay on the center of E6-p53 interaction. Table 2 exhibits six compounds that are chitranone, sesamin, 16-acetylgitoxigenin, tetrahydroalstonine, methylophiogonone A, and phaseollin have a significantly better binding affinity (-6,9 kcal/mol to -7,3 kcal/mol) to E6 on p53 binding site than the positive control. Chitranone, sesamin, and 16-Acetylgitoxigenin have lower docking scores despite their fewer interactions that control positive, probably because of the better fitness compound to E6 surface interaction or shorter inter-atomic surface distance between compounds and protein. Surface distance is one of the parameters calculated in Autodock Vina scoring function. Binding affinity and hydrophobic interaction of the six best compounds do not differ significantly, but tetrahydroalstonine, methylophiogonone A, and phaseolline show better specificity by having more hydrogen bonds.

E7 key role in cancer initiation work in concert with E6. Blocking both protein interaction with cellular protein is important to completely suppress their oncogenic activities. The CR3 E7 residues that interact with pRb are R66, L67, I76, R77, E80, D81, M84. Based on the mutational study conducted by Liu et al. [10], a single mutation in the R66 residue and a mutation in the E80 / D81 residue had a significant effect in inhibiting the interaction of E7 with pRb. Therefore R66, E80, D81 are defined as hot spot residues. Molecular docking performed to CR3 E7 HPV16 results 11 best compounds shown in Table 4.

Table 3. Docking Results of Indonesian Medicinal Plant Active Compounds against Oncoprotein E6 on the Binding Site of p53

Active Compound	Plant Spesies	Docking Score/Binding Affinity (kcal/mol)	Hydrogen Bonds	Hydrophobic Interaction	Total Interaction
Jaceosidin (positive control)	*Artemisia princeps* (Mugwort Korea)	-6,1	**D44**, R48, C106, S111	L108, E114, M137, S138	16,67%
Chitranone	*Plumbago zeylanica* (daun encok)	-7,3	K108	Y43, **F47**, S111, E114, M137	33,33%
Sesamin	*Piper retrofractum* (cabe jawa)	-7,1	R48	Y43, **D44, F47**, S138	50%
16-Acetylgitoxigenin	*Nerium indicum* (jure)	-7,0	R48	R40, Y43, **D44, F47**, C106, K108	50%
Tetrahydroalstonine	*Catharanthus roseus* (tapak dara)	-7,0	S138, R48, **D44**	R40, Y43, **F47**, C106, K108	50%
Methylophiogonone A	*Ophiopogon japonicus* (ophiopogon)	-6,9	R48, K108, S138	**D44, F47**, C106, S111, E144, M137	33,33%
Phaseollin	*Erythrina fusca* (cangkring)	-6,9	E114, M137, S138	Y43, **D44, F47**, K108, C136	50%

DOI: https://doi.org/10.5614/3bio.2021.3.1.2

Table 4. Docking Results of Indonesian Medicinal Plant Active Compounds against Oncoprotein E7 on the Binding Site of pRb

Active Compound	Plant Spesies	Docking Score/Binding Affinity (kcal/mol)	Hydrogen Bonds	Hydrophobic Interaction	Total Interaction
Jaceosidin (positive control)	*Artemisia princeps* (Mugwort Korea)	-5,8	Q70, **D81**	**R66**, V74, T78, L82, L87, T86, G88	28,57%
Columbin	*Tinospora crispa* (brotowali)	-6,9	**R66**	N53, V55, Q70, T78, **D81**, L82, T86, G88	28,57%
Methylophiogonone A	*Ophiopogon japonicus* (ophiopogon)	-6,9	**D81**	N53, V55, **R66**, T64, Q70, V74, R77, T78, L82, T86, G88	42,86%
Serpentine	*Rauvolfia serpetina* (pule pandak)	-6,8	-	N53, V55, **R66**, V74, R77, T78, **D81**, L82, T86, L87, G88	42,86%
Uzarigenin	*Nerium indicum* (jure)	-6,8	N53	**R66**, V74, T78, **D81**, L82, T86, L87, G88	28,57%
Apigenin	*Apium graveolens* (seledri)	-6,6	N53, **D81**	V55, T64, L65, **R66**, T78, L82, T86, G88	28,57%
Coumestrol	*Taraxacum officinale* (jombang)	-6,6	N53	V55, T64, **R66**, T78, L82, T86, L87, G88	14,29%
Kaempherol	*Garcinia latissima* (dolo magota)	-6,6	N53, T64, **D81**	V55, L65, **R66**, T78, L82, T86, G88	28,57%
Phaseollin	*Erythrina fusca* (cangkring)	-6,6	N53	V55, **R66**, T78, **D81**, L82, L87, G88	28,57%
Pelargonidin	*Phaseolus vulgaris* (buncis), *Impatiens balsamina* (pacar air)	-6,5	N53, T64, **D81**	V55, L65, **R66**, T78, L82, T86, G88	28,57%
Rhamnocitrin	*Alpinia galanga* (lengkuas)	-6,5	N53	V55, T64, L65, R66, T78, D81, L82, T86, G88	28,57%
Sesamin	*Piper retrofractum* (cabe jawa)	-6,5	-	R66, V74, R77, T78, D81, L82, T86, G88	42,86%

Table 4 shows the 11 compounds with the best docking scores (-6.5 to -6.9 kcal/mol). This score was significantly better than the positive control docking score. Kaempherol and pelargonidin have relatively better specificity compared to positive control and other compounds because of their hydrogen bonds. All compounds have interactions with hot spot residues either through hydrogen bonds or hydrophobic interactions, so that they have good potency as E7 inhibitors. The total interactions that occurred between the compounds ranged from 28.57% to 42.86%, except for coumestrol which was slightly smaller, namely 14.29%. Based on the results in Table 4, it is concluded that the compounds columbin, methylopiogonone A, serpentine, uzarigenin, apigenin, coumestrol, kaempherol, phaseollin, pelargonidin, rhamnocitrin, and sesamin are potential inhibitors of E7.

Among the compounds that have the potential to act as inhibitors of E6-E6AP, E6-p53, and E7-pRb, phaseollin can be potential inhibitors of the three interactions. Meanwhile, compounds that have the potential to act as inhibitors of E6-E6AP and E6-p53 are chitranone and tetrahydroalstonine.

DOI: https://doi.org/10.5614/3bio.2021.3.1.2

Sesamin and methylophiogonone A have the potential to inhibit E6-p53 and E7-pRb interactions. Further research is needed to determine the potential of the best compounds obtained in this study in vitro and in vivo.

4. Conclusion

The diversity of Indonesian medicinal plants provides as abundant active compounds source for anti-cancer drug discovery. Cervical cancer caused by HPV 16 infections, develop as impact of continuous expression of E6 and E7 oncoproteins in infected cells. In this study, we explored Indonesian medicinal plants active compounds potency an oncoprotein E6 and E7 HPV 16 inhibitors by molecular docking. By observing the docking score, hydrogen bonding, hydrophobic interactions, and interactions of compounds with E6/E7 hot spot protein residues, we suggest potential E6/E7 inhibitors. Elephantin, roemerine, ginkgolide A, phaseollin, anonaine, chitranone, elephantopin, tetrahydroalstonine and vindolinine were found to be potential as E6 inhibitors on E6AP binding site, while chitranone, sesamin, 16-acetylgitoxigenin, tetrahydroalstonine, methylophiogonone A, and phaseollin exhibit potency as E6 inhibitors on p53 binding site. Columbin, methylopiogonone A, serpentine, uzarigenin, apigenin, coumestrol, kaempherol, phaseollin, pelargonidin, rhamnocitrin, and sesamin showed potency as E7 inhibitors. Phaseollin was found to be potential as E6 and E7 inhibitors.

References

[1] World Health Organization (WHO). Global Health Estimates 2020: Deaths by Cause, Age, Sex, by Country and by Region, 2000-2019. WHO; 2020. Accessed December 11, 2020. https://gco.iarc.fr/today/data/factsheets/populations/360-indonesia-fact-sheets.pdf

[2] Smola S. Immunopathogenesis of HPV-associated cancers and prospects for immunotherapy. Viruses. 2017 Sep;9(9):254. DOI: https://doi.org/10.3390/v9090254

[3] Serrano B, Brotons M, Bosch FX, Bruni L. Epidemiology and burden of HPV-related disease. Best practice & research Clinical obstetrics & gynaecology. 2018 Feb 1;47:14-26. DOI: https://doi.org/10.1016/j.bpobgyn.2017.08.006

[4] Murillo R, Ordóñez-Reyes C. Human papillomavirus (HPV) vaccination: From clinical studies to immunization programs. International Journal of Gynecologic Cancer. 2019 Oct 1;29(8). DOI: http://dx.doi.org/10.1136/ijgc-2019-000582

[5] Singh S, Sharma B, Kanwar SS, Kumar A. Lead phytochemicals for anticancer drug development. Frontiers in plant science. 2016 Nov 8;7:1667. DOI: https://doi.org/10.3389/fpls.2016.01667

[6] Sher YP, Lee C, Liu SY, Chen IH, Lee MH, Chiu FF, Leng CH, Liu SJ. A therapeutic vaccine targeting HPV E6/E7 with intrinsic Toll-like receptor 2 agonist activity induces antitumor immunity. American journal of cancer research. 2018;8(12):2528. PMID: https://www.ncbi.nlm.nih.gov/pubmed/30662809

[7] Yim EK, Park JS. The role of HPV E6 and E7 oncoproteins in HPV-associated cervical carcinogenesis. Cancer research and treatment: official journal of Korean Cancer Association. 2005 Dec;37(6):319. DOI: https://dx.doi.org/10.4143%2Fcrt.2005.37.6.319

[8] Pal A, Kundu R. Human papillomavirus E6 and E7: the cervical cancer hallmarks and targets for therapy. Frontiers in microbiology. 2020 Jan 21;10:3116. DOI: https://doi.org/10.3389/fmicb.2019.01336

[9] García-Alai MM, Alonso LG, de Prat-Gay G. The N-terminal module of HPV16 E7 is an intrinsically disordered domain that confers conformational and recognition plasticity to the oncoprotein. Biochemistry. 2007 Sep 18;46(37):10405-12. DOI: https://doi.org/10.1021/bi7007917

[10] Liu X, Clements A, Zhao K, Marmorstein R. Structure of the human Papillomavirus E7 oncoprotein and its mechanism for inactivation of the retinoblastoma tumor suppressor. Journal of Biological Chemistry. 2006 Jan 6;281(1):578-86. DOI: https://doi.org/10.1074/jbc.M508455200

[11] Hoppe-Seyler K, Bossler F, Braun JA, Herrmann AL, Hoppe-Seyler F. The HPV E6/E7 oncogenes: key factors for viral carcinogenesis and therapeutic targets. Trends in microbiology. 2018 Feb 1;26(2):158-68. DOI: https://doi.org/10.1016/j.tim.2017.07.007

[12] Cos P, Vlietinck AJ, Berghe DV, Maes L. Anti-infective potential of natural products: How to develop a stronger in vitro 'proof-of-concept'. Journal of ethnopharmacology. 2006 Jul 19;106(3):290-302. DOI: https://doi.org/10.1016/j.jep.2006.04.003

[13] Woerdenbag HJ, Kayser O. Jamu: Indonesian traditional herbal medicine towards rational phytopharmacological use. Journal of herbal medicine. 2014 Jun 1;4(2):51-73. DOI: https://doi.org/10.1016/j.hermed.2014.01.002

[14] Ekins S, Mestres J, Testa B. In silico pharmacology for drug discovery: methods for virtual ligand screening and profiling. British journal of pharmacology. 2007 Sep;152(1):9-20. DOI: 10.1038/sj.bjp.0707305

[15] Trott O, Olson AJ. AutoDock Vina: improving the speed and accuracy of docking with a new scoring

DOI: https://doi.org/10.5614/3bio.2021.3.1.2

function, efficient optimization, and multithreading. Journal of computational chemistry. 2010 Jan 30;31(2):455-61. DOI: https://doi.org/10.1002/jcc.21334

[16] Wallace AC, Laskowski RA, Thornton JM. LIGPLOT: a program to generate schematic diagrams of protein-ligand interactions. Protein engineering, design and selection. 1995 Feb 1;8(2):127-34. DOI: https://doi.org/10.1093/protein/8.2.127

[17] Pettersen EF, Goddard TD, Huang CC, Couch GS, Greenblatt DM, Meng EC, Ferrin TE. UCSF Chimera—a visualization system for exploratory research and analysis. Journal of computational chemistry. 2004 Oct;25(13):1605-12. DOI: https://doi.org/10.1002/jcc.20084

[18] Krieger E, Joo K, Lee J, Lee J, Raman S, Thompson J, Tyka M, Baker D, Karplus K. Improving physical realism, stereochemistry, and side-chain accuracy in homology modeling: Four approaches that performed well in CASP8. Proteins: Structure, Function, and Bioinformatics. 2009;77(S9):114-22. DOI: https://doi.org/10.1002/prot.22570

[19] Wiederstein M, Sippl MJ. ProSA-web: interactive web service for the recognition of errors in three-dimensional structures of proteins. Nucleic acids research. 2007 Jul 1;35(suppl_2):W407-10. DOI: https://doi.org/10.1093/nar/gkm290

[20] Anderson RJ, Weng Z, Campbell RK, Jiang X. Main-chain conformational tendencies of amino acids. Proteins: Structure, Function, and Bioinformatics. 2005 Sep 1;60(4):679-89. DOI: https://doi.org/10.1002/prot.20530

[21] Daina A, Michielin O, Zoete V. SwissADME: a free web tool to evaluate pharmacokinetics, drug-likeness and medicinal chemistry friendliness of small molecules. Scientific reports. 2017 Mar 3;7(1):1-3. DOI: 10.1038/srep42717

[22] Martinez-Zapien D, Ruiz FX, Poirson J, Mitschler A, Ramirez J, Forster A, Cousido-Siah A, Masson M, Pol SV, Podjarny A, Trave G. Structure of the E6/E6AP/p53 complex required for HPV-mediated degradation of p53. Nature. 2016 Jan;529(7587):541-5. DOI: 10.1038/nature16481

[23] Le Guilloux V, Schmidtke P, Tuffery P. Fpocket: an open source platform for ligand pocket detection. BMC bioinformatics. 2009 Dec;10(1):1-1. DOI: https://doi.org/10.1186/1471-2105-10-168

[24] Otto T, Sicinski P. Cell cycle proteins as promising targets in cancer therapy. Nature Reviews Cancer. 2017 Feb;17(2):93-115. DOI: 10.1038/nrc.2016.138

[25] Houston DR, Yen LH, Pettit S, Walkinshaw MD. Structure-and ligand-based virtual screening identifies new scaffolds for inhibitors of the oncoprotein MDM2. PLoS One. 2015 Apr 17;10(4):e0121424. DOI: https://doi.org/10.1371/journal.pone.0121424

[26] Savjani KT, Gajjar AK, Savjani JK. Drug solubility: importance and enhancement techniques. International Scholarly Research Notices. 2012;2012. DOI: https://doi.org/10.5402/2012/195727

[27] Sastry SV, Nyshadham JR, Fix JA. Recent technological advances in oral drug delivery–a review. Pharmaceutical science & technology today. 2000 Apr 1;3(4):138-45. DOI: 10.1016/S1461-5347(00)00247-9

[28] Lipinski CA. Lead-and drug-like compounds: the rule-of-five revolution. Drug discovery today: Technologies. 2004 Dec 1;1(4):337-41. DOI: https://doi.org/10.1016/j.ddtec.2004.11.007

[29] Zanier K, Charbonnier S, Sidi AO, McEwen AG, Ferrario MG, Poussin-Courmontagne P, Cura V, Brimer N, Babah KO, Ansari T, Muller I. Structural basis for hijacking of cellular LxxLL motifs by papillomavirus E6 oncoproteins. Science. 2013 Feb 8;339(6120):694-8. DOI: https://doi.org/10.1126/science.1229934

[30] Lee HG, Yu KA, Oh WK, Baeg TW, Oh HC, Ahn JS, Jang WC, Kim JW, Lim JS, Choe YK, Yoon DY. Inhibitory effect of jaceosidin isolated from Artemisia argyi on the function of E6 and E7 oncoproteins of HPV 16. Journal of ethnopharmacology. 2005 Apr 26;98(3):339-43. DOI: https://doi.org/10.1016/j.jep.2005.01.054

[31] Patil R, Das S, Stanley A, Yadav L, Sudhakar A, Varma AK. Optimized hydrophobic interactions and hydrogen bonding at the target-ligand interface leads the pathways of drug-designing. PloS one. 2010 Aug 16;5(8):e12029. DOI: https://doi.org/10.1371/journal.pone.0012029

[32] Nittinger E, Inhester T, Bietz S, Meyder A, Schomburg KT, Lange G, Klein R, Rarey M. Large-scale analysis of hydrogen bond interaction patterns in protein–ligand interfaces. Journal of medicinal chemistry. 2017 May 25;60(10):4245-57. DOI: https://doi.org/10.1021/acs.jmedchem.7b00101

[33] Motiejunas D, Wade RJ. Computer-Assisted Drug Design. In Triggle DJ, Taylor JB, editors. Comprehensive Medicinal Chemistry II. Elsevier; 2006 Dec 29.

DOI: https://doi.org/10.5614/3bio.2021.3.1.2

e-ISSN: 2655-8777 http://journals.itb.ac.id/index.php/3bio

Analysis of Bacterial Community Level Physiological Profiling on the Fermentation of Traditional *Pliek u* Using BIOLOG^{TM} EcoPlates

Suji Edwar, Pingkan Aditiawati*

School of Life Sciences and Technology, Bandung Institute of Technology, Indonesia.

Corresponding author; e-mail: pingkan@sith.itb.ac.id
Received 24 August, 2020
Accepted for publication 10 June, 2021

Abstract

Pliek u is an Acehnese traditional condiment made from fermented coconut (*Cocos nucifera*) endosperm. The traditional *pliek u* fermentation process typically involves a diverse bacterial community. This research aimed to discover the physiological profile of the bacterial community diversity in *pliek u* fermentation. BIOLOGTM EcoPlates was used to obtain the physiological functions of the bacterial community during the *pliek u* fermentation process. The bacteria were then isolated from EcoPlate substrate to determine the predominant microorganism. Results from the analysis showed that the value of the Average Well Colour Development (AWCD) increased during the EcoPlates incubation period. The AWCD values in sample IV were higher than the AWCD values in samples I, II, and III. PCA analysis showed that the use of EcoPlate substrate by the bacterial community at the beginning of the fermentation was correlated with the substrate groups of carbohydrate and polymer, and with the substrate groups of carbohydrate and the amino acid at the end of the fermentation. The phylogenetic analysis showed that EC1 had a close relation with *Pseudomonas azotoformans* strain NBRC, while EC3 had a close relation with *Psedomonas lundensis* strain ATCC 49968. In conclusion, there were changes in the use of EcoPlate substrate and the activities of the bacterial community during the *pliek u* fermentation process.

Keywords: *Pliek u*, BIOLOG^{TM} EcoPlate, Fermentation, Bacterial Community

1. Introduction

Pliek u, a fermented food condiment from Aceh, Indonesia, is produced from the fermentation process of coconut (*Cocos nucifera*) endosperm. The process typically involves an uncontrolled (uninoculated) fermentation process of coconut endosperm in 3-4 days. Characteristically, *pliek u* has a specific taste and smell, granular texture, and dark brown (Figure. 1). Acehnese people use *pliek u* as food condiment in cooking to give specific flavor and taste.

During the process of *pliek u* fermentation, it is believed that the coconut endosperm is undergoing several changes because of the activities of a diverse microbial community. Little has been reported, however, regarding the dynamic of these activities during the fermentation of *pliek u*. The profile of this microbial community diversity can be investigated with Community Level Physiological Profiling (CLPP) analysis. This method is based on the different uses of carbon substrate by the microbial community [1]

BIOLOGTM EcoPlate is a relatively simple method to study and to characterize the diversity of the physiological profile of the microbial community. The EcoPlate comprises a blank with 31 carbon substrates that can describe the metabolic activity of the microbial community in the environment [2]. In this study, BIOLOGTM EcoPlates was used to analyze the physiological profile of the bacterial community and to examine the correlation between fermentation time and bacterial metabolic activity in *pliek u* during fermentation.

2. Methodology

2.1. Sample

Samples of *pliek u* were collected from Siron of Aceh Besar Regency in the province of Aceh, Indonesia, where it was traditionally produced. According to the producer, *pliek u* was made from approximately one-year-old freshly grated coconut endosperm. The substrate was fermented for at least 72 hours until the substrate produced oil. Then, the substrate was dried under the sun, and the oil was separated from the

DOI: https://doi.org/10.5614/3bio.2021.3.1.3

pulp using a press machine. Sampling was done every 24 hours during fermentation stages (sample I=0 h, sample II=24 h, sample III=48 h, and sample IV=72 h). The samples were stored at 4°C in a refrigerator until analysis.

Figure 1. Documentation of the traditional *pliek u* fermentation process. (A) grated coconut; (B) during fermentation process; (C) drying process; (D) *pliek u*

2.2. Total Plate Count

Homogenate samples were inoculated on nutrient agar (NA) media with streak plate method and incubated at room temperature (± 28°C) for 24 h. Enumeration was performed to obtain the total plate count number expressed in colony-forming unit per mL (CFU/mL) [3].

2.3. Proximate Analysis and pH

Proximate analysis was conducted according to SNI 01-2891-1992 to determine protein, fat, ash, and lipid contents from samples. Total carbohydrate was calculated by its difference. Subsequently, pH was analyzed based on the Association of Official Analytical Chemists standard procedures [4].

2.4. Community Level Physiological Profile (CLPP)

The samples were then prepared and inoculated into the BIOLOG™ EcoPlate based on the previous method [5] with some modifications. Three grams of sample was suspended into 27 mL nutrient broth and incubated for 12 hours at room temperature (± 28°C). Then, one ml suspension was suspended in 9 ml phosphate buffer saline (PBS) and diluting until 10^{-3}. A 100 µL was pipetted from the 103 dilution and inoculated to each one of the 96 wells in BIOLOG™ EcoPlates. The EcoPlate was put back in the plastic wrapper and incubated at room temperature (± 28°C) in the dark. Absorbance measurements were conducted every 24 hours (0, 24, 48, 72, 96, and 120 h) with BIO-RAD iMark™ microplate absorbance reader at a wavelength of 590 nm. Microbial activity in each microplate was expressed as average well color development (AWCD) was calculated according to Garland and Mills 1991 [6].

$$\text{AWCD} = \sum(C_i - R)/31 \quad (1)$$

Shannon's diversity index (H'), which is related to the number of carbon substrates the bacterial community is able to degrade, was calculated as follow:

$$\text{H}' = -\sum pi \times (\ln pi) \quad (2)$$

Definitions:

Ci: The OD_{590} nm values in 31 carbon wells.
R: The OD_{590} nm value in control well.
pi: The OD_{590} nm value in i well divide mean OD_{590} nm value of 31 wells

2.5. Bacterial Isolation and Characterization

Samples were aseptically taken from the BIOLOG™ EcoPlate well that showed positive results after 120 h

DOI: https://doi.org/10.5614/3bio.2021.3.1.3

incubation. The concentration of the bacterial in the samples was decreased with serial dilutions technique up to 10^{-5}. Then, 100 µL of the samples was inoculated to nutrient agar media and incubated at room temperature ± 28º C for 24 h. The bacterial colonies were separated, purified, and characterized based on colony morphology [3]. These bacterial isolates were referred to as EC1-EC5 in this research.

2.6. Bacterial Identification

The selected bacteria based on substrate carbon utilization and domination were identified by molecular technique. A single isolate colony analysis used PCR (polymerase chain reaction) with 16s rRNA gene primers. Sequencing was performed by Macrogen (Korea). The results sequences were compared in GenBank with the use of the BLAST method to determine their approximate phylogenetic affiliation on the NCBI website (http://www.ncbi.nlm.nih.gov/) [7]. Then, phylogenetic analysis was performed with MEGA-X software and constructed using neighbour-joining algorithm with bootstrap 1000 replication [8].

2.7. Statistical Analyses

HeatMaps were performed on standardized data from the AWCD values at 120 h (BIOLOG™ EcoPlate) with R studio using Pheatmaps packages [9][10]. The results were also submitted to the principal component analysis (PCA) to determine the correlations between the substrates utilization and bacterial community during *pliek u* fermentation using Past3 [11].

3. Results and discussion

3.1. Bacterial Counts and Chemical-nutritional Characteristics

The number of bacteria involved during fermentation was determined by culturing the bacteria on nutrient agar media. Samples were enumerated and expressed in colony forming unit per mL (CFU/mL). Total plate count of bacterial enumeration in the samples decreased along with the time of fermentation. Similar to the number of total bacteria, the substrate pH also decreased in line with the time of fermentation, from 4.43 to 3.96 (Table 1). This strongly suggested that the decrease in the number of total bacteria was probably due to the decrease in pH value [12], as bacterial growth tends to be more bound to a certain pH compared to fungi and yeast [13].

Table 1. Total plate count enumeration of bacteria and chemical-nutritional characteristics of *pliek u* during fermentation.

Sample	Total Plate Count (CFU/mL)	pH	Moisture (%)	Ash (%)	Protein (%)	Fat (%)	Carbohydrate (%)
I	1.8 x 10^8	4.43	56.31	1.20	28.94	3.46	10.09
II	5.6 x 10^8	4.71	nd[1]	nd[1]	nd[1]	nd[1]	nd[1]
III	9.6 x 10^8	4.08	nd[1]	nd[1]	nd[1]	nd[1]	nd[1]
IV	5.0 x 10^8	3.96	48.80	1.03	37.49	3.94	8.74

[1]nd = not determined.

I= fermented *pliek u* 0 h; II= fermented *pliek u* 24 h; III= fermented *pliek u* 48 h; IV= fermented *pliek u* 72 h

Proximate analysis was conducted to evaluate the nutritional change during *pliek u* fermentation. The fermentation process caused biochemical changes in the substrate by the microorganisms' activity [14]. The result of the proximate composition of *pliek u* during fermentation is shown in Table 1. The moisture content on the substrates was high at the beginning of fermentation; however, it decreased at the end of fermentation from 56.31% to 48.80%. The decrease in the moisture content suggested the effects of water evaporation during fermentations that occurred in an open condition. The ash and carbohydrate contents decreased from 1.20% to 1.03% and 10.09% to 8.74% respectively, while the protein and fat contents increased from 28.94% to 37.49% and 3.46% to 3.94% respectively. Extensive hydrolysis of the protein and fat molecules to amino acids, simple fatty acids, and other simple molecules could have caused the increase in protein and fat values. The increase in protein and fat is an indication that *pliek u* can be a source of plant protein and fat [14].

3.2. Community-Level Physiological Profiles (CLPPs)

There was 31 carbon substrates utilization by a bacterial community from *pliek u* samples during fermentation that were calculated based on the BIOLOG™ EcoPlates analysis. AWCD was calculated based on the trendline equation to make it easier to see patterns of changes in AWCD values. The results of the AWCD analysis showed that there was a lag phase from day 0 to day 1, and subsequently an increase in AWCD values with an increase in the incubation time of the EcoPlates. The AWCD values in sample IV were 1.0833 and significantly higher than the AWCD values from samples II, I, and III at the value of 0.2984, 0.2505, and 0.0866 respectively (Figure 2).

DOI: https://doi.org/10.5614/3bio.2021.3.1.3

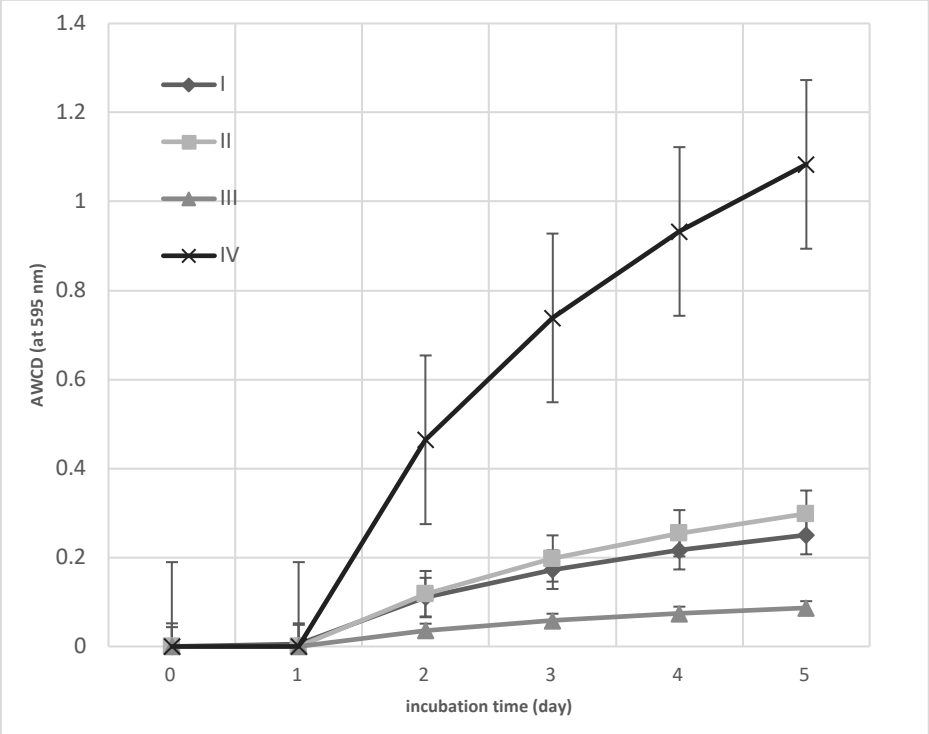

Figure 2. Trendline average well colour development of *pliek u* during fermentation (n = 3). I= fermented *pliek u* 0 h; II= fermented *pliek u* 24 h; III= fermented *pliek u* 48 h; IV= fermented *pliek u* 72 h.

Inoculum density and the structure of the community can influence the rate of substrate utilization by the bacterial community described in the AWCD value in the samples [15]. The number of the bacterial community in the *pliek u* during the fermentation process showed a decrease in the total plate count number from the 24 h of fermentation to the end of fermentation (Table 1). In contrast, the AWCD value at 48 h fermentation showed the lowest AWCD value and at 72 h fermentation showed the highest AWCD value (Figure 2). Thus, there were differences in the structure of the bacterial community at each stage of fermentation. The differences in the diversity or structure of bacterial communities at the stage of *pliek u* fermentation may be owing to the condition of spontaneous fermentation process of *pliek u.* In the spontaneous fermentation, bacteria could enter the substrate via various sources, such as air or the equipment used that contained various microorganisms [16][17].

3.3. Functional Diversity

Shannon index (H') showed functional diversity that encompassed both substrate richness and substrate evenness. Functional diversity, operationally, is defined as the rate of substrates utilization by the microbial community [18]. The H' value of the bacterial community was analyzed at day-0 and day-5 of the EcoPlate incubation (Figure 3). In all samples, there was no significant change in the H' value during the time indicated, which showed that the entire bacterial community on EcoPlate had been active and metabolized the substrate from day-0. Then, the H' values from samples I, II, and IV generally had approximately the same index value in the range of 3.00. In contrast, the H' value in sample III was slightly lower (below 3.00). This result showed that the bacterial community in sample III had a lower ability to utilize the substrate than the bacterial community in samples I, II, and IV.

3.4. Analysis of Substrate Utilization and Multivariate Analysis

The patterns of carbon substrates utilization of the bacterial communities in *pliek u* during fermentation varied based on fermentation times. The number of carbon substrates utilized was lower in samples I and III than in samples II and IV (Figure 4). Heatmap results indicated that at 0 and 48 hours of fermentation, carbon substrate utilization was carbohydrates (N-Acetyl-d-glucosamine, d-Cellobiose, β-Methyl-d-glucoside, d-Mannitol), carboxylic acid (Pyruvic acid methyl ester), and polymer (α-Cyclodextrin). Then, the bacterial community at 24 hours of fermentation was correlated to the use of three polymers (Glycogen, Tween 80, Tween 40), four carbohydrates (i-Erythritol, d-Mannitol, d-Cellobiose, β-Methyl-d-glucoside), two carboxylic acid (2-Hydroxy benzoic acid, γ-hydroxybutyric acid), and two

DOI: https://doi.org/10.5614/3bio.2021.3.1.3

amino acids (l-Threonine, l-Phenylalanine). Finally, the bacterial community at 72 hours correlated to the use of four amino acid substrates (l-Serine, l-Arginine, l-Asparagine, Glycyl-l-glutamic acid), seven carboxylic acids (D-Galactonic acid γ lactone , d-Galacturonic acid, d-Glucosaminic acid, Itaconic acid, 4-Hydroxy benzoic acid, d-Malic acid, γ-Amino butyric acid), five carbohydrates (α-d-Lactose, β-Methyl-D-glucoside, D-Cellobiose, d-Mannitol, N-Acetyl-d-glucosamine), carbon phosphate (Glucose-1-phosphate), amine (Putrescine), and polymer (Tween 40).

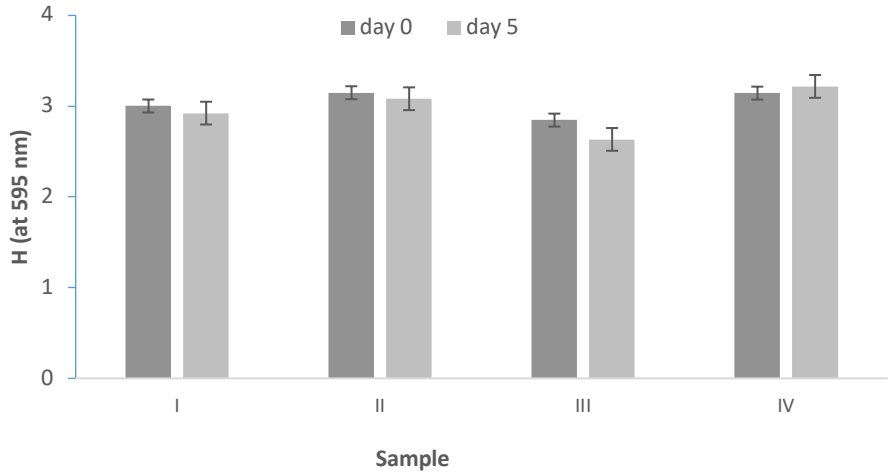

Figure 3. The Shannon index (H') of *pliek u* during fermentation (n = 3), evaluated on the day-0 and the day-5 day of BIOLOG™ EcoPlate incubation

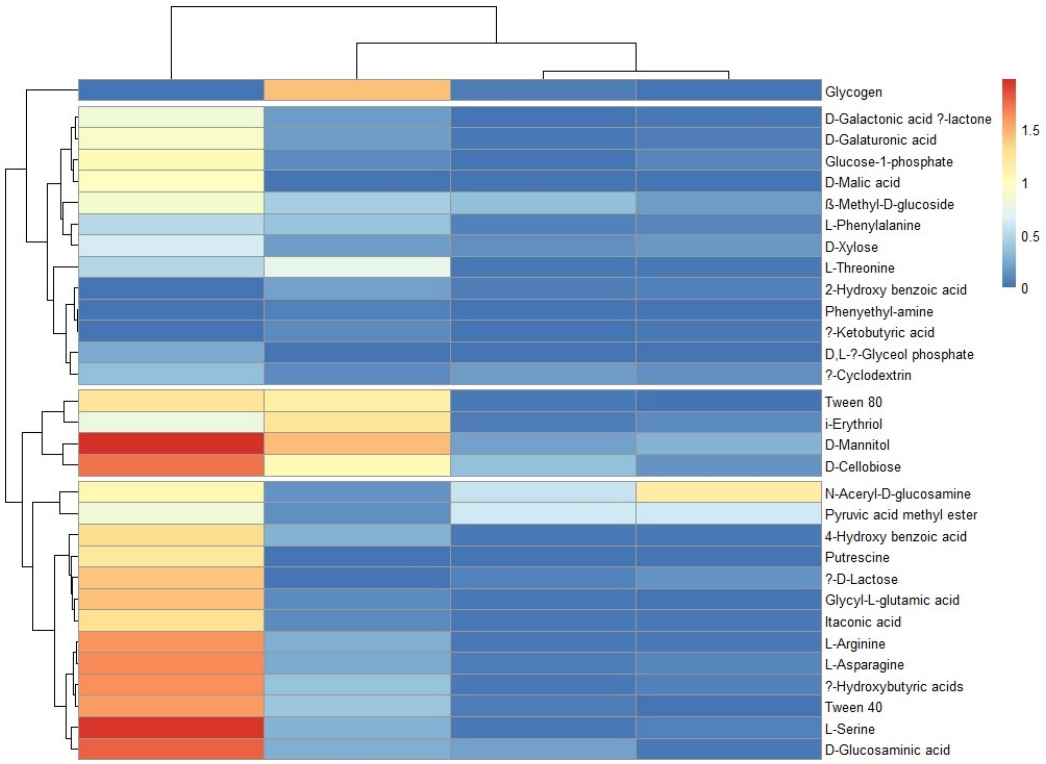

Figure 4. Cluster analyses and HeatMaps for the carbon utilization patterns of the 31 substrates located on the Biolog™ EcoPlates data incubated for 120 h from samples *pliek u* during fermentation (n = 3). Samples I= fermented *pliek u* 0 h; II= fermented *pliek u* 24 h; III= fermented *pliek u* 48 h; IV= fermented *pliek u* 72 h.

DOI: https://doi.org/10.5614/3bio.2021.3.1.3

Based on the Principal Component Analysis (PCA), *pliek u* samples during fermentation were distinguished into three groups based on their metabolic profiles:

- Sample IV with very high biological activity
- Sample II with average biological activity
- Samples I and III with the lowest biological activity (Figure 5).

The result from the PCA also showed that the bacterial community in samples I and III were correlated to the substrate group of carbohydrate, while in sample II the bacterial community was correlated to substrate group carbohydrate and polymer. The bacterial community in sample IV was corelated with substrate group amino acids, carbohydrate, and carboxylic acid.

The data showed that the microbial community-level physiological profiles were different at each stage of fermentation (Figure 5). The use of polymer and carbohydrate substrates by the bacterial community at the 24 h of *pliek u* fermentation was related to the availability of nutrients on the *pliek u* fermentation substrate. Nutrients were available in coconut endosperm at the beginning of fermentation in the form of complex compounds such as polysaccharides, proteins, and fats. At this stage, cellulolytic, proteolytic, and lipolytic microorganisms seemed to have hydrolysed the polysaccharide molecules, such as galactomannan and glucomannan; the protein molecules, such as globulin, albumin, glutelin-1, glutelin-2, and prolamin; the fatty acid molecules such as caproic acid (6: 0), acids, globulins, protein molecules, globulin, albumin, glutelin-1, glutelin-2, and prolamin and fatty acid molecules such as caproic acid (6: 0), acids caprylic (8: 0), capric acid (10: 0), lauric acid (12: 0), meristic acid (14: 0), palmitic acid (16: 0), stearic acid (18: 0), oleic acid (18: 1) and linoleic acid (18: 2) became simple molecules [19][20][21]. Then, there was a change in metabolism from polymer and carbohydrate substrates to amino acids, carboxylic acids, carbohydrates by the bacterial community at the 72 h of fermentation. Changes in the use of these substrates were probably due to the formation of flavour compounds or over fermentation that was correlated to the bacterial community structure in *pliek u* during fermentation.

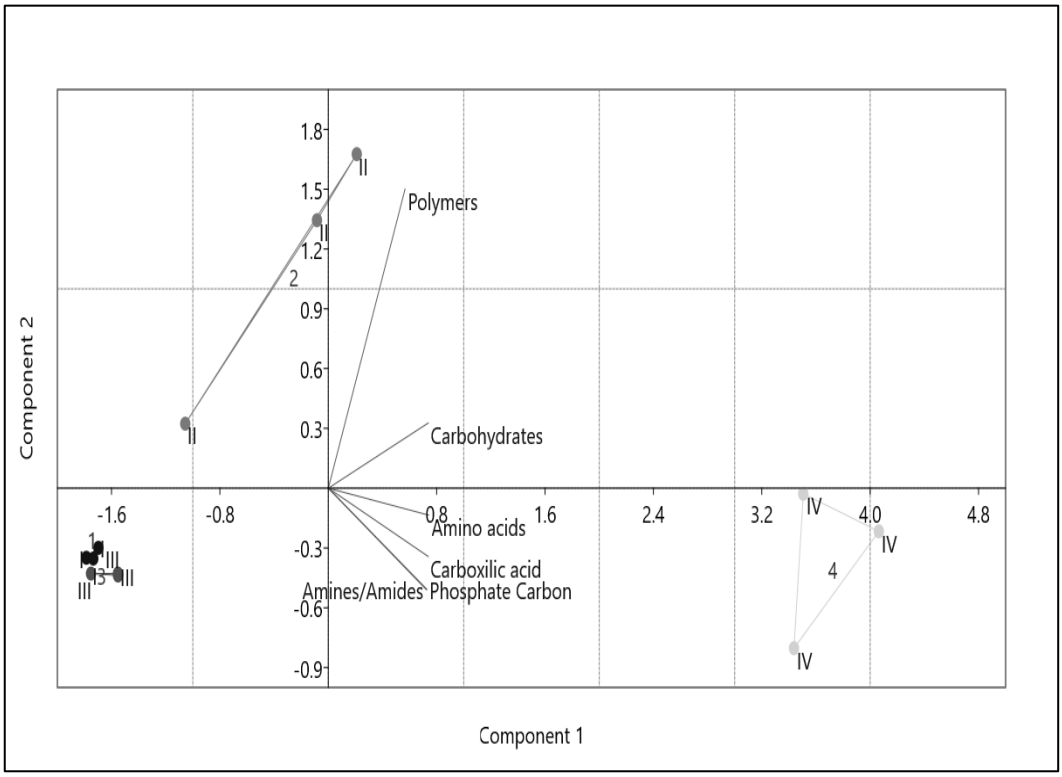

Figure 5. Principal component analysis of substrates utilization bacterial community during *pliek* fermentation from Biolog^{TM} EcoPlates incubated for 120 h (n = 3). I= fermented *pliek u* 0 h; II= fermented *pliek u* 24 h; III= fermented *pliek u* 48 h; IV= fermented *pliek u* 72 h.

The formation of compounds that plays a role in flavours during fermentation can occur through the metabolism of flavour precursor compounds or flavour compounds themselves by microorganisms [22]. In general, the

DOI: https://doi.org/10.5614/3bio.2021.3.1.3

compounds that play a role in flavour formation can come from groups of amino acids, phenols, and ketones [23]. Amino acids have a vital role in the formation of flavour. Each amino acid contributes to a different taste; serine has a combination of sour and umami flavours, arginine tastes bitter but slightly sweet and glutamic acid gives umami or savoury flavours [24]. The amino acid arginine and glutamic acid are the most dominant compared to the other amino acids found in the coconut endosperm. The predominance of umami, bitter, and slightly sweet taste in *pliek u* was suspected from these amino acids.

3.5. Predominant Bacterial in Pliek u Fermentation

The bacteria involved in *pliek u* fermentation were determined by isolating the bacteria from the BIOLOG™ EcoPlate well, which showed positive results. There were five isolated bacterial isolates (Figure 6). The macroscopic characterization showed that EC1, EC3, and EC4 isolates had the same characteristics: round-shaped, convex-elevation, entire-margin, and white opaque colonies. The EC2 isolate was round-shaped, raised-elevation, entire-margin, cream-colored, and large-sized. Then, the EC5 isolate was round-shaped, convex-elevation, entire-margin, and yellowish.

EC1 isolate was present from the 0 h to 72 h *pliek u* fermentation and was found to utilize tween 80, α-Cyclodextrin, pyruvic acid methyl ester, itaconic acid, d-glucosaminic acid, N-Acetyl-d-glucosamine, β- Methyl-d-glucoside, and d-Cellobiose, which were from substrate groups polymer, carboxylic acid, and carbohydrate. EC2 isolate was present at 0 h and 48 h of fermentation and capable to utilize β-Methyl-d-glucoside, d-Mannitol, α-d-Lactose, and glycyl-l-glutamic acid, which were from substrate groups carbohydrate and amino acid. Then, there were only three isolates present at 72 h of *pliek u* fermentation, namely EC3, EC4, and EC5. EC3 isolate was the most dominant compared to the other isolates at 72 h fermentation and was found to utilize tween 40, tween 80, β-Methyl-d-glucoside, d-Xylose, 4-Hydroxy benzoic acid, γ-Amino butyric acid, d- glucosaminic acid, glucose-1-phosphate, glycyl-l-glutamic acid, l-threonine, l-asparagine, l-serine, and l-phenylalanine, which were from substrate groups polymer, carbohydrate, carboxylic acid, phosphate carbon and amino acid. EC4 was capable to utilize d-galactonic acid γ-lactone, d-galacturonic acid, and d, l-α-glycerol phosphate, which were from substrate groups carboxylic acid. Finally, EC5 was found to utilize the amino acid substrate l-arginine. From this result, it was strongly suggested that EC1 and EC3 had an important role in *pliek u* fermentation process.

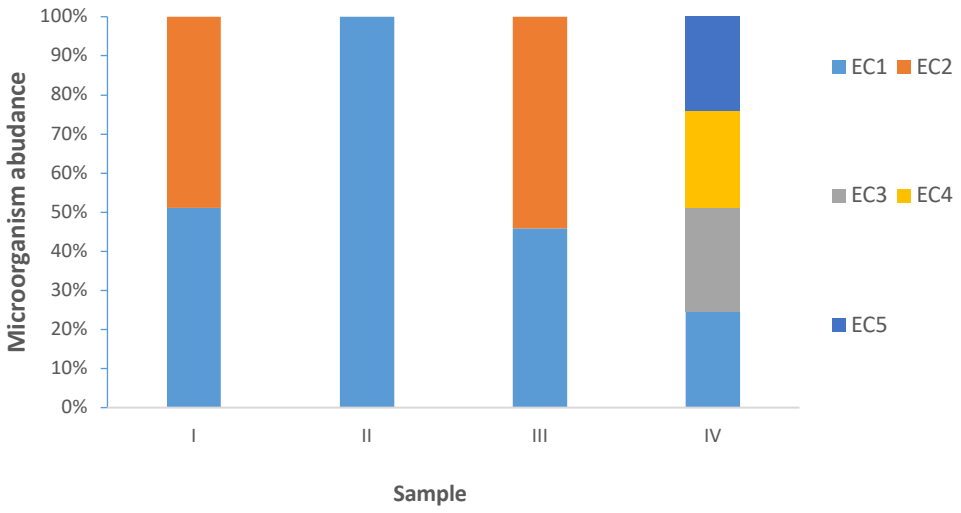

Figure 6. Microorganism abundance during *pliek u* fermentation from samples in BIOLOG™ EcoPlate after 120 h incubation.

The BLAST results of the EC1 sequence on the NCBI gene bank showed that the EC1 had 92.06% ident with *Pseudomonas lactis* strain DSM 29167 and 91.90% ident *Pseudomonas azotoformans* strain NBRC 12693. Then, the results of phylogenetic analysis showed that EC1 isolate had a close relation with the *Pseudomonas azotoformans* strain NBRC 12693 with a bootstrap value of 62 (Figure 7A). *P. azotoformans* has previously been reported in foods such as milk and meat [25]. *P. azotoformans* can hydrolyse compounds, such as citrate, malate, mannitol and mannose,

DOI: https://doi.org/10.5614/3bio.2021.3.1.3

which are a group of organic acids, carboxylic acids and carbohydrates [26]. Furthermore, *P. azotoformans* is also classified as proteolytic and lipolytic bacteria because it can hydrolyse proteins and lipids [27].

The BLAST results of the EC3 sequence on the NCBI showed that the EC3 had 94.25% ident with *Pseudomonas lundensis* strain ATCC 49968 and 93.76% ident with *Pseudomonas helmanticensis* strain OHA11. Based on the phylogenetic analysis results, EC3 isolate had a close relation with *Pseudomonas lundensis* strain ATCC 49968 with a bootstrap value of 94 (Figure 7B). *P. lunden*sis was psychotropics bacteria commonly found in foods such as meat and milk [28]. The main extracellular enzymes secreted by *P. lundensis* were the peptidase and lipase enzymes [29]. *P. lundensis* could produce acids from carbohydrate class compounds such as L-arabinose, D-galactose, D-glucose, D-mannose, D-ribose, maltose, melibiose, and D-xylose. The ability of acid production varied depending on the *P. lundensis* strain [30].

The traditional food fermentation that involves *Pseudomonas* bacteria has been widely reported. This includes fermentation of castor seed oil from Africa, *semayi* (coconut dregs) from Indonesia, *ngapi* (ground fish) from Myanmar, *Ogiri-Nsiko* (crab) from Nigeria. The bacteria is also involved in the fermentation of fish sauce, which is a widespread process in Asia [19]. In the *pliek u* fermentation, the predominant isolates that were isolated from the *pliek u* fermentation process were both bacteria belonging to the genus *Pseudomonas*. This is the first time that *Pseudomonas* presence has been identified in *pliek u* fermentation.

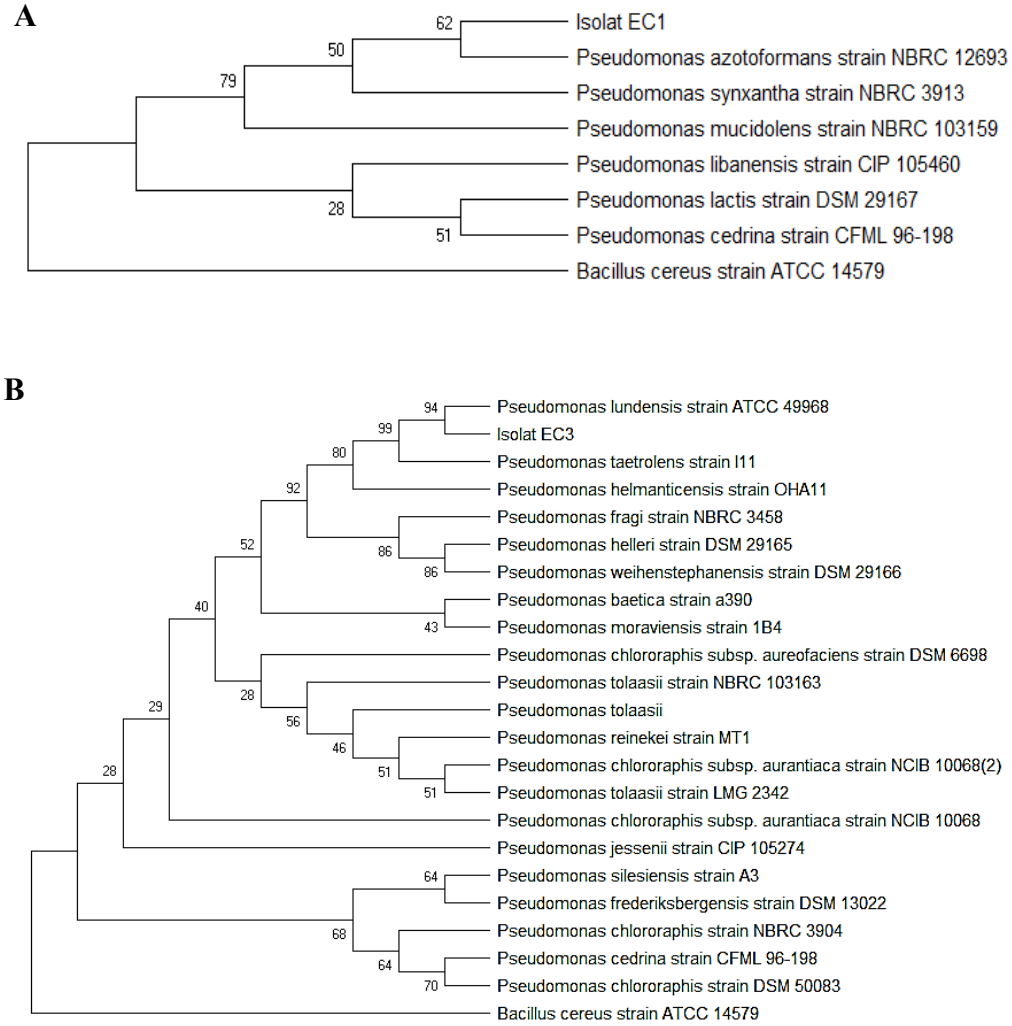

Figure 7. Phylogenetic tree was constructed using neighbor-joining algorithm of nucleotides sequence of 16S rRNA gene (a) EC1 Isolate (b) EC3 Isolate

DOI: https://doi.org/10.5614/3bio.2021.3.1.3

4. Conclusion

The significance of this study showed that there was an alteration in using substrate EcoPlate and the activities of the bacterial community during the process of *pliek u* fermentation. At the beginning of the fermentation, the substrate used was the carbohydrates and polymers substrate group, while at the end of the fermentation it shifted to the amino acids and carbohydrates substrate group. The biological activity of the bacterial community was higher at the end of *pliek u* fermentation. Furthermore, the predominant bacteria isolate EC1 and EC3 can be a candidate inoculum in controlled *pliek u* fermentation.

References

[1] G. L. Kurten dan A. Barkoh, "Evaluation of Community-Level Physiological Profiling for Monitoring Microbial Community Function in Fish Hatchery Ponds," *Texas Park. Wildl.*, 2014. DOI: https://doi.org/10.1080/15222055.2015.1079580

[2] Z. Ge, H. Du, Y. Gao, dan W. Qiu, "Analysis on metabolic functions of stored rice microbial communities by BIOLOG ECO microplates," *Front. Microbiol.*, vol. 9, no. JUL, Jul 2018. DOI: https://doi.org/10.3389/fmicb.2018.01375

[3] J. G. Cappuccino dan N. Sherman, *Microbiology A Laboratory Manual*. 2014.

[4] M. H. Lee, "Official methods of analysis of AOAC International (16th edn)," *Trends Food Sci. Technol.*, 1995.

[5] W. Xu, Z. Ge, dan D. R. Poudel, "Application and Optimization of Biolog EcoPlates in Functional Diversity Studies of Soil Microbial Communities," *MATEC Web Conf.*, vol. 22, hal. 04015, Jul 2015. DOI: https://doi.org/10.1051/matecconf/20152204015

[6] J. L. Garland dan A. L. Mills, "Classification and Characterization of Heterotrophic Microbial Communities on the Basis of Patterns of Community-Level Sole-Carbon-Source Utilization," 1991.

[7] D. Benson, M. Boguski, D. J. Lipman, dan J. Ostell, "The National Center for Biotechnology Information," *Genomics*, 1990. DOI: https://doi.org/10.1016/0888-7543(90)90583-G

[8] S. Kumar, G. Stecher, M. Li, C. Knyaz, dan K. Tamura, "MEGA X: Molecular Evolutionary Genetics Analysis across computing platforms." 2018.

[9] Rstudio Team, "RStudio: Integrated development for R. RStudio, Inc., Boston MA," *RStudio*. 2020.

[10] R. Kolde, "pheatmap : Pretty Heatmaps," *R package version 1.0.8*. 2015.

[11] P. D. Ryan, Ø. Hammer, dan D. A. Harper, "Past: Paleontological Statistics Software Package for Education and Data Analysis," *Palaeontol. Electron.*, 2001.

[12] M. R. Adams dan L. Nicolaides, "Review of the sensitivity of different foodborne pathogens to fermentation," *Food Control*, vol. 8, no. 5–6, hal. 227–239, 1997. DOI: https://doi.org/10.1016/S0956-7135(97)00016-9

[13] J. M. Jay, "Modern Food Microbiology Sixth Edition," 2000.

[14] R. Sharma, P. Garg, P. Kumar, S. K. Bhatia, dan S. Kulshrestha, "Microbial fermentation and its role in quality improvement of fermented foods," *Fermentation*, vol. 6, no. 4, hal. 1–20, 2020. DOI: https://doi.org/10.3390/fermentation6040106

[15] J. Preston-Mafham, L. Boddy, dan P. F. Randerson, "Analysis of microbial community functional diversity using sole-carbon-source utilisation profiles - A critique," *FEMS Microbiol. Ecol.*, vol. 42, no. 1, hal. 1–14, 2002. DOI: https://doi.org/10.1111/j.1574-6941.2002.tb00990.x

[16] A. E. Groenenboom, J. Shindano, N. Cheepa, E. J. Smid, dan S. E. Schoustra, "Microbial population dynamics during traditional production of Mabisi, a spontaneous fermented milk product from Zambia: a field trial," *World J. Microbiol. Biotechnol.*, vol. 36, no. 12, hal. 1–14, 2020. DOI: https://doi.org/10.1007/s11274-020-02957-5

[17] V. Capozzi, M. Fragasso, R. Romaniello, C. Berbegal, P. Russo, dan G. Spano, "Spontaneous food fermentations and potential risks for human health," *Fermentation*, vol. 3, no. 4, hal. 1–19, 2017. DOI: https://doi.org/10.3390/fermentation3040049

[18] J. C. Zak, M. R. Willig, D. L. Moorhead, dan H. G. Wildman, "Functional diversity of microbial communities: A quantitative approach," *Soil Biol. Biochem.*, vol. 26, no. 9, hal. 1101–1108, 1994. DOI: https://doi.org/10.1016/0038-0717(94)90131-7

[19] P. K. Sarkar dan • M J Robert Nout, *Handbook of Indigenous Foods Involving Alkaline Fermentation*. CRC Press, 2014.

[20] U. Patil dan S. Benjakul, "Characteristics of albumin and globulin from coconut meat and their role in emulsion stability without and with proteolysis," *Food Hydrocoll.*, vol. 69, hal. 220–228, Agu 2017. DOI: https://doi.org/10.1016/j.foodhyd.2017.02.006

[21] USDA, "Basic Report: 12104, Nuts, coconut meat, raw," 2019. [Daring]. Available at: https://bit.ly/2zVMEwO. [Accessed: 30-Jun-2020].

[22] R. F. Mcfeeters, "Fermentation Microorganisms and Flavor Changes in Fermented Foods," 2004.

[23] D. Havkin-frenkel dan F. C. Belanger, *Biotechnology in Flavor Production: A Case-based Approach*. New Jersey: Blackwell Publishing, 2008.

DOI: https://doi.org/10.5614/3bio.2021.3.1.3

[24] T. Nishimura dan H. Kato, "Taste of free amino acids and peptides," *Food Rev. Int.*, vol. 4, no. 2, hal. 175–194, Jan 1988. DOI: https://doi.org/10.1080/87559128809540828

[25] E. Circella, A. Schiavone, R. Barrasso, A. Camarda, N. Pugliese, dan G. Bozzo, "Pseudomonas azotoformans belonging to pseudomonas fluorescens group as causative agent of blue coloration in carcasses of slaughterhouse rabbits," *Animals*, vol. 10, no. 2, 2020. DOI: https://doi.org/10.3390/ani10020256

[26] I. Fendri *et al.*, "Isolation, identification and characterization of a new lipolytic Pseudomonas sp., strain AHD-1, from Tunisian soil," *Environ. Technol.*, vol. 31, no. 1, hal. 87–95, 2010. DOI: https://doi.org/10.1080/09593330903369994

[27] J. C. R. Júnior, P. I. T. Junior, A. L. M. Oliveira, E. A. Rios, R. Tamanini, dan V. Beloti, "Proteolytic and lipolytic potential of Pseudomonas spp. From goat and bovine raw milk," *Pesqui. Vet. Bras.*, vol. 38, no. 8, hal. 1577–1583, Agu 2018. DOI: https://doi.org/10.1590/1678-5150-PVB-5645

[28] N. Thompson, "Identification of Novel Strains of Pseudomonas lundensis from Food Samples," no. April, 2018.

[29] J. Aguirre *et al.*, "Characterization of Pseudomonas spp. and Associated Proteolytic Properties in Raw Milk Stored at Low Temperatures," *Front. Microbiol*, vol. 8, hal. 2158, 2017. DOI: https://doi.org/10.3389/fmicb.2017.02158

[30] G. Molin, A. Ternstrom, dan J. Ursing, "Pseudomonas lundensis, a new bacterial species isolated from meat," *Int. J. Syst. Bacteriol.*, vol. 36, no. 2, pp. 339–342, 1986.

DOI: https://doi.org/10.5614/3bio.2021.3.1.3

e-ISSN: 2655-8777 http://journals.itb.ac.id/index.php/3bio

CO_2 Emission and Absorption Estimation in Bandung City by Implementing CO_2 Emission Rate Reduction Simulation Using the Stella Program

Natalia Christiani, Yayat Hidayat*, Sutrisno

School of Life Sciences and Technology, Bandung Institute of Technology, Indonesia.

Corresponding author; e-mail: yayat@sith.itb.ac.id
Received 7 January 2021
Accepted for publication 10 June, 2021

Abstract

Bandung CO_2 emissions continue to increase in line with its population. The emissions source comes from the industrial, transportation, Liquefied Petroleum Gas (LPG), household, and livestock sectors, whereas CO_2 absorption only comes from vegetation through photosynthesis. High CO_2 emissions could decrease air quality and reduce environmental health. This study aims to estimate the amount of CO_2 emissions and their absorption in Bandung by implementing CO_2 Emission Rate Reduction Simulation (CERRS). The simulation comprises four scenarios, namely substitution of vehicle fuel and the application of smart driving techniques, optimization of waste processing in IWPS, processing 90% of livestock waste into biogas, and green space development of 30% of Bandung City area. Estimated CO_2 emission and absorption rates were calculated for the next 10 years (2021-2030) using the Stella program version 9.0.2. The results showed that without implementing the CERRS, the amount of CO_2 emissions in Bandung in 2030 was estimated to reach 10,983,666.82 tons while implementing the CERRS was 2,361,721.30 tons. Without implementing the CERRS, the estimated amount of CO_2 absorptions in 2030 was 214,235.11 tons, while implementing the CERRS was 2,785,703.11 tons. It is expected that the application of the CERRS could reduce the level of CO2 emissions in Bandung by 78.5% and increase CO2 absorptions by 1,200.3%.

Keywords: CO_2 Emissions, CO_2 Absorptions, CERRS

1. Introduction

The population of Bandung City in 2018 reached 2.5 million people [1] with a population growth rate of 0.72%, making this city a metropolitan. Based on data from the Ministry of Home Affairs of the Republic of Indonesia in 2015, Bandung is the 4th most populated city in Indonesia. The annual increase in urbanization activities caused population expansion in this capital city of West Java province. Indeed, West Java province has experienced urbanization since 2000 [2]. Bandung is known as the city of education, which is one reason for urbanization. It happens both from rural to the city and outside Java to the city.

Population expansion in Bandung caused an increase in population activity and an increasing need for land area. Those activities from industrial, transportation, Liquefied Petroleum Gas (LPG), household, and livestock sectors could change the economy, industrial structure, and also the consumption pattern of the local community. Advances in technology, economic factors, and the human desire to improve their standard of living have caused this [3]. These activities produced byproduct wastes, which increases CO_2 emissions [4]. The vegetation must immediately absorb these CO_2 emissions. But in substance, the increasing need for land as housing area has led to a decrease in green open space. The area of green open space functions as a CO_2 absorber is an imbalance with the CO_2 emission rate, which causes the environmental quality of Bandung to decline.

This study offers a program called the CO_2 Emission Rate Reduction Simulation (CERRS). CERRS consists of four scenario steps, namely: (1) substitution of motorized vehicle fuel and application of smart driving techniques, (2) optimization of waste processing at Integrated Waste Processing Site (IWPS), (3) processing 90% of livestock

DOI: https://doi.org/10.5614/3bio.2021.3.1.4

waste into biogas, and (4) construction of 30% green open spaces of Bandung area. This research predicts CO_2 emissions and emission absorptions in Bandung City without applying CERRS, to predict CO_2 emission and emission absorptions in Bandung City by applying CERRS and CO_2 emission from five CO_2 emitting sectors in the Bandung city.

2. Methodology

2.1. Study Area and Sampling Time

This research was conducted from October 2019 to December 2019. Research activities were carried out in Bandung City, West Java (Figure 1).

2.2. Tools and Materials

This research used ArcMap 10.4.1 software to quantify vegetation greenness, Stella 9.0.2 to simulate a dynamic model of CO_2 emission and absorption in Bandung. The research material used is in the form of secondary data as presented in Table 1.

Figure 1. Bandung city map (Source: google earth)

Table 1 Research materials

Type of Data	Source
Landsat ETM 8 imagery for Bandung City 2009 & 2018 and Sentinel-2 in 2018	earthexplorer.usgs.gov and eos.com
Number of industrial sectors in Bandung City	Badan Pusat Statistik, Neraca Energi Indonesia
Number of vehicles in Bandung City	Badan Pusat Statistik
The amount of LPG consumption in Bandung City	Badan Pusat Statistik
Total population of Bandung City	Badan Pusat Statistik
Number of livestock in Bandung City	Badan Pusat Statistik

2.3. Model concept

This study uses the concept of loss-gain emission from urban population activities. CO_2 emissions resulting from the industrial, transportation, LPG, household, and livestock sectors. Then search for information between these components to get a prediction. The conceptualization model is depicted as a causal loop diagram as shown in Figure 2.

DOI: https://doi.org/10.5614/3bio.2021.3.1.4

2.4. Specific Model

We run the model simulation in Stella 9.0.2 which is divided into six submodels, then map them out as a model.

2.4.1.CO2 Emission and Absorption Model

The CO_2 emission and absorption model describes the entire dynamic system of the resulting emission and CO_2 absorption capacity of Bandung city. "Bandung CO_2 emissions" is the accumulation of emissions from industry, transportation, LPG, household, and livestock. These emissions will affect the city's CO_2 according to the amount and rate of each sector. Accumulated CO_2 emissions in Bandung City will be reduced by "Bandung CO_2 absorptions" originating from vegetation and resulting in remaining unabsorbed CO_2 emissions, marked with "Unabsorbed CO_2 emissions". The CO_2 emission and absorption model could be seen in Figure 3.

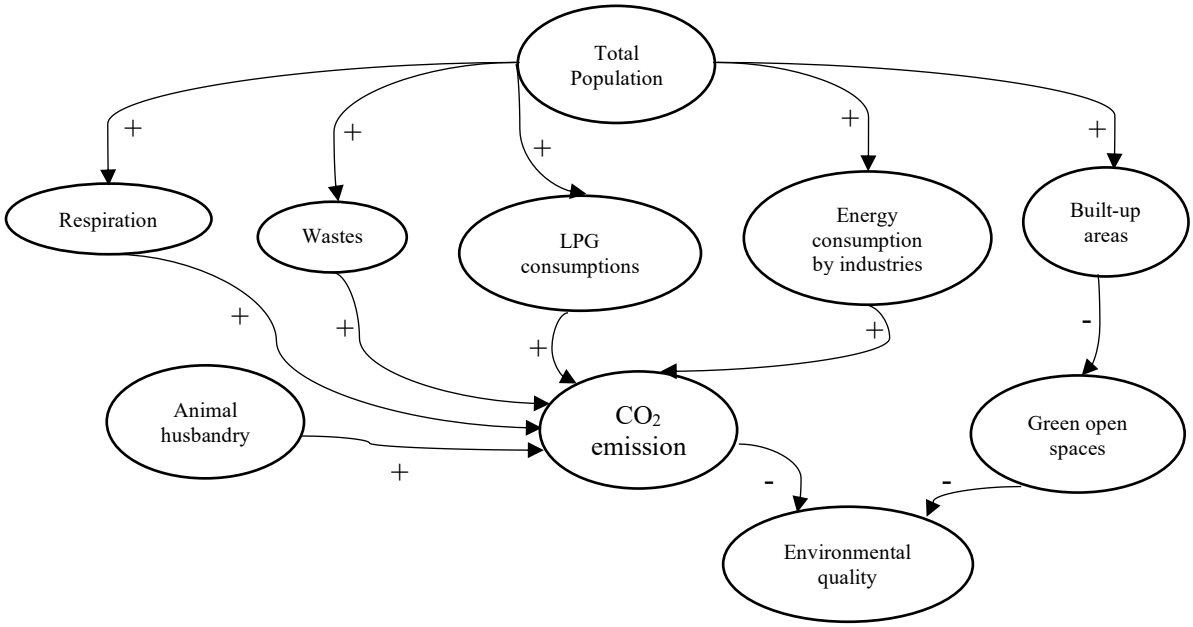

Figure 2. The concept of a model in the form of a causal loop diagram

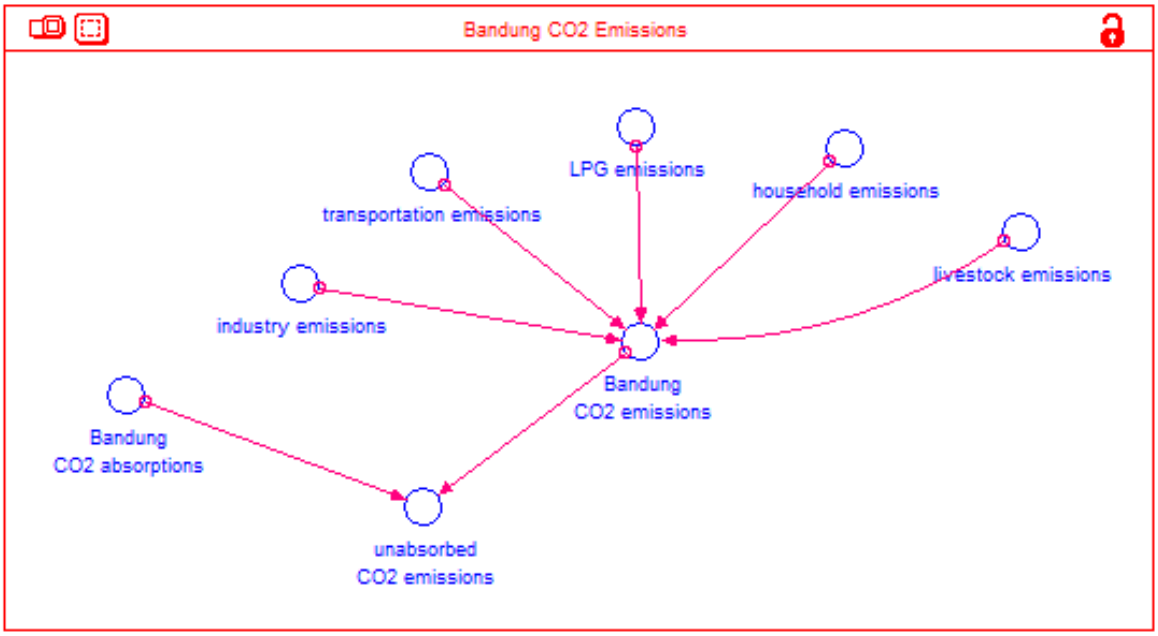

Figure 3. CO_2 emission and absorption model

DOI: https://doi.org/10.5614/3bio.2021.3.1.4

2.4.2.CO2 Absorption Submodel

The CO_2 absorption submodel describes the amount of CO_2 absorption based on the greenness of the land through NDVI quantification, which is equivalent to the absorption capacity of land cover [6] (Table 3). NDVI is calculated through the NDVI algorithm, as seen from Eq. (1). The map is obtained from 2018 Bandung Sentinel-2A imagery downloaded from the eos.com website. The rate of change in the area of land greenness is calculated through the changes in the results of the NDVI images of the Landsat ETM 8 Bandung City in 2009 and 2018.

$$NDVI = \frac{NIR-RED}{NIR+RED} \quad (1)$$

Where:

NIR = reflection in the near-infrared spectrum

RED = reflection in the red range of the spectrum

NDVI results are classified based on the level of greenness of the land according to Permenhut R.I. No: P.12 / Menhut-II / 2012 [5] (Table 2).

The results of NDVI scores were reclassified into five classes [5], where NDVI values ranging from -1 to 1 were converted to 0-100. The rate of increase in green land is assumed to come from the rate of change in the area of greenish land from 2009 to 2018, amounting to 0,00303% per year, and is assumed to have the same rate every year. In the model, each area of green land is multiplied by the respective CO_2 absorption capacity and accumulated into Bandung City's CO_2 absorption. Data and information on the CO_2 absorption submodel could be seen in Table 4 and the CO_2 absorption submodel in the Stella could be seen in Figure 4.

Table 3. CO_2 Absorption Equivalence

Greenness Level of Land	Type of Land Cover (Equivalence)	CO_2 Absorption (t/ha/yr)
No vegetation	Built-up areas	6.12
Very low greenness	Rice fields	12
Low greenness	Grassland	12
Medium greenness	Shrubs	55
High greenness	Trees	569.07

Sources: [5] and [6]

Table 4. Data and information on CO_2 absorption submodel in Bandung City

Greenness Level of Land	Type of Land Cover (Equivalence)	Areas (ha)	CO_2 Absorption (t / ha / yr)
No vegetation	Built-up areas	3,621.27	6.12
Very low greenness	Rice fields	8,968.48	12
Low greenness	Grassland	1,939.53	12
Medium greenness	Shrubs	471.24	55
High greenness	Trees	61.88	569.07

Sources: [5] and [6]

2.4.3.Industry Submodel

The industrial submodel is only based on the amount of natural gas and coal energy used by the industrial sector. The industrial sector that is used is the processing industry, specifically economic activities which include changes both chemically and physically from materials, elements, or components to new products. Processing industry raw materials could come from agricultural, forestry, fishery, mining or quarrying products, and other processing industry activities. In short, the processing industry is a major renewal or change of an item. The industries that are considered are medium and large-scale industries, amounting to 321 units in 2018 [1]. The rate of consumption of natural gas and coal is calculated by reducing the number of processing industries in Bandung, which is 8.86% per year and is assumed to have the same rate every year. CO_2 emissions are obtained through the conversion of data on the amount of energy consumption in the industrial then multiplied by the calorific value and CO_2 emission factor. Data and information on CO_2 emissions from the industrial sector in Bandung could be seen in Table 5. The industrial submodel in Stella could be seen in Figure 5.

2.4.4.Transportation Submodel

The transportation submodel presents four types of motorized vehicles as CO_2 emitters, namely motorbikes, gasoline cars, diesel cars, and buses. CO_2 emissions are obtained through the conversion of data on the amount of energy consumption in the transportation sector then multiplied by the calorific value and CO_2 emission factor. Each type of vehicle has own CO_2 emission factor, as seen in Table 6. The transportation submodel in Stella could be seen in Figure 6.

DOI: https://doi.org/10.5614/3bio.2021.3.1.4

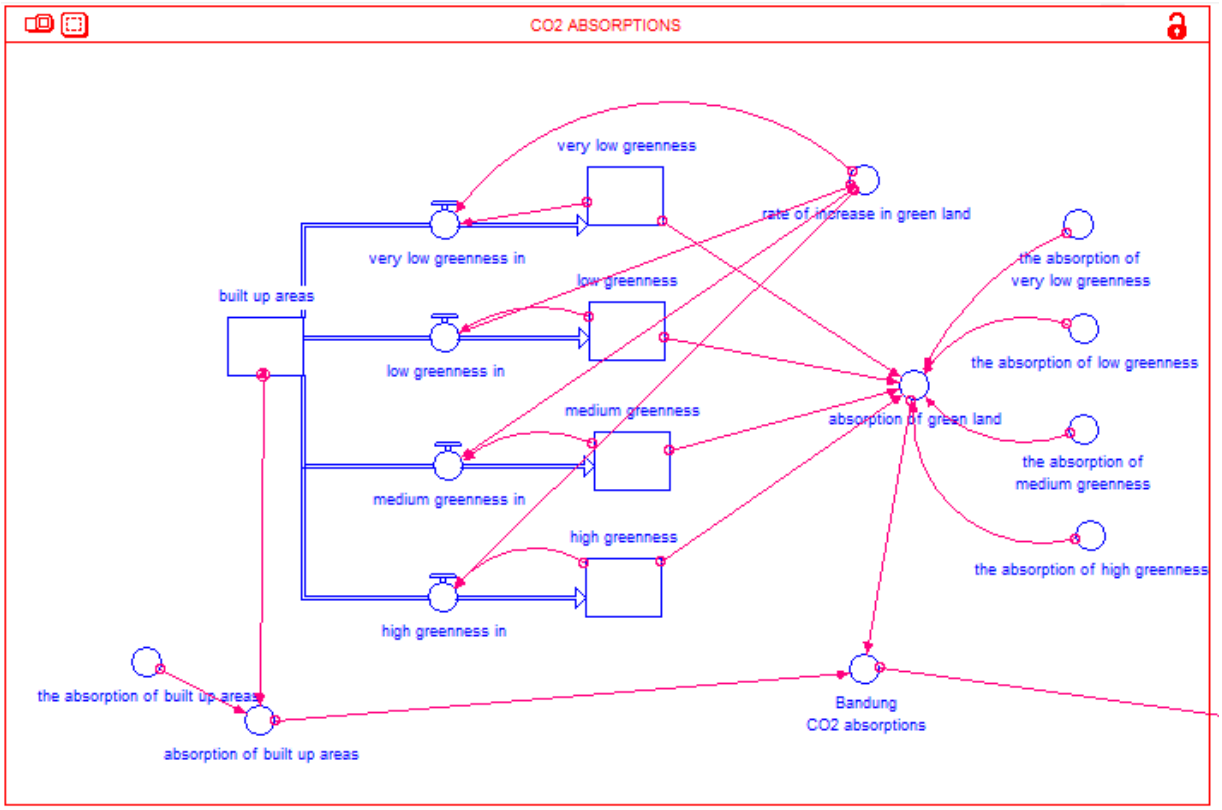

Figure 4. CO_2 absorption submodel

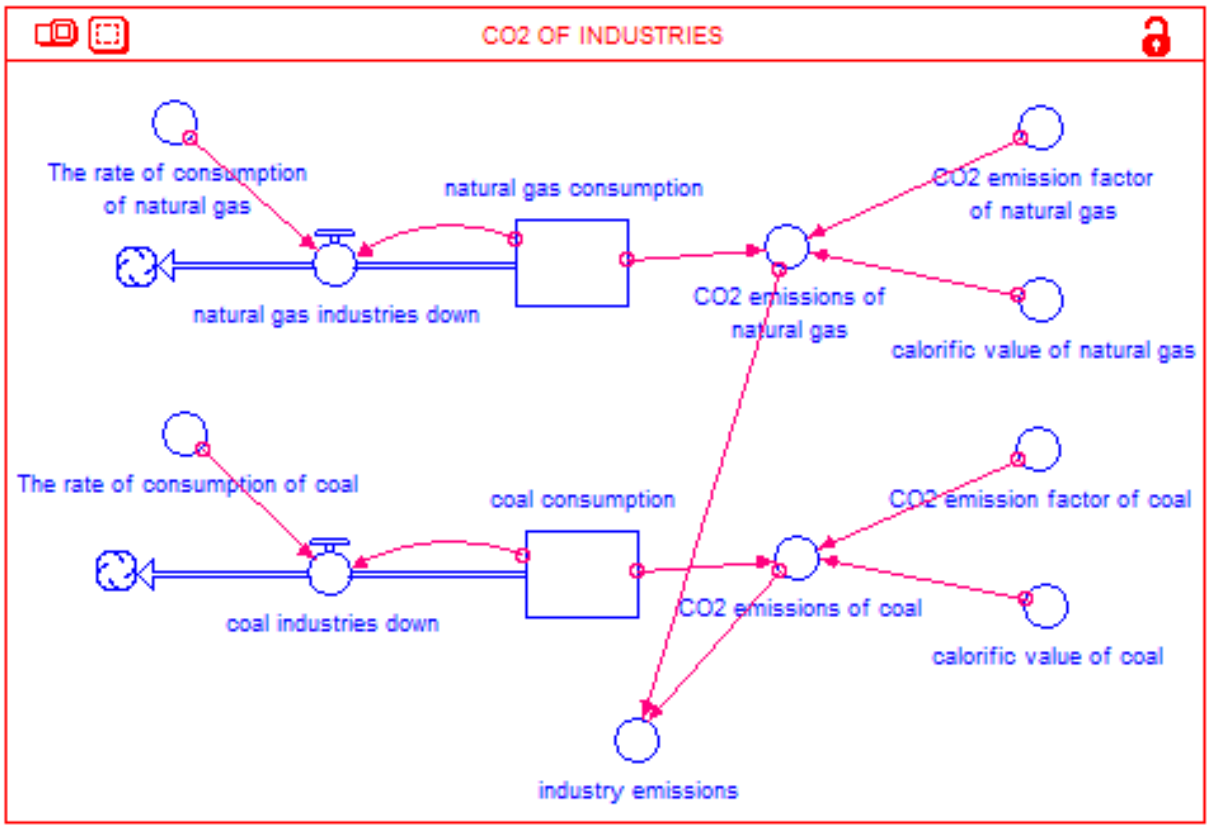

Figure 5. Industry Submodel

DOI: https://doi.org/10.5614/3bio.2021.3.1.4

Table 5. Data and information on industry CO_2 emissions submodel in Bandung City

No	Energy types	Energy consumptions (t)	Calorific value (TJ / t)	CO_2 emission factors (t / TJ)
1	Natural gas	7,675,329.32	$38.5x10^{-3}$	63.1
2	Coal	9,893,000	$18.9x10^{-3}$	96.1

Source: [7]

Table 6. Data and information on transportation CO_2 emissions submodel in Bandung City

Vehicle types	Number of units	The rate of the number of vehicles (% per yr)	Energy consumption (lt / yr / unit)	Calorific value (TJ / L)	CO_2 emission factors (t / TJ)
Motorcycle	1,256,057	8.96	550.8	$33x10^{-6}$	69,300
Gasoline car	402,649	5.99	2320.7	$33x10^{-6}$	69,300
Diesel car	73,576	3.92	1813.2	$36x10^{-6}$	74,100
Bus	6,390	4.2	4263.6	$36x10^{-6}$	74,100

Sources: [7] and [8]

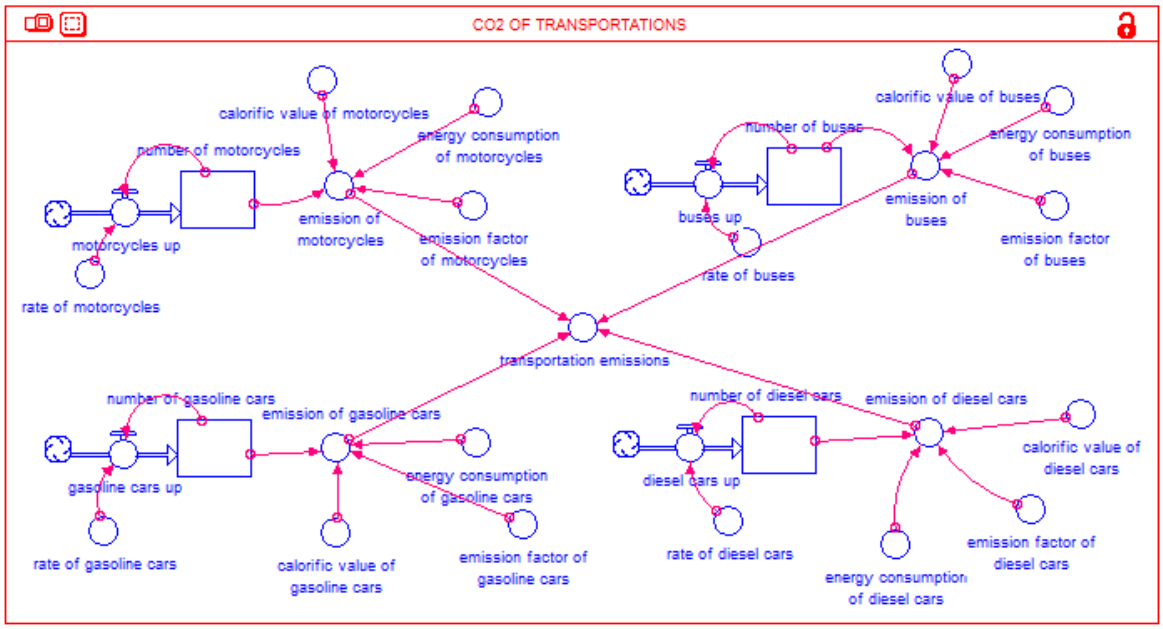

Figure 6. Transportation Submodel

2.4.5.Liquid Petroleum Gasses Consumption Submodel

This submodel calculates Liquid Petroleum Gasses (LPG) which is assumed to be used by all households in Bandung City, with 955,550 heads of households (HH) in 2018 [11]. The city of Bandung experienced an increase in the rate of LPG consumption by 21.92% with an emission factor of 63.1 tons / TJ and a heating value of 0.0461 TJ / ton [8]. CO_2 emissions are obtained through the conversion of data on the amount of energy from LPG consumption in the household then multiplied by the heating value and CO_2 emission factor. LPG consumption submodel in Stella could be seen in Figure 7.

2.4.6.Household Submodel

The household submodel is the amount of CO_2 emissions from respiration and waste generated by residents in Bandung City. The total population of Bandung in 2018 was 2,503,708 people, assuming the amount of waste produced by each person is 0.1825 tonnes/year [10]. A higher population means a higher amount of waste. Bandung City is assumed to experience the same population growth rate every year of 0.72% with a respiration CO_2 emission factor of 0.34 tons/person/year and CO_2 emission factor per tonne of waste is 2.56 tons [10]. CO_2 emissions are obtained through the conversion of data by multiplying the amount of population and waste to each of the CO_2 emission factors. The household submodel in Stella could be seen in Figure 8.

DOI: https://doi.org/10.5614/3bio.2021.3.1.4

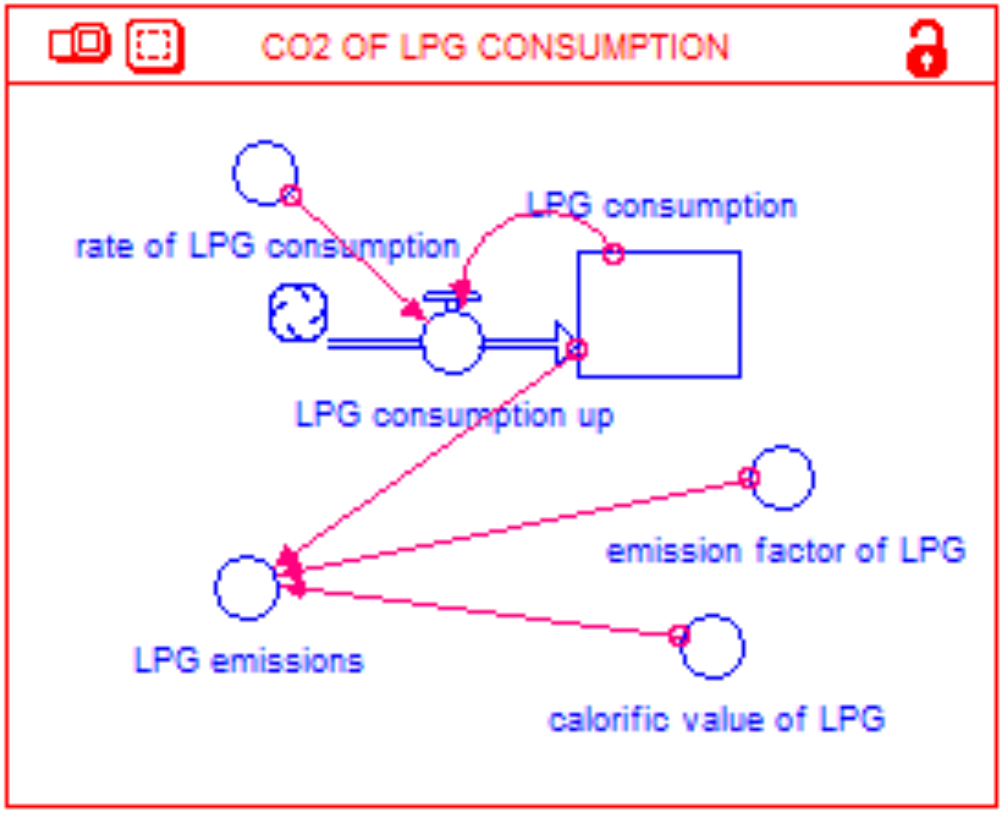

Figure 7. LPG Consumption Submodel

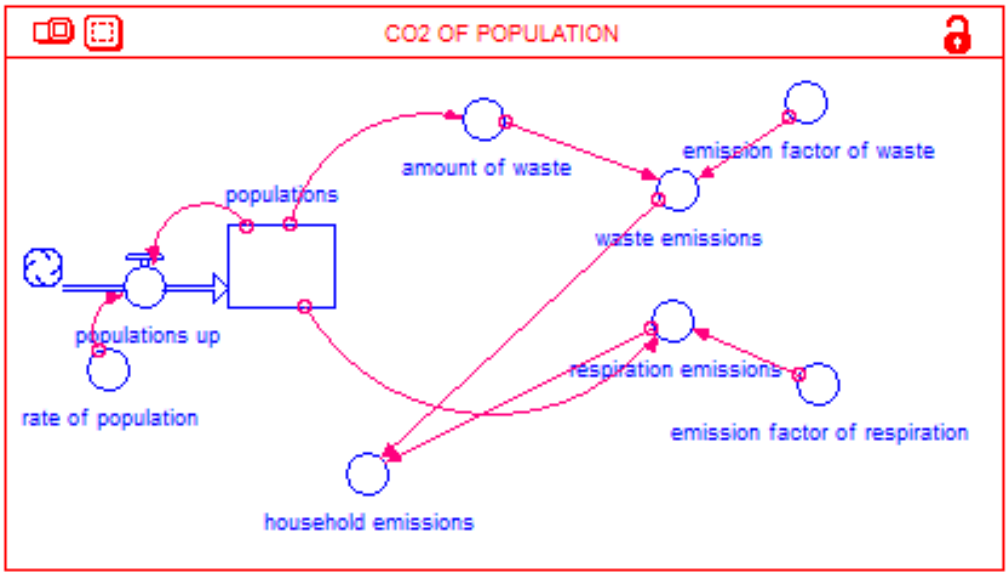

Figure 8. Household Submodel

2.4.7.Livestock Submodel

The livestock submodel is quantified from the emission of enteric fermentation and manure management. The rate of increase and decrease in the number of livestock in Bandung is assumed to be the same every year. CO_2 emissions are obtained through the conversion of data by multiplying the amount of each type of livestock to the CO_2 emission factor. Data and information on the livestock sector could be seen in Table 7. The livestock submodel in Stella could be seen in Figure 9.

DOI: https://doi.org/10.5614/3bio.2021.3.1.4

Table 7. Data and information on livestock CO_2 emissions submodel in Bandung City

Types of livestock	Total	The rate of the number of livestock (%)	CO_2 emission factors (t / head / yr)
Goat	582	4.19	0.12
Sheep	34,684	6.41	0.12
Dairy cows	721	-5.3	2.12
Beef cattle	1,640	19.48	1.1
Buffalo	122	-0.88	1.31
Horse	168	2.68	0.46
Free-range chicken	498,307	22.18	0.00046
Broiler chicken	369,345	18.87	0.00046
Duck	60,647	10.38	0.00046

Sources: [7] and [10]

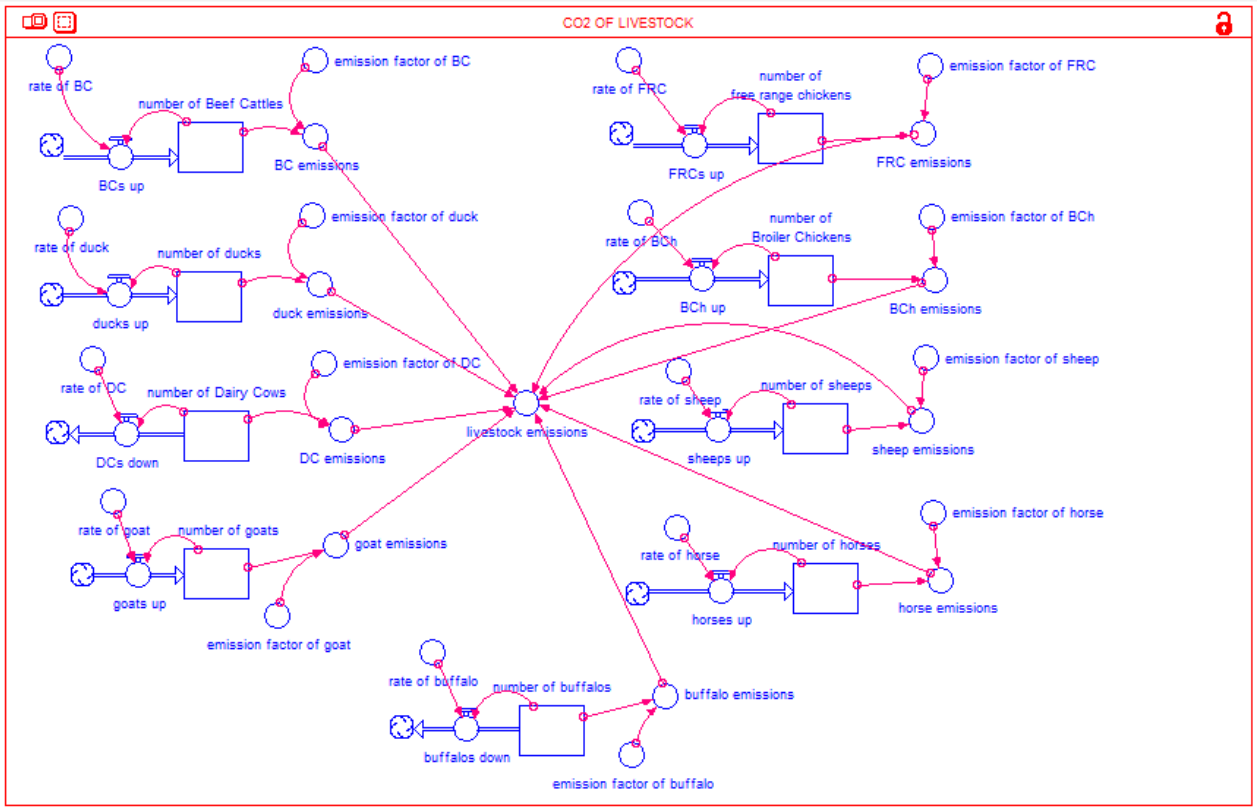

Figure 9. Livestock Submodel

2.5. *Assumptions and Research Limitations*

The assumptions and limitations used in this study are:

1. The model uses a closed approach system, meaning that the calculated CO_2 emission only comes from the Bandung City area, CO_2 outside the Bandung City area is ignored, including the influence of the wind.
2. CO_2 is only absorbed by vegetation in Bandung city.

The rate of increase or decrease in energy from the industrial, LPG, household, transportation, and livestock sector is constant every year.

3. Results and discussion

3.1. *Model Simulation*

Models are applied to estimate CO_2 emissions and absorptions from 2021 to 2030. 2030 is a year that is following the Nationally Determined Contribution (NDC) document related to the Paris Agreement. Indonesia has an ambitious commitment to reduce greenhouse gas (GHG)

DOI: https://doi.org/10.5614/3bio.2021.3.1.4

emissions by 29% below the level of business as usual (BaU) by 2030 [12]. Estimation of CO_2 emissions and absorptions divided into two categories, namely without CERRS intervention and with CERRS intervention. Simulation of CO_2 emission and absorption in Bandung City without CERRS intervention results from Business as Usual, while the simulation of CO_2 emission and absorption with CERRS intervention consists of four scenario stages, namely (1) substitution of motorized vehicle fuel and application of smart driving techniques, (2) optimization of waste processing at IWPS, (3) processing 90% of livestock waste into biogas and (4) building green open space covering 30% of the area of Bandung City.

3.1.1. Estimation of Emissions, Absorptions and Unabsorbed CO2 Emissions without CERRS Simulation Package in Bandung City

Based on the results of the estimation model, the amount of CO_2 emission in Bandung City had a much greater value than its absorption. In 2021, CO_2 emissions in Bandung were 6,958,801.58 tons and would continue to increase to reach 10,983,666.82 tons in 2030, while CO_2 absorption in Bandung City in 2021 was only 214,201.83 tons and increased slightly to become 214,235.11 tons in 2030. Graph and result of CO_2 emission, absorption, and unabsorbed emissions estimate in Bandung City in 2021 and 2030 presented in Table 8 and Figure 10.

Table 8. Estimation using Stella

Year	CO_2 Emissions (t)	CO_2 Absorptions (t)	Unabsorbed CO_2 Emissions (t)
2021	6,958,801.58	214,201.83	6,744,599.75
2030	10,983,666.82	214,235.11	10,769,431.71

Figure 10. Graph of emissions, absorptions, and unabsorbed CO_2 emissions in Bandung City without CERRS simulation package

3.1.2. Estimation of Emissions, Absorptions and Unabsorbed CO2 Emissions by Applying the Phase I Scenarios: Vehicle Fuel Substitution and Smart Driving Techniques

In this scenario, the substitution of diesel fuel to B30 fuel and gasoline fuel to Gas Fuel (BBG) was carried out. B30 fuel is a mixture of 70% diesel fuel and 30% Fatty Acid Methyl Esther (FAME) which is obtained from palm oil. The application of B30 could reduce the composition of diesel use by 30%. FAME is biodiesel that has a higher flash point than diesel so that it affects its low combustibility. Biodiesel is also a cleaner fuel than diesel because it does not contain sulfur and benzene compounds [13]. In the application of BBG as a substitute for gasoline, the resulting emissions are only 10%. This data was obtained based on the results of a trial conducted by the Committee for the Elimination of Lead

DOI: https://doi.org/10.5614/3bio.2021.3.1.4

Gasoline on Euro-2, Euro-3, and Euro-4 vehicles, namely that emissions from BBG are 90% lower than fuel [14].

Smart driving is a driving technique that combines eco-driving, safe driving, and defensive driving. The smart driving technique is simply an efficient, environmentally friendly, safe, comfortable, ethical, and dignified driving method. Some steps in implementing this method are using the highest gear position with low engine speed (2000-2500 rpm), reducing the frequency of acceleration and braking, adjusting tire pressure to those recommended by the vehicle manufacturer, using the hand brake when stopping, and maintaining the vehicle periodically. The results of the training in smart driving techniques that have been carried out in Semarang, Tegal, and Bandung cities have shown a decrease in the level of fuel consumption, which varies from 0 to 40% [15]. In this scenario, 40% applied a reduction in fuel consumption, so that the CO_2 emission reduction in Bandung was 70% and unabsorbed CO_2 emission in Bandung was 71%. The estimation results of this scenario is presented in Figure 11 and Table 9.

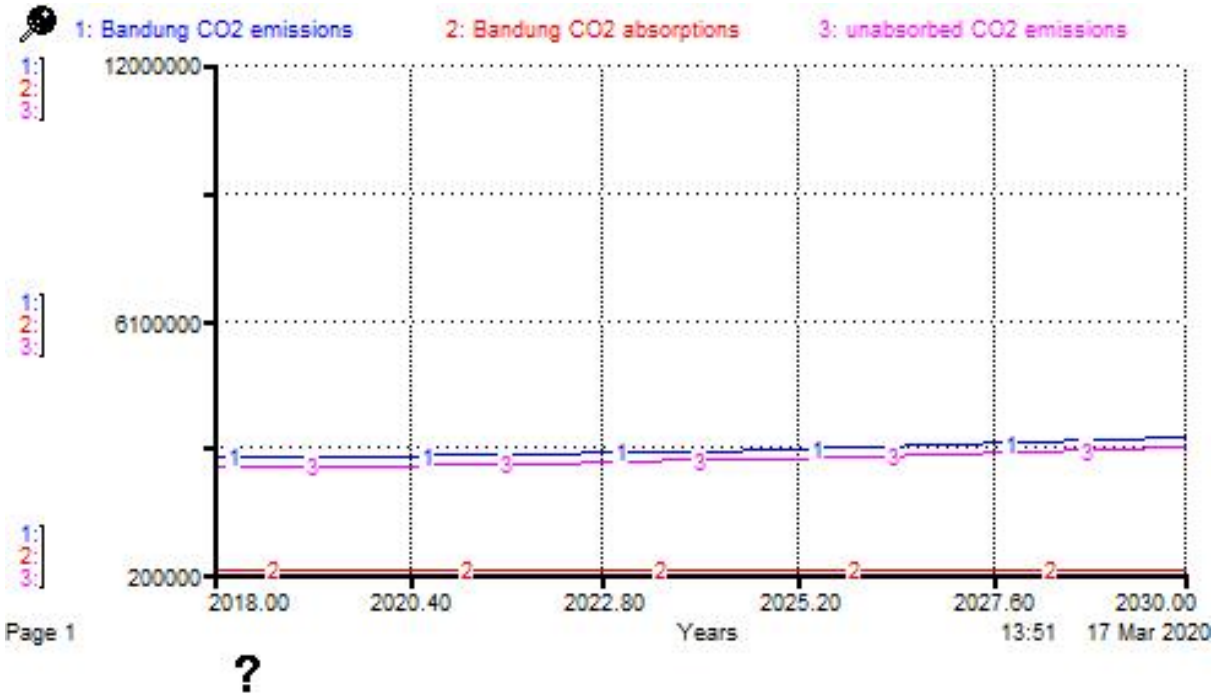

Figure 11. Graph of emission, absorption, and unabsorbed CO_2 emissions in Bandung City by applying the phase I scenarios

Table 9. Estimation using Stella

Year	CO_2 Emissions (t)	CO_2 Absorptions (t)	Unabsorbed CO_2 Emissions (t)
2021	2,901,338.81	214,201.83	2,687,136.98
2030	3,332,409.68	214,235.11	3,118,174.57

3.1.3. Estimation of Emissions, Absorptions and Unabsorbed CO2 Emissions by Applying the Phase II Scenario: Scenario I + Optimization of Waste Management at IWPS

Integrated Waste Processing Site (IWPS) is a place where activities are followed through, sorting, reusing, recycling, reprocessing, processing, and possibly the end [16]. Research at IWPS Janti Village, Waru District, Sidoarjo Regency shows that IWPS in Janti Village has a waste reduction potential of 75%. This is done by processing organic waste into compost, reusing inorganic waste, and recycling inorganic waste into flakes [17]. The second stage scenario could reduce CO_2 emissions in Bandung City by 78% and the unabsorbed CO_2 emissions in Bandung City by 80%. The estimation from this scenario is presented in Figure 12 and Table 10.

DOI: https://doi.org/10.5614/3bio.2021.3.1.4

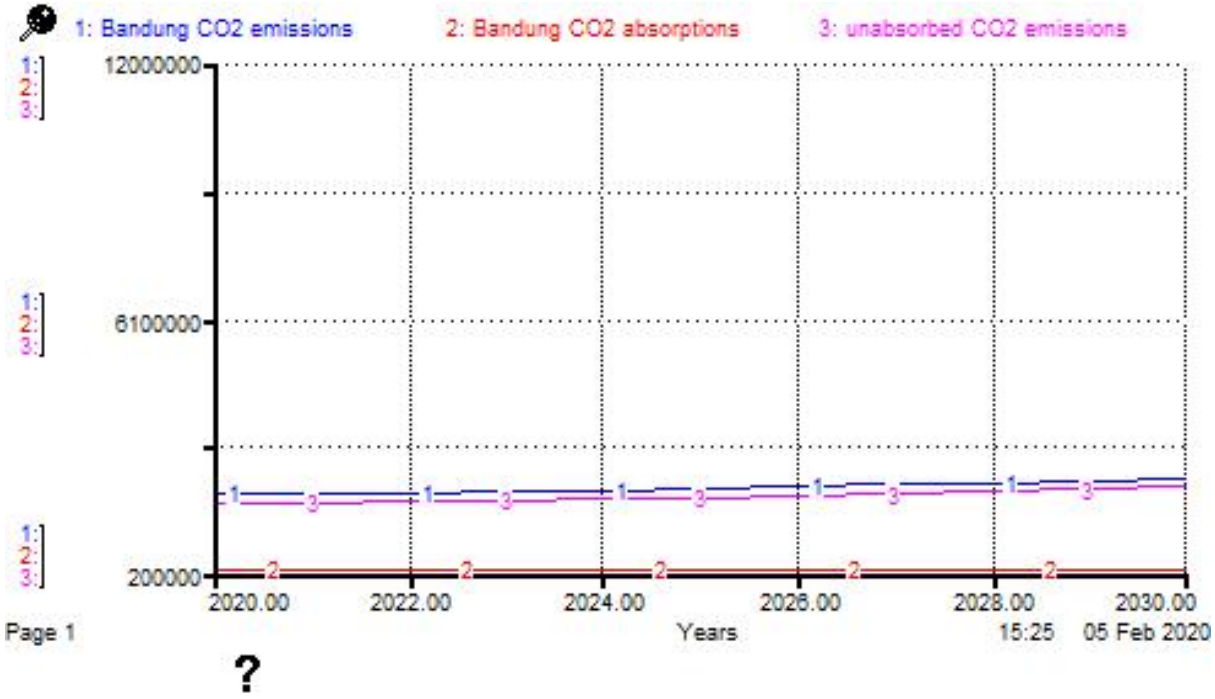

Figure 12. Graph of emission, absorption, and unabsorbed CO_2 emissions in Bandung City by applying the phase II scenarios

Table 10. Estimation using Stella

Year	CO_2 Emissions (t)	CO_2 Absorptions (t)	Unabsorbed CO_2 Emissions (t)
2021	2,007,625.75	214,201.83	1,793,423.92
2030	2,379,604.09	214,235.11	2,165,368.98

3.1.4. Estimation of Emissions, Absorptions, and Unabsorbed CO2 Emissions by Applying the Phase III Scenario: Scenario I + II + Processing 90% of Livestock Waste into Biogas

Biogas comes from decomposing organic matter carried out by microorganisms under anaerobic conditions. The main organic material as a source of biogas production is livestock manure such as cattle, buffalo, pigs, horses, and poultry. Compost from two cows or six pigs could produce biogas in less than two m^3. In addition, one m^3 of biogas is also equivalent to 0.46 kg of LPG or 0.62 liters of kerosene [18]. Scenario stage III could reduce CO_2 emissions in Bandung City by 78.5% and the unabsorbed CO_2 emissions in Bandung City by 80%. The estimation results from this scenario is presented in Figure 13 and Table 11.

3.1.5. Estimation of Emissions, Absorptions and Unabsorbed CO2 Emissions by Applying the Phase IV Scenario: Scenario I + II + III + Development of green open spaces covering an area of 30% of the Bandung City Area

The results of estimating CO_2 emissions in scenario I-IV showed that CO_2 emissions in Bandung City were still not fully absorbed, so efforts still need to be made to achieve carbon neutrality. Carbon-neutral is a state when CO_2 emissions could be absorbed so that emissions are zero. Green Open Space (GOS) in Bandung City has only reached 12% of the area of Bandung City [19], whereas based on Law Number 26 of 2007 concerning Spatial Planning Article 29 paragraph 2 provides that reporting of green open space in the city area is at least 30% of the total area of the city. The proportion of 30% green open space from the area of Bandung City is 5.019,3 Ha. In this scenario, a 30% green open space was built with CO_2 absorption increasing every 4 years. The stage IV scenario was able to increase the absorption of CO_2 emissions in Bandung City by 1,200.3% and reduced the remaining CO_2 emissions in Bandung City by 103,9%. Through the application of stage IV, carbon-neutral could be achieved by 2029. The estimation results of this scenario is presented in Figure 14 and Table 12.

3.1.6. Estimation of CO2 Emissions in Bandung City

After going through stages I-IV, an estimate of the amount of CO_2 emissions in Bandung was obtained based on the five sectors that are provided in Table 13 (sorted from the least contributing sector to the largest).

DOI: https://doi.org/10.5614/3bio.2021.3.1.4

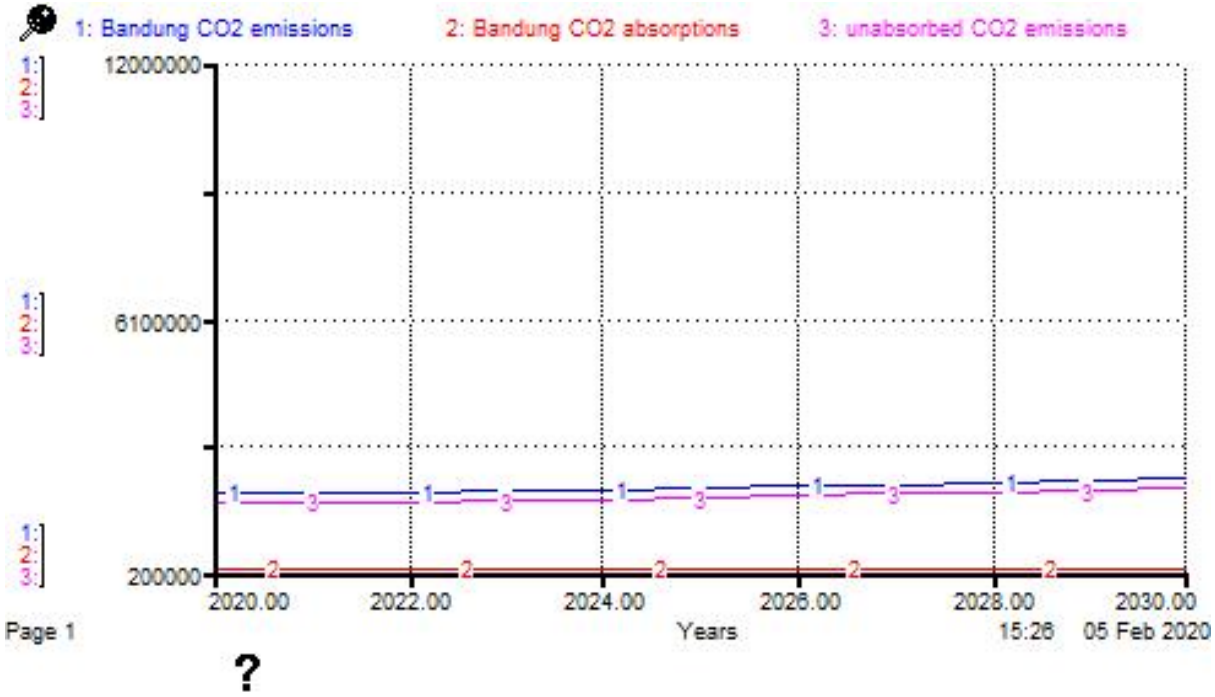

Figure 13. Graph of emission, absorption, and unabsorbed CO_2 emissions in Bandung City by applying the phase III scenarios

Table 11. Estimation using Stella

Year	CO_2 Emissions (t)	CO_2 Absorptions (t)	Unabsorbed CO_2 Emissions (t)
2021	1,996,609.84	214,201.83	1,782,408.01
2030	2,361,721.30	214,235.11	2,147,486.19

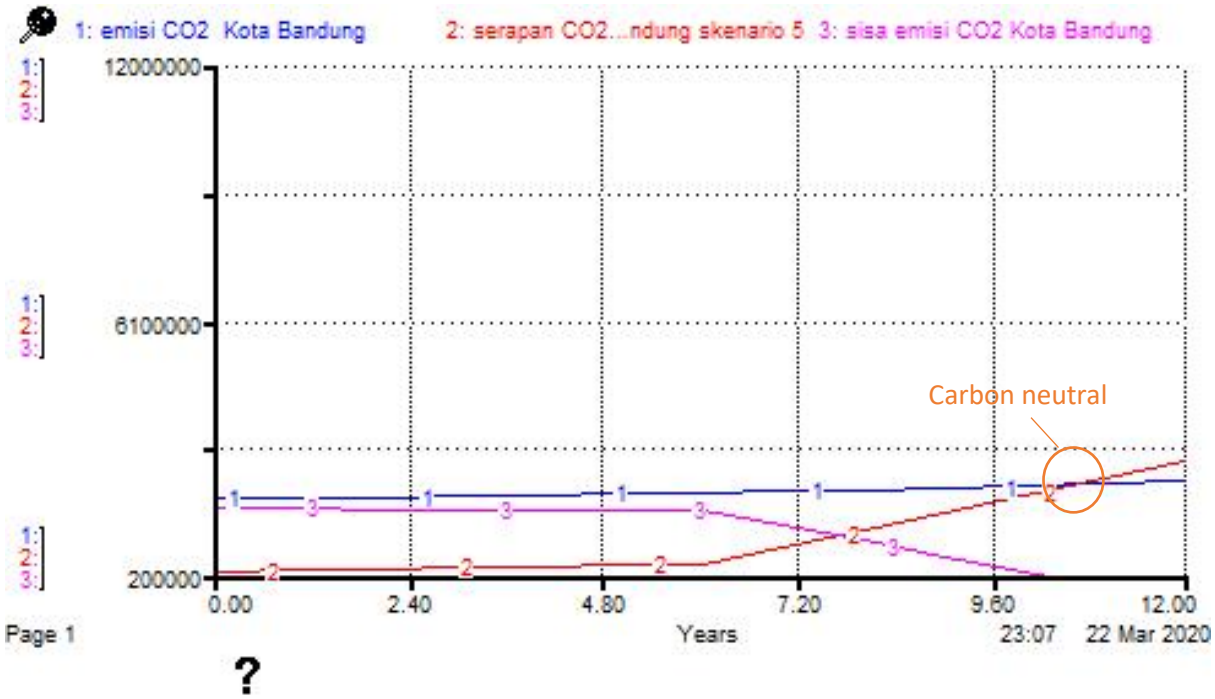

Figure 14. Graph of emission, absorption, and unabsorbed CO_2 emissions in Bandung City by applying the phase IV scenarios

DOI: https://doi.org/10.5614/3bio.2021.3.1.4

Table 12. Estimation using Stella

Year	CO_2 Emissions (t)	CO_2 Absorptions (t)	Unabsorbed CO_2 Emissions (t)
2021	1,996,609.84	1,667,174.97	329,434.87
2030	2,361,721.30	2,785,703.11	-423,981.81

Table 13. Estimated CO2 emissions in Bandung City based on five sectors

Sekctor	Estimation of CO_2 Emissions (t)
Livestocks	1,612.84
LPG	3,730.73
Industries	109,794.84
Transportations	1,000,065.41
Households	1,246,317.49

The effects of estimating CO_2 emissions showed that the application of the CERRS package could reduce CO_2 emissions in the household sector by 43.4%, the transportation sector by 88.44%, and the livestock sector by 90%. Since the present study provides useful information about the benefit of increasing green open space in a city as well as applying some programs for reducing CO_2 emissions, the study suggests it is necessary to make policies that could give the best result and convenient implementation for the community. The dynamic simulation model of CO2 emissions and absorptions like this study did have to be established and improved as soon as possible. It could help the decision-maker have complete data for the program which gives the emission highest.

4. Conclusion

Based on the results, several points can be concluded, i.e.,

1. The number of CO_2 emissions in Bandung without CERRS intervention was estimated to be 6,958,801.58 tons in 2021 and 10,983,666.82 tons in 2030, the number of CO_2 absorption in Bandung without CERRS intervention was estimated to be 214,201.83 tons in 2021 and 214,235.11 tons in 2030.
2. The number of CO_2 emission in Bandung without CERRS intervention was estimated to be 1,996,609.84 tons (down 71.3%) in 2021 and 2,361,721.30 tons (down 78.5%) in 2030, the number of CO_2 absorption in Bandung with CERRS intervention was estimated to be 1,667,174.97 tons (up 678%) in 2021 and 2,785,703.11 tons (up 1,200.3%) in 2030.
3. CO_2 emissions in 2030 with CERRS intervention are thought to come from the household sector (1,246,517.49 tons), followed by the transportation sector (1,000,065.41 tons), the industrial sector (109,794.84 tons), LPG consumption (3,730.73 tons), and the livestock sector (1,612.84 tons).

References

[1] Statistics of Bandung Municipality. Bandung Municipalitiy in Figures 2019. [Internet]. Bandung: BPS Kota Bandung; 2019 [cited 2019 September 25]. Available from: https://bandungkota.bps.go.id/publication/2019/08/16/bd52ff3d885d75c04ddcfb17/kota-bandung-dalam-angka-2019.html

[2] Badan Pusat Statistik. Kebutuhan Data Ketenagakerjaan untuk Pembangunan Berkelanjutan. [Internet]. Direktur Statistik Kependudukan dan Ketenagakerjaan Badan Pusat Statistik; 2019 [cited 2019 September 25]. Available from: https://www.ilo.org/wcmsp5/groups/public/@asia/@ro-bangkok/@ilo-jakarta/documents/presentation/wcms_346599.pdf

[3] Agung P, Hartono D and Awirya A. Pengaruh Urbanisasi terhadap Konsumsi Energi dan Emisi CO_2: Analisis Provinsi di Indonesia. Jurnal Ekonomi Kuantitatif Terapan [Internet]. 2017 May [cited 2019 August 20];10(1):9-17. DOI: https://dx.doi.org/10.24843/JEKT.2017.v10.i01.p02

[4] Pratama, Riza. Efek Rumah Kaca terhadap Bumi. Buletin Utama Teknik [Internet]. 2019 Jan [cited 2019 August 20];14(2):120-126. Available from: https://jurnal.uisu.ac.id/index.php/but/article/view/1096

[5] Menteri Kehutanan Republik Indonesia. Peraturan Menteri Kehutanan Republik Indonesia Nomor P.12/Menhut-II/2012 [Internet]; 2012 [cited 2019 September 2]. Available from: https://www.forda-mof.org/files/P.12_2012_RencouldaTeknikRehabilitasiHutanLahanDAS_.pdf

DOI: https://doi.org/10.5614/3bio.2021.3.1.4

[6] Ludang, Yetrie. Keragaman Hayati Ruang Terbuka Hijau Berbasis Pengetahuan Ulayat di Kota Palangkaraya. Tangerang: An1mage; 2017.

[7] Boer, R., Dewi, R. G., Siagian, U. W. R., Ardiansyah, M., Surmaini, E., Ridha, D. M., Gani, M., Rukmi, W. A., Gunawan, A., Utomo, P., Setiawan, G., Irwani, S., Parinderati, R. Pedoman Penyelenggaraan Inventarisasi Gas Rumah Kaca Nasional [Internet]. Jakarta: Kementrian Lingkungan Hidup; 2012 [cited 2019 November 27]. Availbale from: https://kemenperin.go.id/download/18859

[8] Dinas Lingkungan Hidup Provinsi DKI Jakarta. Inventarisasi dan Penyusunan Profil Emisi Gas Rumah Kaca Provinsi DKI Jakarta [Internet]. 2018 [cited 2019 November 18]. Available from: https://lingkunganhidup.jakarta.go.id/wp-content/uploads/2019/10/2018-Laporan-AkhirInventarisa si-GRK.pdf.

[9] Dinaryanto, Okto. Pengaruh Jenis Burner terhadap Konsumsi Bahan Bakar LPG. Jurnal Angkasa [Internet]. 2010 April [cited 2019 November 20];2(1):77-84. Available from: http://stta.ac.id/data_lp3m /Okto.pdf

[10] Nur, Rizka Permatayakti. Model Dinamika Sistem Penyerapan Emisi CO_2 di Kota Bogor [Thesis]. Departemen Manajemen Hutan, Fakultas Kehutanan, Institut Pertanian Bogor; 2014.

[11] Badan Pusat Statistik Provinsi Jawa Barat. Provinsi Jawa Barat dalam Angka 2019 [Internet]. BPS Provinsi Jawa Barat; 2019 [cited 2019 November 18]. Available from: https://jabar.bps.go.id/publication/2019/08/16/b0a6b953b7 6cbe2239dc912d/provinsi-jawa-barat-dalam-angka-2019.html

[12] Direktorat Jenderal Pengendalian Perubahan Iklim. Kontribusi Penurunan Emisi GRK Nasional, Menuju NDC 2030 [Internet]; 2017 [cited 2019 November 18]. Available from: http://ditjenppi.menlhk.go.id/berita-ppi/3150-kontribusi-penurunan-emisi-grk-nasional,-menuju-ndc-2030.html.

[13] Djamin dan Wirawan. Pengaruh Komposisi Biodiesel terhadap Kinerja Mesin dan Emisi Gas Buang. Jurnal Teknik Lingkungan [Internet]. 2010 September [cited 2019 November 18];11(3):381-387. Available from: http://ejurnal.bppt.go.id/index.php/JTL/article/view/1183

[14] Alfarizi, Moh Khory. BBG 90 Persen Lebih Rendah Emisi daripada BBM, Bisa Setara Euro6 [Internet]. 2019 [cited 2019 November 18]. Available from: https://tekno.tempo.co/read/1253417/ bbg-90-persen-lebih-rendah-emisi-daripada-bbm-bisa-setara-euro6.

[15] Sinaga, Nazaruddin. Pelatihan Teknik Mengemudi Smart Driving untuk Menurunkan Emisi Gas Rumah Kaca dan Menekan Biaya Transportasi Angkutan Darat. Proceeding Seminar Nasional Tahunan Teknik Mesin XII (SNTTM XII) [Internet]. 2013 October [cited 2019 November 18]. Available from: http://eprints.undip.ac.id/75836/

[16] Peraturan Pemerintah Republik Indonesia Nomor 81 Tahun 2012. Peraturan Pemerintah Republik Indonesia Nomor 81 Tahun 2012 tentang Pengelolaan Sampah Rumah Tangga dan Sampah Sejenis Sampah Rumah Tangga [Internet]; 2012 [cited 2019 November 18]. Available from: https://peraturan.bpk.go.id/Home/Details/5295/pp-no-81-tahun-2012

[17] Pertiwi, Puspita Cahyani. Alternatif Optimasi Pengolahan Sampah di TPST Desa Janti, Kecamatan Waru, Kabupaten Sidoarjo [Thesis]. Teknik Perencouldaan Wilayah dan Kota, Universitas Brawijaya; 2019.

[18] Hariansyah. Pemanfaatan Kotoran Ternak Sapi sebagai Penghasil Biogas. Jurnal Teknik Protech [Internet]; 2009 April. [cited 2019 November 19];8(1). Available from: https://www.researchgate.net/publication/322128695

[19] Ispranoto, Tri. Ruang Terbuka Hijau di Bandung Masih Kurang 3.000 Hektare [Internet].; 2019 [cited 2019 November 18]. Available from: https://news.detik.com/berita-jawa-barat/d-4408922/ruang-terbuka-hijau-di-bandung-masih-kurang-3000-hektare.

DOI: https://doi.org/10.5614/3bio.2021.3.1.4

3BIO: Journal of Biological Science, Technology and Management 3(1):42-55
e-ISSN: 2655-8777 http://journals.itb.ac.id/index.php/3bio

Optimal Feeding Frequency on the Growth Performance of Whiteleg Shrimp (*Litopenaeus vannamei*) during Grow-out Phase

Alif Ihsanario, Ahmad Ridwan*

School of Life Sciences and Technology, Bandung Institute of Technology, Indonesia.

Corresponding author; e-mail: ridwan@sith.itb.ac.id
Received 13 April, 2021
Accepted for publication 24 June, 2021

Abstract

Whiteleg shrimp (*Litopenaeus vannamei*) is a fisheries commodity that has experienced a vast increase in production since the early 1970s. As one of the largest contributors to the global shrimp market, Indonesia always tried to increase its shrimp production. To fulfill the global market demand, whiteleg shrimp farmers have met with countless obstacles, e.g., sub-optimal growth problem. Optimal feed management is one of the determining factors that account for the growth and production efficiency of whiteleg shrimp. Feed management practices include feeding frequency, methods of feed monitoring, and controlling. This literature review aims to provide an insight into the optimal feeding frequency for the growth, survival, and feed efficiency of whiteleg shrimp production. The method used for this review was a narrative review approach following the PRISMA scheme for literature sorting, which includes identification, screening, eligibility test, and inclusion. There were eight primary literatures from journals with H indices of 18, 50, 55, 72, 80, and 164 (four articles from Q1 journals and three from Q2 journals) and one article without index. Data analysis revealed that the growth rate was significantly affected by the feeding frequency of on-demand feeding system (AQ1) ($P < 0.05$), although no significant difference was found in regards to the survival rate and the FCR ($P > 0.05$). The optimal feeding frequency for industrial-scale shrimp production was found in the on-demand feeding system (AQ1).

Keywords: frequency, feed, growth, survival, FCR, *Litopenaeus vannamei*

1. Introduction

During five years of 2013 - 2017, The Central Statistics Department (Badan Pusat Statistik) has noted an average annual growth of 6.43% on whiteleg shrimp (*L. vannamei*) export. According to the Ministry of Oceanography and Fisheries' data, the export volume from 2017 alone amounted to 147 thousand tons and increased in the following year up to 180 thousand tons [1]. In 2018, Indonesia is the 6th largest exporter of whiteleg shrimp on a global scale. The global market volume of shrimps amounts to 4.66 million tons in 2018, with the whiteleg shrimp being the main commodity. According to Research and Markets [2], the growth of global shrimp market is currently at a CAGR (compound annual growth rate) of 3.7% and the volume is predicted to reach 5.83 million tons in 2024. This indicates a vast development in the fisheries industry, especially in regards to whiteleg shrimp commodity. In response to that opportunity, the Ministry of Oceanography and Fisheries initiated a program called '*Percepatan Pengembangan Tambak Udang Nasional,*' aimed to accelerate the production of whiteleg shrimp to better equip Indonesia to compete in the global market, with a target of 1.29 million tons of product by 2024 [1].

Feed is one of the biggest contributory components in the success or failure of shrimp farming, with its share as the main source of balanced nutrition for shrimp. In a study by Tacon & Metian [3], in 2012 shrimp feed was in the third position (6.18 million tons) of the largest commodity feed production globally, after the first order of carp feed (11.03 million tons) and both tilapia feed (6.67 million tons). In each report on the operation of commodity cultivation, it can be ascertained that feed is the largest contribution to operational costs, at least 50-60% of the total costs incurred per cycle [4]. In addition to being named the biggest factor in economic efficiency, improper feed management is the main cause of water quality degradation in aquaculture, which will indirectly require more maintenance or mitigation costs. Boyd et al.

DOI: https://doi.org/10.5614/3bio.2021.3.1.5

[5] estimated that only about 10-30% of nutrients in feed are absorbed by the digestive system of commodity animals, while the rest is trapped in water in the form of untouched feed, feces, or excretion products.

Using feed with balanced nutrition and implementing feed management is the key to efficient cultivation economically and environmentally friendly [6]. In general, it has been agreed that the use of high-quality feed is highly recommended because the operational costs will be more efficient. After all, the absorption of nutrients will be more optimal and the accumulation of nutrients in the water will be much reduced. Shipton & Hasan [7] found that feed with a formulation that is not under the nutritional needs of commodity animals will lead to inefficient cultivation and increase production costs. The use of high-quality feed with appropriate formulations is a prerequisite for profitable cultivation, but ultimately the success of cultivation will depend on the application of proper feed management [8, 9].

Effective feed management strategy requires the consideration of the shrimp's physiology on the feeding behaviour and digestion [8]. According to Cardona et al. [10], feeding frequency affects enzymatic activity in shrimp's digestion, which will accelerate the digestion process and ultimately the shrimp's growth. The study conducted by Peixoto et al. [11] have proven that feeding frequency affects digestive activity and whiteleg shrimp's growth in the nursery phase. Feeding frequency has been reported to cause an increase in shrimp's performance, although it is yet to be clear whether only one or more factors are involved, e.g., feed waste reduction or the reduced degradation of water quality [12].

Despite studies regarding feeding frequency being conducted since the late '90s, for example, the study done by Velasco et al in 1999 [13], no indisputable conclusion has been drawn. Hence, it could be assumed that researchers are still considering the possibility of feeding frequency effect on shrimp's growth. This literature review was conducted to evaluate the effect of feeding frequency management on the growth performance of whiteleg shrimp. The expected output would be the possible recommendation of feeding frequency management that would optimize the growth of whiteleg shrimp in the most efficient way and the most lucrative option for the aquaculture industry.

This study aimed to, i.e., (1) determine the feeding frequency for the most optimal growth of whiteleg shrimp, (2) determine the feeding frequency for the most optimal survival of whiteleg shrimp, (3) determine the feeding frequency for the most optimal FCR (feed conversion ratio) of whiteleg shrimp, and (4) determine the feeding frequency for the most optimal economic return.

2. Research Method

This study is categorized under literature review with the format of semi-systematic review. On a brief note, this literature review was conducted by comparing and analyzing qualitative and quantitative data from the primary literature that has been previously and meticulously shortlisted [14]. Data analysis was conducted with quantitative and descriptive methods.

2.1. Searching and Shortlisting Primary Literature

In the literature review, primary literature is the main component, both as the source of data and as the object of discussion. Therefore, finding and sorting the right primary literature is crucial to produce good literature reviews. Primary literature was searched via Google Scholar and the Elsevier repository with the keywords "vannamei," "feeding" and "frequency", whilst applying Boolean operator "AND" in between every keyword. The search results returned from the repositories were then sorted according to the relevance to the topic at hand, having high credibility, having the required data and parameters, and published in 2005 and onwards.

The process of identification, screening, eligibility, and inclusion in sorting the candidate primary literature was a method provided by the PRISMA (*Preferred Reporting Items for Systematic Reviews and Meta-Analyses*). Although the PRISMA was primarily intended for systematic reviews or meta-analyses, it has been extensively used in other literature review formats, especially semi-systematic reviews [15]. Overall, the searching and sorting process of primary literature is provided in the flow diagram in figure 1. Eight primary literature were obtained through the entire sorting process, originating from various journals with credibility index (H Index) of 18, 50, 55, 72, 80, and 164 (four articles from Q1 journals and three articles from Q2 journals), and one article without a Scopus index but was included due to the relevant data and information it contained (Table 1).

2.2. Data Analysis

Data analysis of growth, survival, and FCR of whiteleg shrimp was conducted using MetaInsight application. Significance tests between each feeding frequency treatment were conducted with the Bayesian random effect model method, with credibility of 95% [16]. The eight primary literature have several variations in the experimental variables. Variations in methods include the research period, the culture system used, the protein content in shrimp feed, the stocking density of shrimp in the experimental unit, and the main variable analyzed in this literature study, namely the feeding frequency. The different methods used by each primary literature are important to highlight because they have the potential to bias the analysis results obtained (table 2). Since water quality parameter throughout all primary literature were reported to be within the ideal range for

DOI: https://doi.org/10.5614/3bio.2021.3.1.5

shrimp [17] (except for one case explained later in this article), mostly the analysis will neglect the influence of water quality.

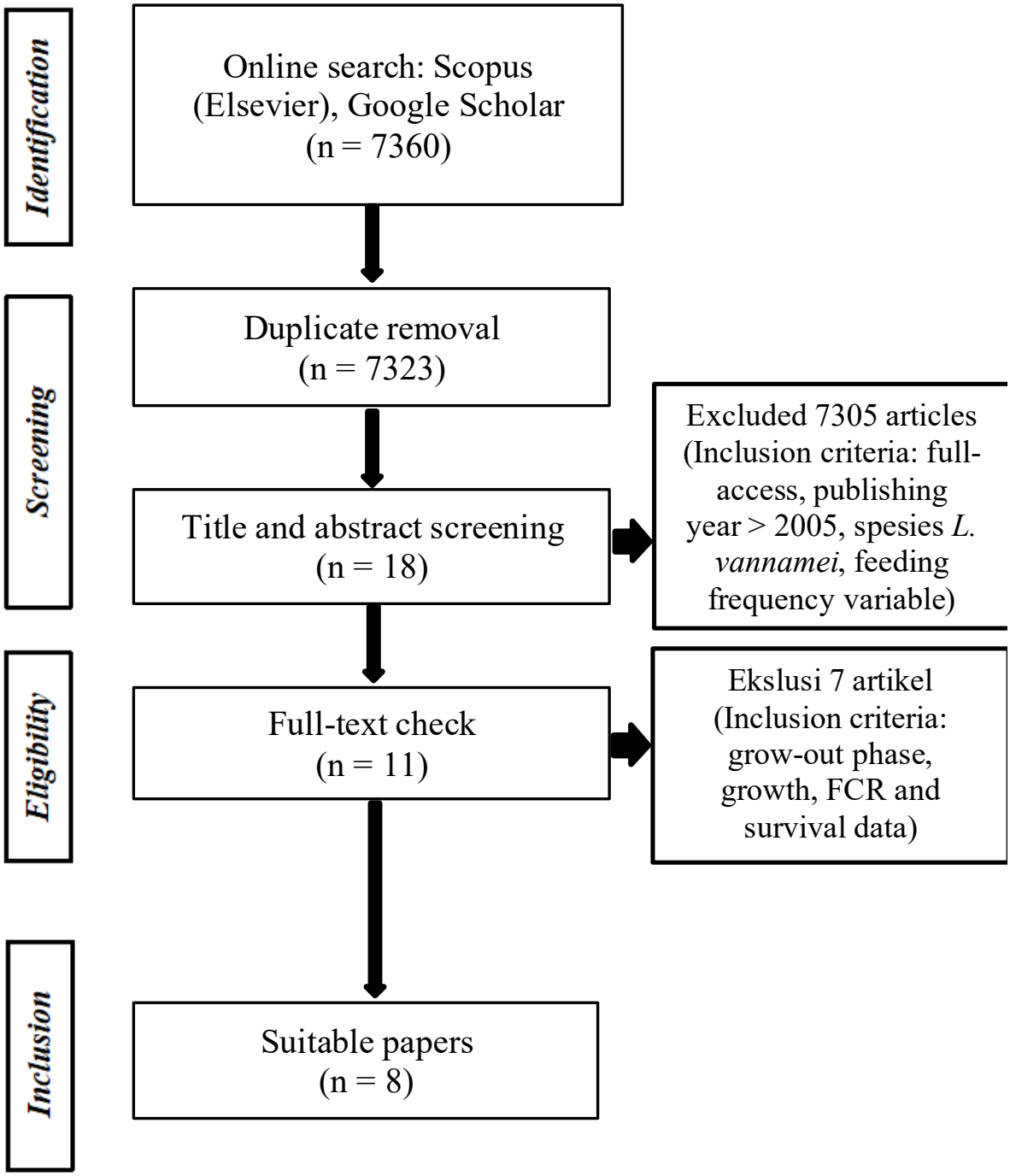

Figure 1 Flow diagram of literature review using PRISMA

DOI: https://doi.org/10.5614/3bio.2021.3.1.5

Table 1. List of primary literature

No	Year	Publication	Article Title	Pages	Authors	Journal
1	2020	International Journal, Scopus indexed	Optimizing feed automation: improving timer-feeders and on demand systems in semi-intensive pond culture of shrimp *Litopenaeus vannamei*	Vol. 519, Page 734-759	Reis, J., Novriadi, R., Swanepoel, A., Jing ping, G., Rhodes, M., Davis, D. A.	Aquaculture ISSN: 00448486 **H Index: 164 Q1**
2	2020	International Journal, Scopus indexed	Effects of feeding frequency on growth, feed utilization, digestive enzyme activity and body composition of *Litopenaeus vannamei* in biofloc-based zero-exchange intensive systems	Volume 522, Article number 735079	Wujie Xu, Yu Xu, Haochang Su, Xiaojuan Hu, Yunna Xu, Zhuojia Li,Guoliang Wen, Yucheng Cao	Aquaculture ISSN: 00448486 **H Index: 164 Q1**
3	2019	International Journal, Scopus indexed	The Effect of Dosage Combination and Feeding Frequency on Growth and Survival Rate of v*annamei* Shrimp Juveniles in Ponds	Volume 370, Page 012-033	Zainuddin Z., Aslam yah S., Nur K., Hadijah	IOP Conf. Series: Earth and Environmental Science ISSN: 17551315 **H Index: 18**
4	2019	International Journal, Scopus indexed	Multiple feedings enhance the growth performance and feed efficiency of juvenile *Litopenaeus vannamei* when fed a low-fish meal amino acid-supplemented diet	Volume 27, Issue 2, Pages 337-347	Nunes, A.J.P., Sabry-Neto, H., da Silva, F.H.P., de Oliveira-Neto, A.R., Masagounder, K.	Aquaculture Internati onal ISSN: 09676120 **H Index: 50 Q2**
5	2019	International Journal, Scopus indexed	Feed management and the use of automatic feeders in the pond production of Pacific white shrimp *Litopenaeus vannamei*	Volume 50, Issue 1, Pages 54-64	Ullman, C., Rhodes, M., Hanson, T., Cline, D., Davis, D.A	Journal of the World Aquaculture Society ISSN: 17497345 **H Index: 55 Q2**
6	2019	International Journal, Scopus indexed	Effect of feeding frequency on growth and digestive enzyme activity in *Litopenaeus vannamei* during the grow-out phase in biofloc system	Volume 25, Issue 3, Pages 577-584	Nery, R. C., Costa, C.B., Rodr igues, F., Soares, R., Bezerra, R.S., Peixoto, S.	Aquaculture Nutrition ISSN: 13535773 **H Index: 72 Q1**
7	2016	International Journal	Effects of feeding frequency on growth, feed conversion ratio, survival rate and water quality of white leg shrimp (*Litopenaeus vannamei*, Boone, 1931)	Volume 4, Issue 3, Pages 293-297	Mazdak Aalimahmoudi, Alireza Reyshahri, Siamak Salehipour Bavarsad, Milad Maniat	International Journal of Fisheries and Aquatic Studies ISSN: 23475129
8	2006	International Journal, Scopus indexed	Effects of feeding frequency on feed leaching loss and grow-out patterns of the white shrimp *Litopenaeus vannamei* fed under a diurnal feeding regime in pond enclosures	Volume 25 2, Issue 2-4, Pages 494-502	Carvalho, E. A., Nunes, A.J.P.	Aquaculture ISSN: 00448486 **H Index: 164 Q1**

DOI: https://doi.org/10.5614/3bio.2021.3.1.5

Table 2 Primary literature on variable variations

Literature	Days of culture	Culture system	Feed protein (%)	Stocking density (shrimps m^{-2})	Feeding method	Feeding time range	Feeding frequency (day^{-1})
Reis *et al*. **(2020)**	**91**	*Zero water exchange* **(***outdoor***)**	**40**	**26**	*On-demand automatic feeding* **dan** *timed automatic feeding*	**7.00 - 19.00**	**36 dan** *on-demand* **(AQ1)**
Xu *et al*. **(2020)**	**56**	*Biofloc-based*, *zero water exchange* **(rumah kaca)**	**40,1**	**300**	*Timed automatic feeding*	**6.00 - 24.00**	**3, 6 dan 12**
Nery *et al*. **(2019)**	**63**	*Biofloc-based* **RAS**	**35**	**150**	*Hand-feeding*	**8.00-16.00**	**1, 2, 3 dan 4**
Zainuddin *et al*. **(2019)**	**56**	*Flow through*	**24,97**	**40**	*Hand-feeding*	**6.00 - 18.00**	**3, 4 dan 5**
Ullman *et al*. **(2019)**	**91**	*Biofloc-based*, *zero water exchange* **(***outdoor***)**	**40**	**38**	*On-demand automatic feeding, timed automatic feeding* **dan** *hand-feeding*	**8.00 - 19.00**	**2, 6 dan** *on-demand* **(AQ1)**
Nunes *et al*. **(2019)**	**91**	*Flow through* **(***outdoor***)**	**32**	**100**	*Timed automatic feeding* **dan** *hand-feeding*	**7.30 - 17.30**	**2, 4, 10**
Aalimahmoudi *et al*. **(2016)**	**56**	*Flow through* **(***indoor***)**	**42**	**57**	*Hand-feeding*	**7.00 - 23.00**	**2, 4 dan 6**
Carvalho & Nunes (2006)	**84**	*Flow through* **(***outdoor***)**	**40**	**80**	*Hand-feeding*	**7.00 - 17.00**	**2, 3, 4, 5 dan 6**

3. Results and discussion

3.1. Whiteleg Shrimp Growth Performance based on Feeding Frequency

The growth performance of whiteleg shrimp can be assessed through several parameters, including the ones found from the primary literature; growth rate (g/week), survival (%) and feed conversion ratio or FCR. From the eight primary literature, ten values of average growth rates based on feeding frequency were obtained as shown in Figure 2. The feeding frequencies that are applied from the experiments from the primary literature includes one (1x), two (2x), three (3x), four (4x), five (5x), six (6x), ten (10x), twelve (12x) and thirty-six (36x) times per day, and a feeding treatment using on-demand, acoustic automatic feeder (AQ1), where the feed is automatically discharged into the shrimps only if there is feeding stimulus from the shrimps.

The lowest growth rate was found in the 1x treatment, with a growth rate of 0.62 ± 0.47 g/week. The growth rate of the shrimps increased to 0.87 ± 0.35 g/week at 2x feeding frequency and then reached 0.97 ± 0.47 g/week at 3x feeding

DOI: https://doi.org/10.5614/3bio.2021.3.1.5

frequency before plummeting down to 0.7 ± 0.19 g/week and 0.63 ± 0.29 g/week at 4x and 5x feeding frequencies, respectively. The growth rate then saw an increase up to 1.36 ± 0.48 g/week at 6x feeding frequency but dropped drastically to 0.88 ± 0.06 g/week at 10x feeding frequency. From this point, increase in feeding frequency was followed by an increase in the growth rate as well; at 12x and 36x feeding frequencies, the growth rate was at 1.85 ± 0.08 g/week and 1.97 ± 0.19 g/week, respectively. The final treatment, the on-demand acoustic automatic feeder (AQ1), produced the highest growth rate of 2.46 ± 0.15 g/week.

In using the Bayesian random-effect model, one treatment is treated as a "control" which will be used as the main comparison against other treatments. In this analysis, treatment of 4x feeding frequency was used as a control because it is a common feeding frequency used in aquaculture industry practice [17]. Based on Figure 3, the results of statistical inference show that of all the feeding frequency treatments, only the AQ1 treatment has a significant effect (P <0.05), indicated by the range of the credible interval (CrI) line which inside the range of 0.415 - 1.07 (marked in green) and does not intersect the x = 0 line or line-of-no-effect. The 1x to 36x treatments have a credible interval (CrI) line span that crosses the line-of-no-effect. This indicates that there is no significant influence.

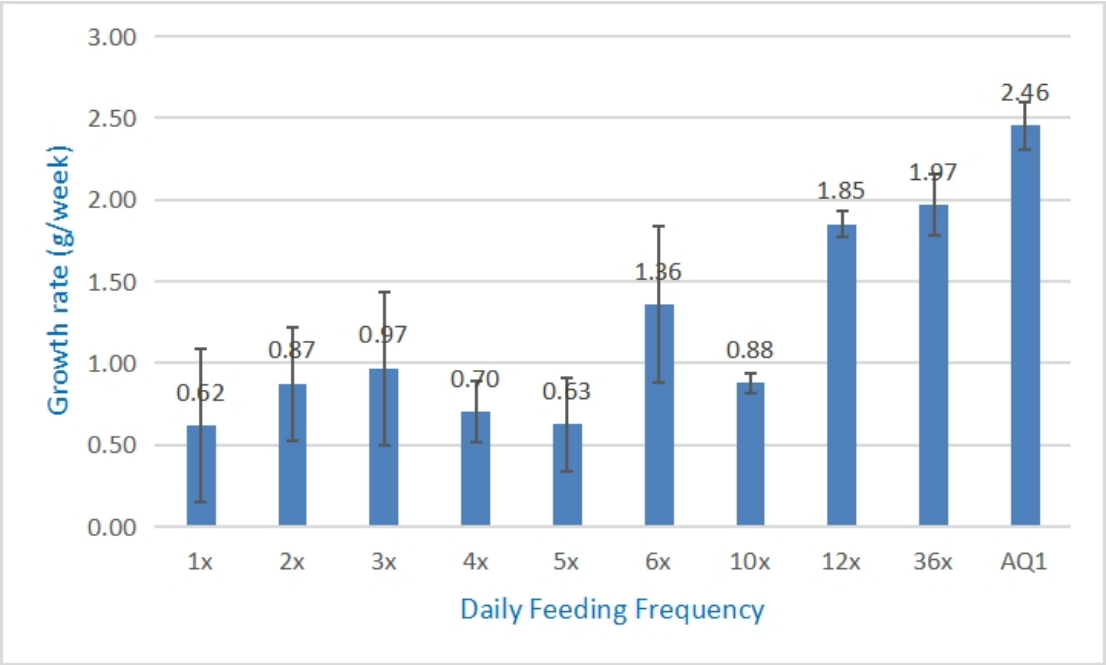

Figure 2 Growth rate based on feeding frequency

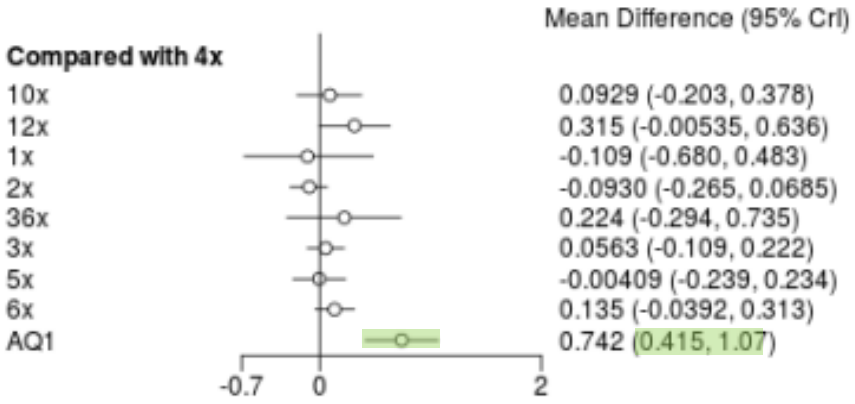

Figure 3 Forest plot of growth rate based on feeding frequency

DOI: https://doi.org/10.5614/3bio.2021.3.1.5

Based on Figure 4, the lowest shrimp survival rate is found in on-demand feeding (AQ1), which is 72.61 ± 14.74%. The survival rate from treatments 1x to 5x show no significant difference, with values of 78.3 ± 1.3%, 76.15 ± 10.61%; 76.69 ± 14.41%, 79.72 ± 12.38% and 80.84 ± 6.96%, respectively. Then, at the 6x feeding frequency, the survival rate decreased to 74.9 ± 17.67%. At 10x feeding, the highest survival rate was 94.24 ± 6.1%, then it decreased slightly to 90.15 ± 1.77% at a feeding frequency of 12x. The subsequent addition of the feeding frequency at 36x and AQ1 on-demand system resulted in a drastic reduction in survival rates of 77.6 ± 13.04% and 72.61 ± 14.74, respectively.

Based on the Forest plot in Figure 5, there was no significant difference in the frequency of feeding on the survival rate of white shrimp (P> 0.05). This is indicated by the range of the credible line intervals in each treatment that intersects the line-of-no-effect. However, the statistical inference is not too conclusive. The overall credible interval for survival data is relatively wide, with the widest interval found in the 36x treatment (-44.0, 30.4), which reduces the reliability of the inference.

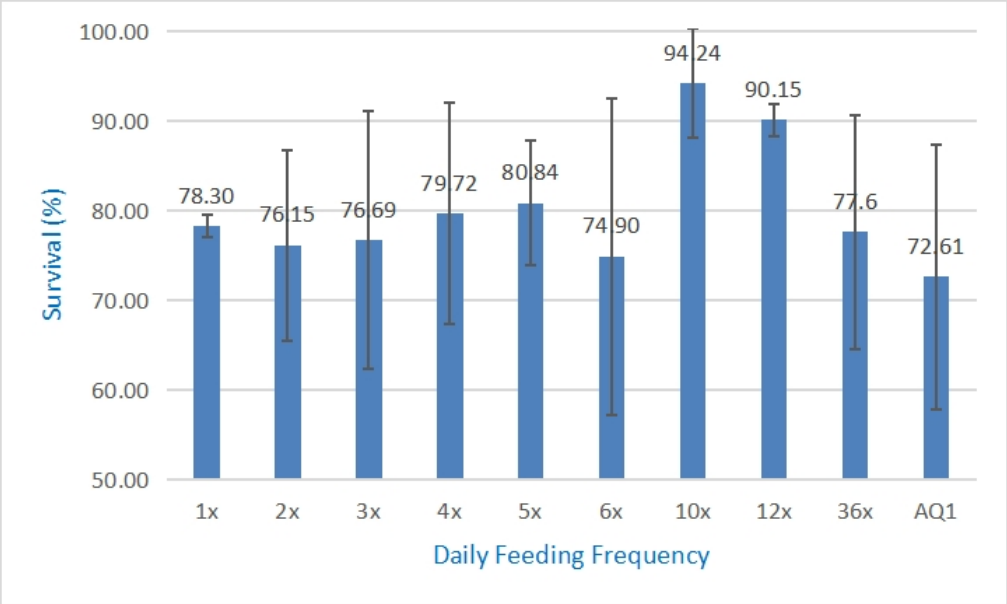

Figure 4 Survival based on feeding frequency

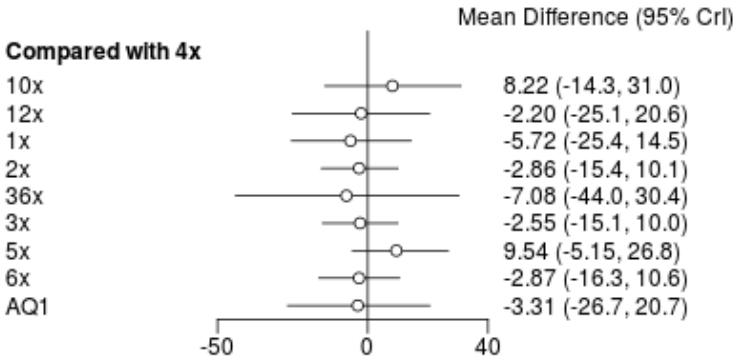

Figure 5 Forest plot of survival based on feeding frequency

The feed conversion ratio (FCR) between treatments of feeding frequency can be seen in Figure 6. Treatment 1x gives an FCR of 1.71, followed by a decrease in the efficiency of feed use in treatment 2x, with an FCR of 2.08, and then a further decrease to 1.95 on treatment 3x before spiking to the highest FCR of 2.30 at treatment 4x. Furthermore, along with the increase in feeding frequency, the FCR decreased, from 1.98 in treatment 5x to 1.83, 1.74, 1.19 then reaches the lowest point or the most efficient use of feed in treatment 36x with an FCR of 0.99. In treatment

DOI: https://doi.org/10.5614/3bio.2021.3.1.5

AQ1, the use of feed was still classified as very efficient, with an FCR of 1.11.

Although the inter-treatment FCR data showed quite a contrast, especially the FCR of treatments 12x, 36x, and AQ1 compared to other treatments, the statistical inference did not show a significant difference (P> 0.05). It can be seen from the Forest plot in Figure 7 that none of the treatments' credible intervals intersect nor cross the line-of-zero-effect. Similar to the Forest plot results for survival data, the overall credible interval range in the FCR Forest plot data is still too wide to provide reliable inference. The reason being is that the FCR at 36x treatment (0.99) is very far compared to 4x treatment or control treatment (2.3), but there was no significant difference from statistical analysis.

However, the credible interval at 36x treatment is still too wide (-1.48, 1.56) to conclude. In short, for the time being, the initial hypothesis regarding the effect of feeding frequency on FCR was rejected because the statistical analysis did not show any significant difference. If the analysis was to be carried out with a larger sample and with low heterogeneity, it would be possible to see a significant difference, especially in the 36x, AQ1, and 12x treatments, where the FCR difference was visible compared to the 4x treatment.

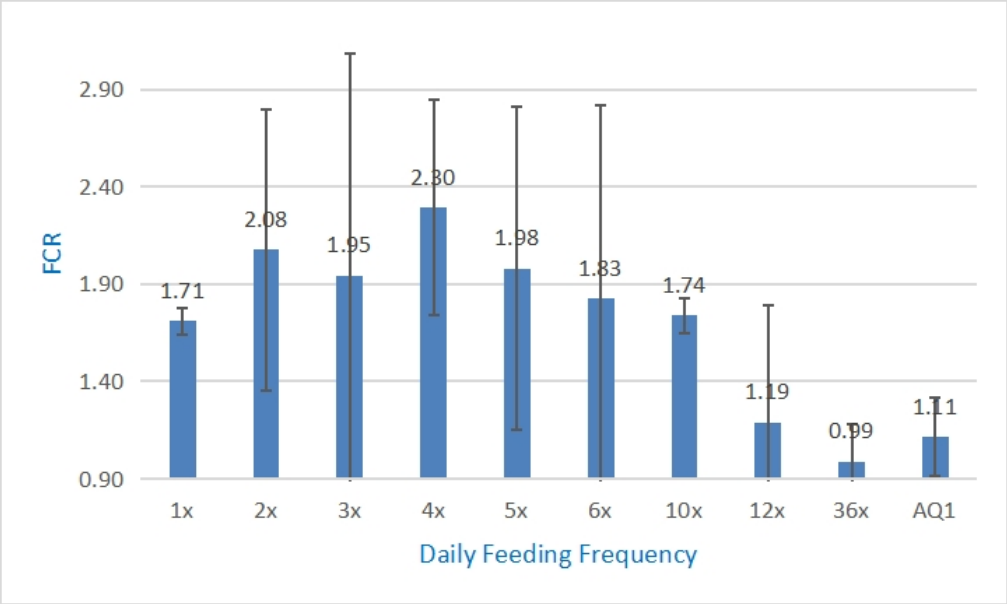

Figure 6 FCR based on feeding frequency

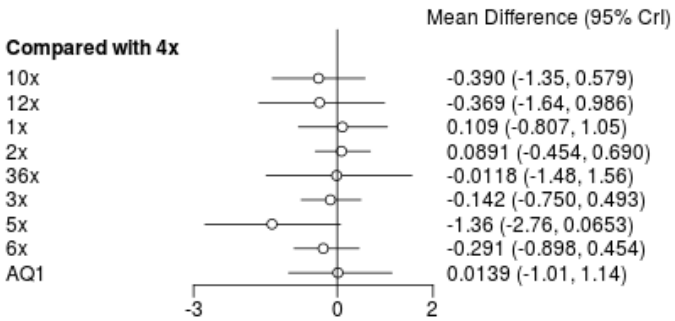

Figure 7 Forest plot of FCR based on feeding frequency

3.2. Feeding Frequency's Relation to Whiteleg Shrimps' Endogenous Factors

Most organisms exhibit biological rhythms, which are adaptive strategies, for them to adapt certain physiological processes to occur at the most favorable moments [18]. The dark/light cycle is one of the environmental factors that most influence the formation of biological rhythms of organisms. Biological components generate these rhythms called pacemakers, which consistently express the pattern of origin even though the organism has been isolated from environmental influences [19].

DOI: https://doi.org/10.5614/3bio.2021.3.1.5

The experiment conducted by Santos et al. [20] was based on the premise that white shrimp also have an endogenous circadian rhythm that is influenced by the light/dark cycle. After being observed, the endogenous rhythm of shrimp is that they tend to be more active in the dark phase or at night after 19:00, or in other words, they are nocturnal animals. The percentage of locomotion and feeding activities conducted in a day was 67.7 ± 2.5% and 81.9 ± 2.3% of those activities were performed at night.

As evidence that feeding activity on white shrimp is more effective at night, Santos et al. [20] measured the amount of feed consumed during daytime and nighttime. It can be seen from the graph that the total daily feed intake at night was 1.1 ± 0.2 g/day in the dark phase compared to 0.2 ± 0.1 g/day in the light phase. Based on these findings, it was concluded that in the endogenous rhythm of white shrimp, most of the feeding activity occurs at night.

Another finding regarding the feeding rhythm of white shrimp was reported by Hernandez-Cortes et al. [21], where white shrimp were fed once every 2 hours for 5 days to see the pattern of feed consumption in a day. For 5 days a consistent pattern was found, the peak of feed consumption by white shrimp occurred from 20.00 to 24.00. Within this range, the amount of feed consumed reached 30.4% of the daily intake.

If we review the eight primary literature, it can be seen that the feeding schedule which includes the dark phase (6:00 to 24:00) results in a higher growth rate when compared to the feeding schedule which only covers the light phase (6:00 to 18:00). Based on the illustration of the feeding schedule applied by the eight primary literature (Figure 8), shrimp fed until the dark phase produced a minimum growth of 0.65 g/week which was obtained from treatment 2x by Aalimahmoudi et al. [22] and a maximum of 2.49 g/week from the AQ1 treatment by Reis et al. [23]. On the other hand, shrimp fed only during the light phase showed a low growth rate with a minimum value of 0.44 g/week from treatment 3x by Zainuddin et al. [24] and a maximum value of 0.91 g/week from treatment 3x by Carvalho & Nunes [25].

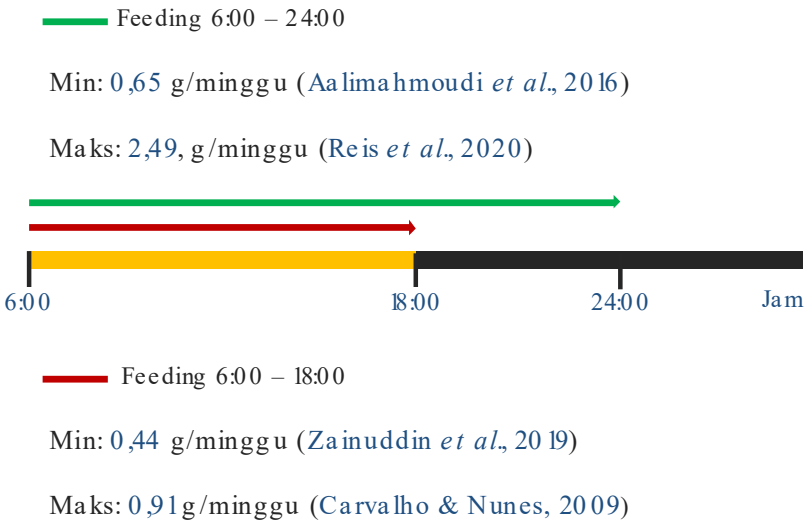

Figure 8 Growth rate comparison of with and without dark phase feeding

This phenomenon correlates with the findings of Hernandez-Cortes et al. [18] and Santos et al. [20] who showed that most of the feeding activities of white shrimp occur at night. Feeding only in the light phase is not following the endogenous rhythm of feeding white shrimp, hence the literature that applied that feeding schedule lacks optimal shrimp growth. The feeding schedule does not, however, appear to produce a strong effect on the survival rate and FCR data. According to these findings, it can be concluded that to optimize the growth rate of white shrimp, the feeding schedule must include the peak period of white shrimp feeding activity, which is around 20:00 to 24:00.

The experiment of Xu et al. [26] reported that feeding frequency affects the activity of digestive enzymes, specifically proteases, carbohydrases, and lipases. As the feeding frequency increased from 3 times, 6 times to 12 times a day, there was a significant increase in proteases in the stomach. The increase in enzymatic activity will certainly increase the effectiveness of digestion and absorption of nutrients, which are the basic ingredients for growth, showed by the increase in the growth rate of the feeding treatment 3 times to 12 times per day [26].

It is also worth mentioning that FCR is also influenced by increased enzymatic activity, as observed by Xu et al. [26], where the FCR decreased from 1.39; 1.30 to 1.19 at feeding frequencies of 3, 6, and 12 times/day, respectively. The main

DOI: https://doi.org/10.5614/3bio.2021.3.1.5

FCR data (Figure 6) also displays a trend of FCR decline from 4x to 36x treatment. Thus, it can be concluded that the optimization of growth rate and FCR can be done by increasing enzymatic activity to increase nutrient absorption by increasing the feeding frequency to 36x or by applying an on-demand system (AQ1).

3.3. Relation between Whiteleg Shrimps' Exogenous Factors and Feeding Frequency

At a glance, DO parameters from all analyzed literature fall into the DO range that is adequate for shrimp needs, ranging from 4 mg/L to 6.9 mg/L. However, treatment AQ1 from one of the primary literature [27] reported an acute drop in DO (<3 mg/L) occurring about 25 times per examination in the early morning. Lack of data and explanations for how long DO values last throughout the night before being checked in the morning makes it difficult to draw definitive conclusions regarding the effect of the low DO. The authors mentioned that one repetition of the AQ1 treatment had to be discontinued at week 11 because they DO levels reached lethal levels and the mortality rate was too high. According to Cheng et al. [28], hypoxia or sub-optimal DO levels in water (1 - 5 mg/L) will inhibit shrimp growth because feeding behavior and feed-to-meat conversion efficiency are not as intense as under normal DO conditions. Hypoxia is reported to reduce the total haemocyte count (THC) which elevates shrimps' sensitivity and susceptibility to various types of pathogens [28].

Apart from DO, a contrasting temperature parameter discrepancy is found in one of the primary literature. The experiment by Nery et al. [29] took the second-lowest position with a growth rate of 0.57 g/week. When compared with other experiments, this discrepancy could be caused by several factors such as the location of the culture pond which was located indoors, and the culture water temperature which averaged 24.8 ± 0.7 °C throughout the experiment, while the water temperature of other experiments ranged from 27.69 °C [25] up to 30.2 ± 1 °C [30]. These findings are important to highlight because, according to Wyban et al. [31], the growth performance of *L. vannamei* is very sensitive to small changes in temperature. In addition, the optimal temperature (the temperature that produces the best growth) of *L. vannamei* is size-specific, where the optimal temperature for small size (<5 g) is around 30 °C, and for larger shrimp it is between 27 °C, whereas 23 °C was rated as sub-optimal for all shrimp sizes [31]. If Nery et al. [29] optimized the temperature parameter in the experiment, an increase in shrimp growth performance can be predicted.

Experiments by Zainuddin et al. [24] occupied the lowest position, with a growth rate of only 0.44 g / week. This phenomenon may be related to the low levels of crude protein (CP) in the feed used in the experiment. All primary literature except Zainuddin et al. [24] applied pellet feeds with CP levels ranging from 32% to 40%. In fact, according to Lee & Lee [32], the optimal CP levels for whiteleg shrimp growth in juvenile, sub-adult, and adult phases were 34.5%, 35.6%, and 32.2%, respectively.

Feed leaching is the phenomenon where the nutritional content of the feed dissolves and dissipates into the water due to being submerged for too long. According to Carvalho & Nunes [25], the loss of CP content from feed leaching peaks between two and three hours after the feed is submerged, reaching a maximum of 6.91%. Despite this, findings by Smith et al. [33] showed that the loss of CP of 15% after submerging the feed for 4 hours had no significant impact on growth. Moreover, the effect of feed leaching was expected to be more pronounced under more culture-intensive conditions, where there are no flocs or natural food sources present [25].

In retrospect, the trend in FCR shown in Figure 6 is decreasing trend as the frequency of feeding increases, especially after treatment 4x. The decrease in FCR or the increase in feed efficiency is thought to be influenced by the increase in the consumption of relatively fresh feed due to reduced feed leaching during this short feeding period [34]. The reason is, in the treatment of low feeding frequency such as 1x to 4x, the percentage daily feed portion given at each feeding time is more than that of the high feeding frequency treatments. For example, in the 1x treatment because the feeding is only once, the feeding covers 100% of the total daily portion, then for the 2x treatment because the feeding is done twice, each provision amounts to 50% of the total daily portion, and so on. The implication is that at lower feeding frequencies, the shrimp will leave a lot of uneaten feed, which will eventually be lost through leaching because it only has a limited capacity to digest food in the first hour [35]. This has been shown to increase FCR and also slow down the growth rate. Meanwhile, by dividing the portion into smaller feeds that are more frequent according to the GPT of white shrimp, the FCR and growth rate will be optimized.

The culture system certainly has a positive impact on the growth performance of white shrimp, in this case in terms of food supply. For example, in the 6x feeding frequency treatment, the culture system in the experiment of Xu et al. [26] is a biofloc, so even though the interval between feeding is quite long, shrimp have an alternative source of food in the form of flocs to compensate the nutritional needs. In the treatment of the same feeding frequency, Aalimahmoudi et al. [22] implemented feeding at 3-hour intervals. This is because the culture system applied is not biofloc but flow-through and water quality control is carried out by changing the water by as much as 20% per day. The implication is that the impact of feed leaching is more visible because there is no alternative feed source [25]. As a result, the absorption of feed nutrients in shrimp in the experiment of Aalimahmoudi

DOI: https://doi.org/10.5614/3bio.2021.3.1.5

et al. [22] was not optimal and the growth rate was affected (0.88 g/week), compared to Xu et al. [26] which resulted in a growth rate of 1.67 g/week (Figure 9). Experiments by Ullman et al. [27] also use a biofloc system based on zero water discharge, and the growth rate can reach 1.89 g/week. This is different from Carvalho & Nunes [25] in which a conventional flow-through system was applied.

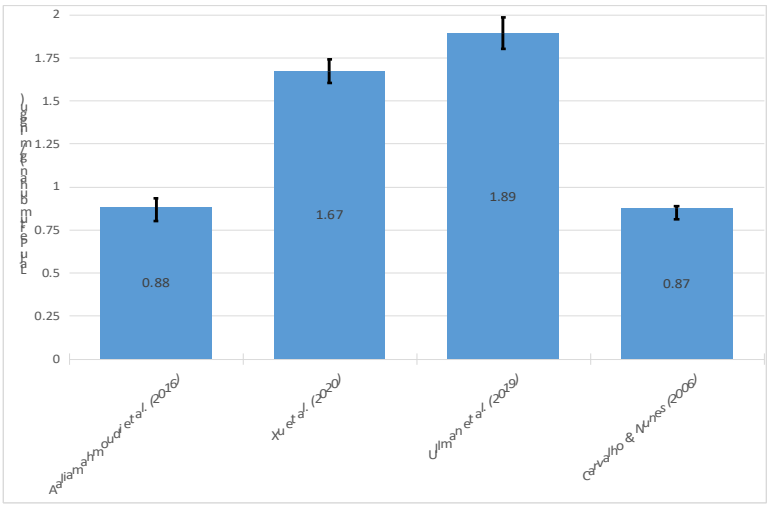

Figure 9 Growth rate of treatment 6x

Tacon et al. [9] reported that ponds undergo rapid development of microbial food chains, starting from the growth of autotrophic microbial communities characterized by the appearance of a greenish color in the water. It then turns into heterotrophic communities that appear in the water in the form of suspended particles or "floc". The composition of the floc is reported to include bacteria, algae, diatoms, flagellates, ciliates, amoebae, rotifers, nematodes, and gastrotrich. Some findings by Moss et al. [36] stated that the organisms in the floc were not only an alternative source of nutrition but also had a positive impact on enzyme activity and the microbiome of the digestive tract of shrimp. In addition, the stomach is the first digestive organ to pass by food after the mouth, so the production and secretion of enzymes by biofloc microorganisms may contribute to the increased activity of protease and amylase enzymes in the stomach [29, 37]. Thus, it can be concluded that the biofloc culture system can optimize the overall growth performance of shrimp.

3.4. Optimizing Feeding Frequency

Overall AQ1 treatment is the best feeding system because it not only adjusts the best feeding frequency for shrimp but also the amount of feed. Bador et al. [38] found that in considering both endogenous factors (circadian rhythm, molting, etc.) As well as exogenous factors (temperature, salinity, etc.), fluctuations in the amount of feed consumption were observed. Therefore, applying fixed feeding frequency and feed portions throughout the entire cycle of production potentially jeopardizes the growth rate, survival, and FCR of shrimps. The on-demand system guarantees the best feed efficiency without having to perform difficult calculations by relying on acoustic sensors, especially in the involvement of endogenous and exogenous factors that are difficult to control. If a simulation of whiteleg shrimp production is carried out for one cycle (90 days) at a stocking density of 100 individuals/m2 by considering the parameters of growth rate, survival rate, and FCR of all feeding frequency treatment, the projected gross profit (only feed cost deduction) can be seen in Table 3.

Based on these projection results, the most profitable production is yielded by treatment AQ1, with a gross profit of Rp. 133,563,737 per unit area of 0.1 ha. Although the additional costs of the AQ1 feeder and sensor equipment have not been accounted for (around Rp. 6 million per unit), 0.1 ha of pond area only requires 1 unit, so the resulting profit remains superior. The valuation of shrimp produced by AQ1 treatment is very high because the shrimp prices in the market are not equal for all sizes, but each size has its price (the latest shrimp size prices can be seen on the app.jala.tech page). For example, shrimp harvested at 10 g would be priced at Rp. 51,000 per kilogram, whereas at 11 g it would be priced at Rp. 52,000 and at 12.5 g it would be priced at Rp. 55,000. For the size of the shrimp harvest produced by the AQ1 treatment (31.57 g), the market is valued at Rp. 85,000 per kilogram. Therefore, although AQ1 treatment shows the lowest survival parameter (72.61%), on a larger scale it produces the largest profit.

DOI: https://doi.org/10.5614/3bio.2021.3.1.5

Table 3 Projection of gross profit based on feeding frequency treatments

Treatment	Final weight (kg)	Total feed (kg/0,1 ha)	Biomass (kg/0,1 ha)	Price (kg^{-1})	Yield value ($0,1\ ha^{-1}$)	Gross profit ($0,1\ ha^{-1}$)
1x	7.97	1067	624	Rp44,000	Rp27,463,166	Rp1,847,522
2x	11.24	1778	856	Rp52,000	Rp44,518,489	Rp1,838,271
3x	12.46	1859	956	Rp55,000	Rp52,562,602	Rp7,951,288
4x	9.04	1654	720	Rp49,000	Rp35,302,966	-Rp4,392,553
5x	8.04	1286	650	Rp44,000	Rp28,580,946	-Rp2,286,476
6x	17.46	2388	1308	Rp63,000	Rp82,384,102	Rp25,076,151
10x	11.31	1855	1066	Rp52,000	Rp55,445,431	Rp10,918,485
12x	23.79	2552	2144	Rp77,000	Rp165,109,725	Rp103,869,027
36x	25.33	1946	1965	Rp77,000	Rp151,343,280	Rp104,643,068
AQ1	31.57	2555	2293	Rp85,000	Rp194,877,123	Rp133,563,737

4. Conclusion

Based on the discussion that has been carried out, several conclusions can be drawn from this literature review: (1) the most optimal feeding frequency (P <0.05) for the growth rate of whiteleg shrimp (*L. vannamei*) is feeding with the on-demand system (AQ1), (2) the feeding frequency did not have a statistically significant effect on the survival of whiteleg shrimp (*L. vannamei*) (P> 0.05), (3) the feeding frequency did not have a statistically significant effect on shrimp FCR (*L. vannamei*) (P> 0.05), and (4) the most optimal feeding frequency for white shrimp production on an industrial scale is the on-demand system (AQ1).

References

[1] KKP, 2020. Program Percepatan Pengembangan Tambak Udang Nasional. Diambil dari https://kkp.go.id/an-component/media/upload-gambar-pendukung/DitJaskel/publikasi-materi-2/menarik-minat/Materi%20Pembahas%20Direktur%20KKI%20Budidaya.pdf

[2] Research and Markets, 2019. Shrimp Market: Global Industry Trends, Share, Size, Growth, Opportunity and Forecast 2019-2024

[3] Tacon, A. G. J., & Metian, M., 2015. Feed Matters: Satisfying the Feed Demand of Aquaculture. *Reviews in Fisheries Science & Aquaculture*, 23, 1–10. DOI: https://doi.org/10.1080/23308249.2014.987209

[4] Van, T. P. T. H., Rhodes, M.A., Zhou, Y., Davis, D.A., 2017. Feed management for Pacific white shrimp Litopenaeus vannamei under semi-intensive conditions in tanks and ponds. *Aquac Res.* 00:1–10. DOI: https://doi.org/10.1111/are.13348

[5] Boyd, C. E., Tucker, C., McNevin, A., Bostick, K., & Clay, J., 2007. Indicators of resource use efficiency and environmental performance in fish and crustacean aquaculture. Reviews in Fisheries Science, 15, 327–360. DOI: https://doi.org/10.1080/10641260701624177

[6] Davis, D. A., Roy, L. A., & Sookying, D., 2008. Improving cost effectiveness of shrimp feeds. In: L. E. Cruz-Suarez, D. Ricque-Marie, M. Tapia-Salazar, M. G. Nieto-Lopez, D. A. Villarreal-Cavazos, J. P. Lazo & T. Viana (Eds.), *Avances en Nutricion Acuicola IX. IX Simposio Internacional de Nutricion Acuicola* (pp. 271–280). Monterry, Nuevo Leon, Mexico: Universidad Autonoma de Nuevo Leon.

[7] Shipton, T. A., & Hasan, M. R., 2013. An overview of the current status of feed management practices. In: M. R. Hasan & M. B. New (Eds.), *On-farm feeding and feed management in aquaculture* (pp. 3–20), FAO Fisheries and Aquaculture Technical Paper No. 583. Rome: FAO.

[8] Davis, D. A., Amaya, E., Venero, J., Zelaya, O., & Rouse, D. B., 2006. A case study on feed management to improving production and economic returns for the semi-intensive pond production of *Litopenaeus vannamei*. In: L. E. Cruz Suarez, D. R. Maria, M. T. Salazar, M. G. N. Lopez, D. A. V. Cavazos, A. C. P. Cruz & A. G. Ortega (Eds.), Avances en Nutricion Acuıcola VIII. *Memorias del Octavo Simposio Internacional de Nutricion Acuıcola* (pp. 282–303). Monterrey, Nuevo Leon, Mexico: Universidad Autonoma de Nuevo.

DOI: https://doi.org/10.5614/3bio.2021.3.1.5

[9] Tacon, A. G. J., Cody, J. J., Conquest, L. D., Divakaran, S., Forster, I. P., & Decamp, O. E., 2002. Effect of culture system on the nutrition and growth performance of Pacific white shrimp *Litopenaeus vannamei* (Boone) fed different diets. Aquaculture Nutrition, 8, 121–139. DOI: https://doi.org/10.1046/j.1365-2095.2002.00199.x

[10] Cardona, E., Lorgeoux, B., Geffroy, C., Richard, P., Saulnier, D., Gueguen, Y., Chim, L., 2015. Relative contribution of natural productivity and compound feed to tissue growth in blue shrimp (Litopenaeus stylirostris) reared in biofloc: assessment by C and N stable isotope ratios and effect on key digestive enzymes. Aquaculture 448: 288–297. DOI: https://doi.org/10.1016/j.aquaculture.2015.05.035

[11] Peixoto, S. R. M., Silva, E., Costa, C. B., Nery, R. C., Rodrigues, F. F., Silva, J. F., Soares, R., 2018. Effect of feeding frequency on growth and enzymatic activity of *Litopenaeus vannamei* during nursery phase in biofloc system. Aquaculture Nutrition, 24(1), 579–585. DOI: https://doi.org/10.1111/anu.12591

[12] Lara, G., Hostins, B., Bezerra, A., Poersch, L. H., & Wasielesky, W. J., 2017. The effects of different feeding rates and re-feeding of *Litopenaeus vannamei* in a biofloc culture system. Aquacultural Engineering, 77, 20–26. DOI: https://doi.org/10.1016/j.aquaeng.2017.02.003

[13] Velasco, M., Lawrence, A. L., Castille, F. L., 1999. Effect of variations in daily feeding frequency and ration size on growth of shrimp, *Litopenaeus vannamei* (Boone), in zero-water exchange culture tanks. Aquaculture. Volume 179, Issues 1–4, Pages 141-148, ISSN 0044-8486, DOI: https://doi.org/10.1016/S0044-8486(99)00158-1.

[14] Mikolajewicz, N. & Komarova, S. 2019. Meta-Analytic Methodology for Basic Research: A Practical Guide. Frontiers in Physiology. 10. DOI: https://doi.org/10.3389/fphys.2019.00203.

[15] McAlister F. A., Clark H. D., van Walraven C., Straus S. E., Lawson F. M., Moher D., Mulrow C. D. 1999. The medical review article revisited: has the science improved? Ann Intern Med 131:947–951. DOI: https://doi.org/10.7326/0003-4819-131-12-199912210-00007

[16] Higgins, J. P. T., Thomas, J., Chandler, J., Cumpston, M., Li, T., Page, M. J., Welch, V. A. (editors). 2020. Cochrane Handbook for Systematic Reviews of Interventions version 6.1 (updated September 2020). Cochrane. Available from www.training.cochrane.org/handbook.

[17] FAO, 2016. FAO Statistical Yearbook: Fishery and Aquaculture Statistics. The organization of Food and Agriculture of the United Nations, Rome. http://www.fao.org/3/478cfa2b-90f0-4902-a836-94a5dddd6730/i3740t.pdf.

[18] Lopez-Olmeda, J. F., Sanchez-Vázquez, F.J., 2011. Thermal biology of zebrafish (*Danio rerio*). *J. Therm. Biol.* 36, 91–104. DOI: https://doi.org/10.1016/j.jtherbio.2010.12.005

[19] Vera, L. M., Madrid, J. A., Sánchez-Vázquez, F. J., 2006. Locomotor, feeding and melatonin daily rhythms in sharpsnout seabream (*Diplodus puntazzo*). *Physiol. Behav.* 88, 167–172. DOI: https://doi.org/10.1016/j.physbeh.2006.03.031

[20] Santos, A. D. S., López-Olmeda, J. F., Sánchez-Vázquez, F. J., Fortes-Silva, R., 2016. Synchronization to light and mealtime of the circadian rhythms of self-feeding behavior and locomotor activity of white shrimp (*Litopenaeus vannamei*). Comp. Biochem. Physiol. Part A Mol. Integr. Physiol. 199, 54–61. DOI: https://doi.org/10.1016/j.cbpa.2016.05.001.

[21] Hernandez-Cortes, P., Quadros-Seiffert, W., Navarrete del Toro, M.A., Portillo, G., Colado, G., Garcia-Carreño, F.L., 1999. Rate of ingestion and proteolytic activity in digestive system of juvenile white shrimp, Penaeus vannamei, during continual feeding. J. Appl. Aquac. 9 (1), 35–45. DOI: https://doi.org/10.1300/J028v09n01_03

[22] Aalimahmoudi, M., Reyshahri, A., Bavarsad, S. S., Maniat M. 2016. Effects of feeding frequency on growth, feed conversion ratio, survival rate and water quality of white leg shrimp (Litopenaeus vannamei, Boone, 1931). International Journal of Fisheries and Aquatic Studies, Vol. 4, Issue 3, Pages 293-297.

[23] Reis, J., Novriadi, R., Swanepoel, A., Jingping, G., Rhodes, M., Davis, D. A. 2020. Optimizing feed automation: improving timer-feeders and on demand systems in semi-intensive pond culture of shrimp *Litopenaeus vannamei*. Aquaculture. Vol. 519, 734759. ISSN 0044-8486. DOI: https://doi.org/10.1016/j.aquaculture.2019.734759

[24] Zainuddin Z., Aslamyah S., Nur K., Hadijah, 2019. The Effect of Dosage Combination and Feeding Frequency on Growth and Survival Rate of Vannamei Shrimp Juveniles in Ponds. IOP Conf. Series: Earth and Environmental Science. 370, 012033. IOP Publishing Ltd. DOI: https://doi.org/10.1088/1755-1315/370/1/012033

[25] Carvalho, E. & Nunes, A. 2006. Effects of feeding frequency on feed leaching loss and grow-out patterns of the white shrimp *Litopenaeus vannamei* fed under a diurnal feeding regime in pond enclosures. Aquaculture. 252. 494-502. DOI: https://doi.org/10.1016/j.aquaculture.2005.07.013.

DOI: https://doi.org/10.5614/3bio.2021.3.1.5

[26] Xu, W., Xu, Y., Su, H., Hu, X., Xu, Y., Li, Z., Wen, G., Cao, Y. 2020. Effects of feeding frequency on growth, feed utilization, digestive enzyme activity and body composition of *Litopenaeus vannamei* in biofloc-based zero-exchange intensive systems. *Aquaculture*, Volume 522, Article number 735079. DOI: https://doi.org/10.1016/j.aquaculture.2020.735079

[27] Ullman, C., Rhodes, M. A., Davis, D. A., 2019. Feed management and the use of automatic feeders in the pond production of Pacific white shrimp *Litopenaeus vannamei*. *Aquaculture* 498, 44–49. DOI: https://doi.org/10.1016/j.aquaculture.2018.08.040.

[28] Cheng W., Liu C. H., Hsu J. P., Chen J. C. 2002. Effect of hypoxia on the immune response of giant freshwater prawn Macrobrachium rosenbergii and its susceptibility to pathogen Enterococcus. Fish and Shellfish Immunology. 13: 351e65. DOI: https://doi.org/10.1006/fsim.2001.0411

[29] Nery, R., Costa, C. B., Rodrigues, F., Soares, R., Bezerra, R. D. S., Peixoto, S. Effect of feeding frequency on growth and digestive enzyme activity in *Litopenaeus vannamei* during the grow-out phase in biofloc system. Aquacult Nutr. 2019; 25: 577– 584. DOI: https://doi.org/10.1111/anu.12880

[30] Nunes, A.J.P., Sabry-Neto, H., da Silva, F.H.P., de Oliveira-Neto, A.R., Masagounder, K. 2019. Multiple feedings enhance the growth performance and feed efficiency of juvenile *Litopenaeus vannamei* when fed a low-fish meal amino acid-supplemented diet. Aquaculture International, Vol. 27, Issue 2, Pages 337-347. DOI: https://doi.org/10.1007/s10499-018-0330-7

[31] Wyban, J., Walsh, W. A., Godin, D. M., 1995. Temperature effects on growth, feeding rate and feed conversion of the Pacific white shrimp (*Penaeus vannamei*), Aquaculture, Volume 138, Issues 1–4, Pages 267-279, ISSN 0044-8486, DOI: https://doi.org/10.1016/0044-8486(95)00032-1.

[32] Lee, C., Lee, K. J. 2018. Dietary protein requirement of Pacific white shrimp *Litopenaeus vannamei* in three different growth stages. Fish Aquatic Sci 21, 30. DOI: https://doi.org/10.1186/s41240-018-0105-0

[33] Smith, D. M., Burford, M. A., Tabrett, S. J., Irvin, S. J., Ward, L., 2002. The effect of feeding frequency on water quality and growth of the black tiger shrimp (*Penaeus monodon*). *Aquaculture* 207, 125 – 136. DOI: https://doi.org/10.1016/S0044-8486(01)00757-8

[34] Wade, N. M., Bourne, N., Simon, C. J., 2018. Influence of marker particle size on nutrient digestibility measurements and particle movement through the digestive system of shrimp. Aquaculture 491, 273–280.DOI: https://doi.org/10.1016/j.aquaculture.2018.03. 039.

[35] Pontes, C. S., Arruda, M. D., 2005. Artificial food access and digestive tract filling of juvenile marine shrimp *Litopenaeus vannamei* (Boone) (Crustacea, Decapoda, Penaeidae) during light and dark phases in 24-hour period. *Revista Brasileira De Zoologia* 22 (4), 1039–1043.

[36] Moss, S. M., Divakaran, S. & Kim, B .G. 2001. Stimulating effects of pond water on digestive enzyme activity in the Pacific white shrimp, *Litopenaeus vannamei* (Boone). Aquaculture Res., 32, 125– 132. DOI: https://doi.org/10.1046/j.1365-2109.2001.00540.x

[37] Xu, W. J., Pan, L. Q., Zhao, D. H., Huang, J., 2012. Preliminary investigation into the contribution of bioflocs on protein nutrition of *Litopenaeus vannamei* fed with different dietary protein levels in zero-water exchange culture tanks. *Aquaculture* 350- 353, 147–153. DOI: https://doi.org/10.1016/j.aquaculture.2012.04.003.

[38] Bador, R., Blyth, P., Dodd, R., 2013. Acoustic Control Improves Feeding Productivity at Shrimp Farms. *Global Aquacuture Advocate*. pp. 77–78.

DOI: https://doi.org/10.5614/3bio.2021.3.1.5

3Bio Journal of Biological Science, Technology and Management
Guidelines for Authors

Submitting your manuscript: Manuscript for publication should be submitted electronically to 3BIO: Journal of Biological Sciences, Technology and Management to facilitate rapid publication and minimize administrative costs. All manuscripts should be submitted through online submission system. A user ID and password for the site can be obtained on first use. Online submission ensures the quickest possible review and allows authors to track the progress of their papers. In order to submit a NEW Manuscript to 3BIO: Journal of Biological Sciences, Technology and Management, you must be a registered user of 3BIO Journal, if you do not register, please register before you submit a NEW Manuscript. Submissions by anyone other than one of the authors will not be accepted. The submitting author takes responsibility for the paper during submission and peer review.

Other relevant correspondence should be sent to The Editorial Office of the 3BIO Journal of Biological Science, Technology and Management, c/o Dr. Rudi Dungani, School of Life Sciences and Technology, Institut Teknologi Bandung, Jl. Ganesha 10 Bandung 40132, Indonesia. Phone +62-22-2500258 Fax +62-22-2534107 E-mail: support3BIO@sith.itb.ac.id

Type of articles: Articles may be in the form of Research article, Review article or Short communication. Research articles are reports of recent advances on the research of selected topics. Short communications are concise, but independent report representing a significant contribution in the field.

Manuscript form: All manuscript must be written in English. Please ensure the following when submitting your manuscript to 3BIO:

1. The manuscript has not been submitted/published earlier in any journal and is not under consideration for publication elsewhere (or an explanation has been provided in Comments to the Editor section).
2. All authors have seen and approved the manuscript and have contributed significantly for the manuscript.
3. The submitted file should be in OpenOffice, Microsoft World, RTF, or WordPerfect document file format.
4. Cover letter should be written in Comments to the Editor section or submitted as a separate file in the Supporting Files section.
5. The text is single-spaced, uses a 12-point font, employs italics rather than underlining (except with URL addresses), and all illustrations, figures and tables are place within the text at the appropriate points, rather than at the end of the document.
6. The text adheres to the stylistic and bibliographic requirements outlined in the Author Guidelines, which is found in the 'Guidelines to references' page.
7. Where available, URLs for the references should be provided.

Referencing: 3Bio uses Vancouver citation style. Vancouver is a numbered referencing style commonly used in medicine and science, and consists of:

- Citations to someone else's work in the text, indicated by the use of a number.
- A sequentially numbered reference list at the end of the document providing full details of the corresponding in-text reference.

It follows rules established by the International Committee of Medical Journal Editors, now maintained by the U.S. National Library of Medicine. It is also known as Uniform Requirements for Manuscripts submitted to Biomedical Journals.

File Size and Format: Manuscripts will be distributed to reviewers via the Web. However, reviewers who use telephone modems may experience unacceptable download delays if the files are too large. A number of simple tricks can be used to avoid unnecessarily large files. Do not scan pages of text. Do not scan printed Figures unless no original digital document exists.

If a scanned figure is unavoidable, please use Adobe PhotoShop or a similar program to edit the file and reduce the file size (not necessarily the image size) as much as possible before submission. For example, crop the picture to exclude surrounding "white space." Do not carelessly use colour. Black and white line drawings or gray-scale figures should not be saved as color documents; this will increase file sizes without increasing the information content of the file. Do not use colour unless absolutely needed to convey information.

Readability: A paper may be returned to the corresponding author for no other reason than that it suffers due to poor English. Papers must be understandable and communicate an unambiguous message. The editors and staff can make only a limited number of edits, and it is the responsibility of the authors to obtain help from a colleague who is fluent in English if that is needed. Most problems occur when there are nuances in meaning, and the authors bear the primary responsibility for clarity. Poor English may ultimately be a reason to refuse a paper.

Table of Content